STUDIES ON THE FUNCTION OF THE *PRD*-1 GENE IN *NEUROSPORA CRASSA*

DI WU

A THESIS SUBMITTED TO

THE FACULTY OF GRADUATE STUDIES

IN THE PARTIAL FULFILMENT OF THE REQUIREMENTS

FOR THE DEGREE OF

MASTER OF SCIENCE

GRADUATE PROGRAM IN BIOLOGY

YORK UNIVERSITY

TORONTO, ONTARIO

JUNE 2018

Abstract

In *Neurospora crassa*, conidiation is controlled by the circadian clock which consists of more than one oscillator. The *frequency* (*frq*) gene is a key component in the FRQ oscillator. The *prd*-1 mutant was found to lengthen the period of the circadian rhythm and disrupts the FRQ-less rhythm, but how this mutant affects the oscillators was unclear. This thesis aims to study the function of the *prd*-1 gene. Building on previous research, knocking out *prd*-1 is lethal; strains expressing PRD-1-FLAG were constructed; *prd*-1 expression showed non-circadian rhythmicity; co-IP and MS analysis discovered ribosomal proteins bind to PRD-1; the *prd*-1 mutant responds to amino acids differently in growth; and the deletion of the C-terminus of *prd*-1 was found to be lethal. The results of these various experiments outlined that the *prd*-1 gene may affect the circadian rhythm via nutrient sensing pathways especially the TOR pathway.

Acknowledgements

I would like to express my whole-hearted gratitude to my supervisor Dr. Patricia Lakin-Thomas for the continuous generous support in my study, research work, finance and daily life during the three years, and for numerous helpful comments, insightful inspiring conversations and open-minded mercy to my mistakes. Her immense understanding of the world, pure enthusiasm on science and patience on me are the most precious traits I admire. This thesis cannot be accomplished without her close supervision.

I would like to thank my supervision committee member Dr. Katalin A. Hudak for her encouraging comments, valuable guidance and constant support throughout my thesis.

My sincere appreciation also goes to Lalanthi Ratnayake for myriad helps during the time in York University.

I also feel grateful to all the colleagues Aryan Lajevardi, My Ha Le, Alexandra Pana, Dr. Keyur Adhvaryu and Chanhee Seo for helps in experimental work and company.

I would like to thank the Department of Biology and York University for support in more than financial aspects, offering me an unforgettable research experience.

Friends and people I met here are also deeply appreciated.

Finally, my every stair I stepped on cannot be performed without infinite support from my parents and family. Their concerns and cares on me are always engraved in my memory.

Table of Contents

Abstract ..... **ii**

Acknowledgements ..... **iii**

Table of Contents ..... **iv**

List of Tables ..... **ix**

List of Figures ..... **x**

List of Abbreviations ..... **xiii**

Chapter 1 Introduction **1**

1.1 CIRCADIAN RHYTHMS 1

1.1.1 History and definitions 1

1.1.2 Importance in human health 3

1.2 MOLECULAR CIRCADIAN CLOCKS 4

1.2.1 Transcription-translation feedback loop (TTFL) 4

1.2.2 Molecular circadian clock in Drosophila 6

1.2.3 Molecular circadian clock in mammals 8

1.2.4 Molecular circadian clock in cyanobacteria 10

1.2.5 Molecular circadian clock in plants 13

1.3 MOLECULAR CIRCADIAN CLOCK IN *NEUROSPORA CRASSA* 15

1.3.1 *Neurospora crassa* 15

1.3.2 FRQ-WCC oscillator 16

1.3.3 FRQ-less oscillator 18

1.4 THE *PRD-1* GENE IN *NEUROSPORA* 19

1.4.1 Effects of the *prd*-1 mutation 19

1.4.2 Identification of the *prd*-1 gene 19

1.5 OBJECTIVE OF THE THESIS 21

Chapter 2 Essentiality of the *prd*-1 gene and its C-terminus **23**

2.1 INTRODUCTION 23

2.2 MATERIALS AND METHODS 26
2.2.1 Strains 26
2.2.2 Microconidia purification 26
2.2.3 Race tube assay 27
2.2.4 Spore PCR 27
2.2.5 DNA agarose gel electrophoresis 27
2.2.6 Regular PCR 28
2.2.7 Assembly PCR 28
2.2.8 Techniques related to molecular cloning 28
2.2.9 Transformation of *Neurospora* 29
2.2.10 Crossing 29
2.3 RESULTS 31
2.3.1 Microconidia purification is effective to select homokaryons 31
2.3.2 The *prd*-1 gene is essential for *Neurospora crassa* 31
2.3.3 The failure to construct knock-in DNA cassette by assembly PCR 34
2.3.4 The construction of knock-in DNA cassette and guide RNA expression plasmid by restriction endonucleases 34
2.3.5 The construction of knock-in transformants 39
2.3.6 The essentiality of C-terminus of the *prd*-1 gene 39
2.4 CONCLUSION 45

Chapter 3 Rhythmicity of the *prd*-1 gene 47

3.1 INTRODUCTION 47
3.2 MATERIALS AND METHODS 51
3.2.1 Strains 51
3.2.2 Race tube assay 51
3.2.3 Protein extraction 51
3.2.4 Nuclei isolation 52
3.2.5 Western blotting and immunodetection 52
3.2.6 Genomic DNA extraction 53

3.2.7 Regular PCR 53
3.2.8 Techniques related to molecular cloning 54
3.2.9 Transformation of *Neurospora* 54
3.2.10 Spore PCR 54
3.2.11 Microconidia preparation 54
3.2.12 Crossing 54
3.2.13 Culture and harvest of time courses 54
3.2.14 Coomassie blue staining 55
3.2.15 Digoxigenin (DIG)-conjugated DNA probe 55
3.2.16 RNA extraction 55
3.2.17 Northern blotting and immunodetection 56
3.2.18 Data analysis and statistics 57
3.3 RESULTS 58
3.3.1 Preliminary test of PRD-1-FLAG strains from lab stock 58
3.3.2 Construction of *ccg-prd*-1-flag plasmid 63
3.3.3 Construction of native-*prd*-1-flag plasmid 63
3.3.4 Construction of transformants expressing FLAG-tagged PRD-1 69
3.3.5 The rhythmicity of the *prd*-1 mRNA 72
3.3.6 The rhythmicity of PRD-1 76
3.4 CONCLUSION 79

Chapter 4 Interacting partners of PRD-1 81

4.1 INTRODUCTION 81
4.2 MATERIALS AND METHODS 81
4.2.1 Strains and cell culture 81
4.2.2 Nuclei isolation and protein extraction 82
4.2.3 Co-IP for Western blotting 82
4.2.4 Western blotting 83
4.2.5 SDS-PAGE gel staining 83
4.2.6 Co-IP and Mass Spectrometry 83

4.2.7 Data analysis 84
4.3 RESULTS 84
4.3.1 Nuclei isolation is not necessary for IP 84
4.3.2 Capture efficiency of Anti-FLAG M2 Affinity Gel 85
4.3.3 Candidates of PRD-1 binding partners 85
4.4 CONCLUSION 89
Chapter 5 Growth responses under different conditions 90
5.1 INTRODUCTION 90
5.1.1 The association between glucose concentration and the *prd*-1 gene. 90
5.1.2 The association between amino acids and the *prd*-1 gene. 90
5.1.3 The measurement of growth rate and growth limit 91
5.2 MATERIALS AND METHODS 92
5.2.1 Strains 92
5.2.2 Culture 92
5.2.3 The measurement of dry weight 92
5.3 RESULTS 93
5.3.1 The determination of the standard growth curve 93
5.3.2 The growth response to glucose concentration gradient 94
5.3.3 The growth response to amino acids 95
5.4 CONCLUSION 98
Chapter 6 Discussion 99
6.1 LETHALITY OF PRD-1^{KO} 99
6.2 DOSE EFFECT OF THE EXPRESSION OF PRD-1 100
6.3 FLUCTUATION OF PRD-1-FLAG 101
6.4 THE ROLE OF PRD-1 IN RIBOSOME-ASSOCIATED BIOLOGICAL PROCESSES 101
6.5 THE POTENTIAL ROLE OF PRD-1 IN NUTRIENT SENSING 103
6.6 PRD-1 AND THE REGULATION OF THE CIRCADIAN RHYTHM 104
6.7 FUTURE WORK AND PERSPECTIVE 106

Appendices 109

APPENDIX A: GENOTYPE OF THE STRAINS 109

APPENDIX B: RECIPES 111

APPENDIX C: PRIMER INFORMATION 113

APPENDIX D: SEQUENCES 116

APPENDIX E: MASS SPECTROMETRY DATA 125

References 128

List of Tables

Table 2.1 Primers used for the amplification of fragments in Figure 2.4b 37

Table 3.1 The schedule for sampling every 4 hours 55

Table 3.2 The results (Mean ± SE, n=5) of race tube analysis to test the phenotype. 59

Table 3.3 The results (Mean ± SE, n=3) of race tube analysis to test the phenotype. 70

Table 4.1 List of candidates binding to PRD-1 86

List of Figures

Figure 1.1 Schematic diagram of TTFL. 5

Figure 1.2 The schematic diagram of the TTFL in *Drosophila*. 7

Figure 1.3 The schematic diagram of the TTFL in mammals. 9

Figure 1.4 The schematic diagram of post-translational regulation of the circadian clock in cyanobacteria 12

Figure 1.5 The schematic diagram of TTFLs in proposed clock model in *Arabidopsis thaliana*. 14

Figure 1.6 The schematic diagram of circadian clock regulation in *Neurospora crassa*. 17

Figure 1.7 Organization of the *prd*-1 gene 20

Figure 2.1 Schematic results of sorbose plates with/without hygromycin selection. 32

Figure 2.2 Result of *prd*-1^{KO} spore PCR after microconidia purification. 33

Figure 2.3 Result of spore PCR from both ends of race tube. 33

Figure 2.4 The construction of knock-in DNA cassette by assembly PCR. 36

Figure. 2.5 Schematic graph of the construction of plasmids carrying knock-in cassette 37

Figure 2.6 DNA gel pictures of digested plasmids. 38

Figure 2.7 Spore PCR of the knock-in transformants. 41

Figure 2.8 The purification of homokaryotic knock-in transformants of #567 42

Figure 2.9 The race tubes of selected *prd*-1^{+}-flag homokaryons 43

Figure 2.10 The purification of homokaryotic knock-in transformants of #26 triggered by CRISPR gene editing. 44

Figure 3.1 Spore PCR results of some prd-1 transformants in Table 3.1. 61

Figure 3.2 Western Blotting results by Anti-FLAG M2 antibody 61

Figure 3.3 Western Blotting results by Anti-FLAG M2 antibody 62

Figure 3.4 PCR of genomic DNA to test epitope tag. 62

Figure 3.5 Plasmid map of pBM61-ccg-*prd*-1-flag. 64

Figure 3.6 Construction of pBM61-ccg-*prd*-1-flag. 64

Figure 3.7 Plasmid map of pBM61-native-*prd*-1-flag. 66

Figure 3.8 Colony PCR result of native-*prd*-1-flag plasmids 67

Figure 3.9 Restriction enzyme test of native-*prd*-1-flag transformants. 67

Figure 3.10 Restriction enzyme test of pJET-native-*prd*-1 subclones. 67

Figure 3.11 Restriction enzyme test of pBM61-native-*prd*-1-flag transformants. 67

Figure 3.12 Construction of native-*prd*-1-FLAG. 68

Figure 3.13 Construction of transformants expressing FLAG-tagged PRD-1. 71

Figure 3.14 DNA probes in the 1.5% agarose gel. 73

Figure 3.15 Agarose gel (upper panel) and Northern blot (lower panel) of 40μg total RNA 73

Figure 3.16 The results of circadian time course of the *prd*-1 mRNA. 75

Figure 3.17 Western blotting results using Anti-FLAG M2 antibody 76

Figure 3.18 The results of circadian time course to assay PRD-1-FLAG. 78

Figure 3.19 Representative picture of the race tubes..... 80

Figure 4.1 Western blotting results detected by Anti-FLAG antibody. 87

Figure 4.2 IP capture efficiency assay. 88

Figure 5.1 The standard growth curve in 1% glucose Vogel's medium. 93

Figure 5.2 The maximum growth in Vogel's media with a gradient of glucose concentration. 94

Figure 5.3 The growth in Vogel's media with 50mM amino acids. 96

Figure 5.4 Simulated growth curves 97

List of Abbreviations

ANOVA	Analysis of Variance
bd	band
BLAST	Basic Local Alignment Search Tool
Bmal1	Brain and Muscle Arnt-Like protein 1
BSA	Bovine Serum Albumin
chol-1	Choline mutant
CLOCK	Circadian Locomotor Output Cycles Kaput
Ccg	Clock-controlled genes
csp-1	conidial separation 1
DD	constant dark
DIG	Digoxigenin
ECL	Enhanced Chemiluminescence
FGSC	Fungal Genetics Stock Center
FLO	FRQ-Less Oscillator
FRH	FRQ-interacting Helicase
FRQ	Frequency
GFP	Green Fluorescent Protein
gRNA	guide RNA
HR	Homologous Recombination
HRP	Horseradish peroxidase
IAA	Iodoacetate
IP	Immunoprecipitation
LL	Constant light
KI	Knock in
KO	Knock out
MS	Mass Spectrometry
NCBI	National Center for Biotechnology Information
NHEJ	non-homologous end-joining

NI	Nuclei Isolation
NLS	Nuclear Localization Signal
PCR	Polymerase Chain Reaction
PER	Period
prd	period
PVDF	polyvinylidene difluoride
RFP	Red Fluorescent Protein
SCN	suprachiasmatic nuclei
SDS-PAGE	Sodium dodecyl sulfate polyacrylamide gel electrophoresis
TTFL	Transcription-translation feedback loop
WCC	White Collar Complex
WT	wild type

Chapter 1 Introduction

Organisms have developed diverse approaches to adapt to the environmental changes on the earth. Biological rhythms, oscillations at a biochemical, physiological, or behavioral level, are a ubiquitous feature reflecting periodic environmental changes in the world that corresponds to the periodic celestial movement: the relative position of Earth to the Sun and to the Moon. According to the period of biological rhythms, they can be categorized as ultradian (less than 24 h), circadian (about 24 h), infradian (more than 24 h), or even circannual rhythms (about one year) (Wollnik, 1989). During the struggle with nature, called evolution, organisms gain the endogenous biological clocks which can predict the periodic environmental changes such that they can be prepared to optimize their living condition. This internal mechanism can maintain the rhythms even in the absence of the environmental stimulus.

1.1 Circadian Rhythms

1.1.1 History and definitions

A biological rhythm with a 24-hour period is called a circadian (from Latin circa, “about”; di, “day”—i.e., “about a day”) rhythm (Huang et al., 2011; Ishida et al., 1999). The circadian rhythms are the most common ones in everyday life and the circadian clock helps regulate functions of human bodies including: blood pressure, hormone levels, body temperature, appetite, alertness, sleep schedule, and daily performance (Arendt, 2010; Ishida et al., 1999; Tsang et al., 2014). Circadian rhythms have been observed in a large number of multi- and unicellular organisms, including vertebrates, invertebrates, plants, fungi and bacteria (Dunlap, 1999; Wollnik, 1989). Such oscillations are believed to be produced by one or multiple endogenous oscillators and persist with a period of ~24 h in the absence of environmental time cues.

The origin of circadian research began with de Mairan in the 18th century, a French

scientist who noted the movements of leaves of the sensitive heliotrope plant (probably *Mimosa pudica*) (McClung, 2006), and the daily movements sustained when he moved the plant to the constant darkness. More significant, a regular period of the movements was found, leading him to a presumption that an endogenous system is controlling the movements. In 1832 de Candolle measured the free-running period of *M. pudica* and found it was 22 to 23 h, notably implying that these rhythms were not simply responses to environmental time cues (McClung, 2006).

In 1954, Colin Pittendrigh showed that eclosion in *Drosophila pseudoobscura* follows the circadian rhythm. The first clock mutant was identified in *Drosophila* in 1971 by Ron Konopka and Seymour Benzer and was called the "*period*" (*per*) gene (Golombek and Rosenstein, 2010). This gene was cloned in 1984 and scientists began studying the circadian rhythm at the molecular level.

As a mechanism to perceive, predict and adapt to surrounding periodic changes, the circadian clock has five fundamental characteristics. Firstly, the circadian clock is endogenous. The free running rhythm in constant conditions can be maintained without a zeitgeber (German for time givers). Secondly, the circadian clock is stable. The period and amplitude of the free running rhythm can stabilize for a relatively long time. Thirdly, the free running period is approximately 24 h, but not exactly equal to 24 h. Fourthly, the circadian clock can be entrained (synchronized) by external stimuli, like light, temperature or feeding. Fifthly, the circadian clock is temperature compensated, which means the free running period is substantially unchanged at constant conditions within a certain range of temperatures.

Typically, the circadian system is conceptualized as a network among three components. Input pathways are capable of relaying the environmental signals to timekeeping oscillators; the oscillator operates to generate the pace in the absence of the zeitgebers; the output pathways are activated transiently and repetitively according to the fluctuation of the core oscillator. The entrainment of the circadian rhythm depends on the interaction and

synchronization among these three parts. The phase of the circadian rhythm can be reset by light pulses, temperature pulses or temperature steps (Lakin-Thomas et al., 1990; Liu et al., 1997; Liu et al., 2003). The phase alteration is not a simple response to exogenous time cues. Different phase alteration responding to the entrainment given at different circadian time suggest intricate regulations in the circadian system (Liu, 2003).

1.1.2 Importance in human health

The alignment between the clock and physiological events is demonstrated to have great significance for organisms particularly for humans.

Many components of the endocrine system display robust circadian rhythms in mammals (Tsang et al., 2014). Several hormones were found to have circadian rhythms: melatonin, cortisol, gonadal steroids, prolactin, thyroid hormone and growth hormone (Gnocchi and Bruscalupi, 2017). As a hormone helping to adjust the sleep/wake cycle, the timing of melatonin secretion is regulated by the suprachiasmatic nucleus (SCN), which is the master pacemaker to drive circadian rhythms in mammals (Panda et al., 2002). The secretion begins approximately 2 hours before natural sleep time and the concentration of melatonin is highest during the middle of the night. Melatonin is also a stable marker of circadian phase used in research as well as clinical practice (Golombek and Rosenstein, 2010).

Organisms are able to use temperature changes as synchronization cues. The changes of temperature can induce alterations in the phase response behavior, sometimes even the rhythmicity itself (Balzer and Hardeland, 1988). Similarly, scheduled physical activity has been reported to phase-shift and entrain the circadian rhythm of rodents. In humans, timed physical exercise produced phase-advance shifts. Regular physical exercise also facilitated entrainment of the circadian rhythms (Yamanaka et al., 2006). These findings suggest that artificial arrangement of the zeitgeber is useful to adjust the circadian rhythm to social timetables.

Numerous reports have shown that shift workers have a higher incidence of diabetes,

obesity, and cardiovascular events (Arendt, 2010; Huang et al., 2011). Genome-wide association studies have also suggested associations between clock gene variation and obesity and metabolic syndrome, implying the impact of the circadian clock on human metabolic disease (Huang et al., 2011). Feeding an isocaloric high-fat diet at a deliberately altered circadian time results in increased weight gain in mice (Arble et al., 2009), suggesting that the synchronization of feeding with the circadian clock is critical in the homeostasis of body weight. The disruption of clock genes gives rise to a spectrum of reproductive and metabolic changes in animal models. Emerging evidence that mutated or knock-out clock genes strongly influence reproductive competency in mice has been found (Boden and Kennaway, 2006).

The discovery of the genetic basis for circadian rhythms has expanded our knowledge of the dynamic regulation of behavior and physiology in the human body. More broadly, the research about circadian clocks advances the development of clinical practice and disseminates the awareness that the synchronization between internal and external time is essential for personal welfare.

1.2 Molecular Circadian Clocks

1.2.1 Transcription-translation feedback loop (TTFL)

Circadian clocks are endogenous mechanisms that synchronize physiological and behavioral processes in organisms with external time cues. Circadian clocks seem to be the fruits of convergent evolution, because the operation principles of circadian clocks share a structurally analogous network based on the studies of diverse organism (Czeisler and Gooley, 2007; Dunlap, 1999) The molecular clocks mentioned here are oscillators that generate the intrinsic motivation to drive the circadian rhythms.

These circadian molecular clocks are composed of transcription–translation feedback loops (TTFLs) that are autoregulatory and interlocked. According to this scheme, the clocks have a set of components that can positively or negatively modulate the expression of

relevant genes (Dunlap, 1999). The positive elements activate the transcription of the negative elements and clock-controlled genes (ccgs). The negative elements suppress the function of the positive elements. The negative elements are translocated and accumulated into the nucleus leading to their transcription becoming substantially repressed. Following the decay of the negative elements, the transcriptional function of the positive elements is renewed (Figure 1.1). The negative feedback with delay is the key to maintain the period. The duration of these processes is about 24 hours and the oscillation of the transcriptional activity gives rise to the circadian rhythms (Dunlap, 1999; King and Takahashi, 2000). The TTFLs are widely accepted as the pacemaker of the circadian clock.

Regardless of the conservative blueprint, the components of the circadian clock in different organisms are distinct. Following are some model systems that are well characterized in recent decades.

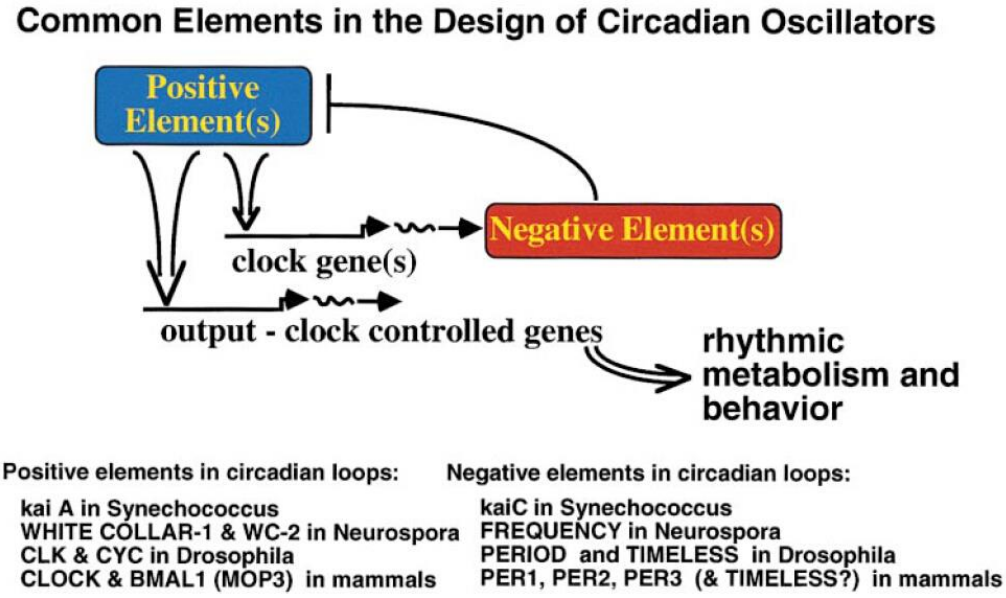

Figure 1.1 Schematic diagram of TTFL. The translated protein (negative element) negatively regulates the transcription factor (positive element) which causes the rhythmic expression of clock and clock-controlled genes. (Adapted from Dunlap, 1999)

1.2.2 Molecular circadian clock in *Drosophila*

Since the identification of the *per* mutant and the *per* gene, several approaches to genetic screening have been carried out in *Drosophila*. Researchers have identified several genes that, together with period, play key roles in the circadian clock. For *Drosophila*, it seems that most of the core genes have been identified — new mutant alleles tend to fall into previously defined complementation groups (Young and Kay, 2001). The studies of these genes all suggest that the TTFL composes a light-responsive molecular clock in *Drosophila*.

The rhythmic regulation of the expression of PERIOD (PER) and TIMELESS (TIM) is the pivot of these loops (Figure 1.2). Transcription factors CLOCK (CLK) and CYCLE (CYC) function as a heterodimer to drive the expression of PER and TIM via the E-boxes in their promoter. Once PER and TIM are translated, the casein kinase 1ε orthologue Double-time (DBT) binds to either PER or PER/TIM complex and phosphorylates them. The TIM-free PER will be degraded and the DBT/PER/TIM complex can enter the nucleus. The gradually accumulated PER and TIM can repress the transcriptional activity of CLK/CYC in the nucleus while DBT is slowly removed from the DBT/PER/TIM complex (Young and Kay, 2001). Since the expression of TIM that stabilize PER decreases, the degradation of the phosphorylated PER is enhanced. The expression of PER and TIM is reactivated when the nuclear PER is at a low level. Delays in PER and TIM accumulation and nuclear translocation of the DBT/PER/TIM complex are important for the generation of a 24-hour period (Tataroglu and Emery, 2015). The synthesis and degradation of PER and TIM are tightly regulated throughout the day to set the pace of the circadian pacemaker (Tataroglu and Emery, 2015). In general, the abundances of key regulators PER and TIM are tightly regulated by the TTFLs to maintain the circadian rhythms in *Drosophila.*

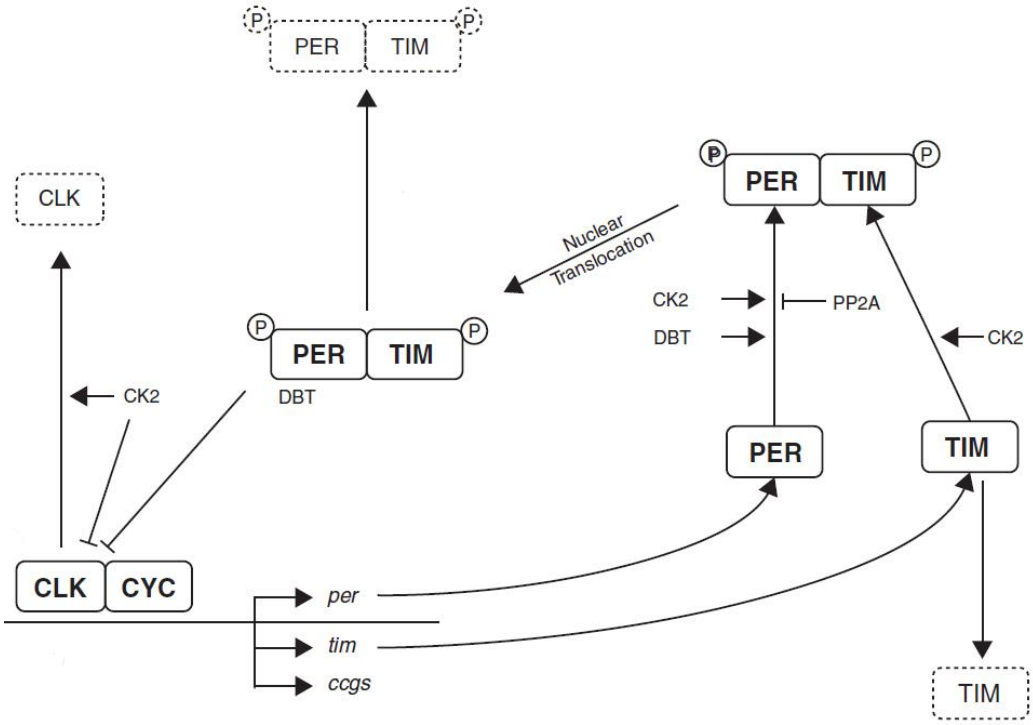

Figure 1.2 The schematic diagram of the TTFL in *Drosophila*. The CLK/CYC heterodimer binds to E-box of the promoter of per/tim and activate the transcription. PER is phosphorylated by DBT and TIM binds to phosphorylated PER for stabilization. Then the complex inhibits the activity of CLK/CYC in the nucleus and the proteins are degraded when their expression is decreasing. The transcriptional activity of CLK/CYC is renewed when the nuclear PER is at a low level and a new cycle starts. (Adapted from Tataroglu and Emery, 2015)

1.2.3 Molecular circadian clock in mammals

Many circadian rhythms have been discovered in mammals including blood pressure, body temperature, hormone levels, the number of immune cells in blood, and the sleep-wake cycle (Ishida et al., 1999). Prior to 1997, no mammalian clock genes had been identified at the molecular level (King and Takahashi, 2000). Studies involving mice with mutations that possessed aberrant rhythmic phenotypes uncovered clock genes in the 1990s. Researchers showed that virtually all cells have the capacity to generate circadian oscillations (Panda et al., 2002; Reddy et al., 2006). Further works demonstrated that the mammalian circadian system could be conceptualized as a hierarchical system. The master clock, a clock located in the suprachiasmatic nuclei (SCN) of the anterior hypothalamus and entrained by light signals in the eye (Avivi et al., 2001), synchronizes independent peripheral oscillators distributed throughout the body (Steinlechner, 2012).

At molecular level, the cell-autonomous circadian rhythms in mammals are based on the TTFLs (Figure 1.3). The core clock genes identified in mammals are *Clock* (Circadian Locomotor Output Cycles Kaput), *Bmal*1 (brain and muscle Arnt-like protein 1), *Per*1 (Period), *Per*2, *Per*3, *Cry*1 (Cryptochrome), and *Cry*2. The positive element CLOCK and its heterodimeric partner BMAL1, which are basic helix–loop–helix (bHLH)–PER-ARNT-SIM (PAS) transcription factors, bind to the promoter of negative elements containing E-boxes (PER1, PER2, PER3, CRY1 and CRY2) (Takahashi, 2017). The transcription of PER1, PER2, CRY1 and CRY2 are activate in the subjective daytime. Similar with the heterotrimer in *Drosophila*, PER and CRY interact with each other as well as with the CK1δ (serine/threonine kinases casein kinase 1δ) and CK1ε in the cytoplasm (Lee et al., 2001). The proteins as a complex enter the nucleus at night to repress their own transcription via the interaction with transcriptional factors CLOCK-BMAL1. *Per* and *Cry* transcription declines due to the repression and the PER and CRY protein abundances decrease. PER and CRY proteins are subsequently degraded by the proteasome. Once the inhibition is relieved by the

turnover of the repressor complex, CLOCK–BMAL1 functions to start a new cycle of transcription-translation processes (Takahashi, 2017). Importantly, the mutation of PER2 and its regulatory kinase CK1δ, have been found to underlie human sleep-timing disorders (Young and Kay, 2001), thus demonstrating a clear role in humans' circadian clock.

Beyond targeting *Per* and *Cry*, the CLOCK–BMAL1 complex also activates the nuclear receptors REV-ERBα and REV-ERBβ (Preitner et al., 2002; Zhang et al., 2015). The rhythmic expression of REV-ERBα and REV-ERBβ leads to the repression of BMAL1 and CLOCK, which induces a rhythm in these genes that is in antiphase with PER expression rhythms (Zhang et al., 2015).

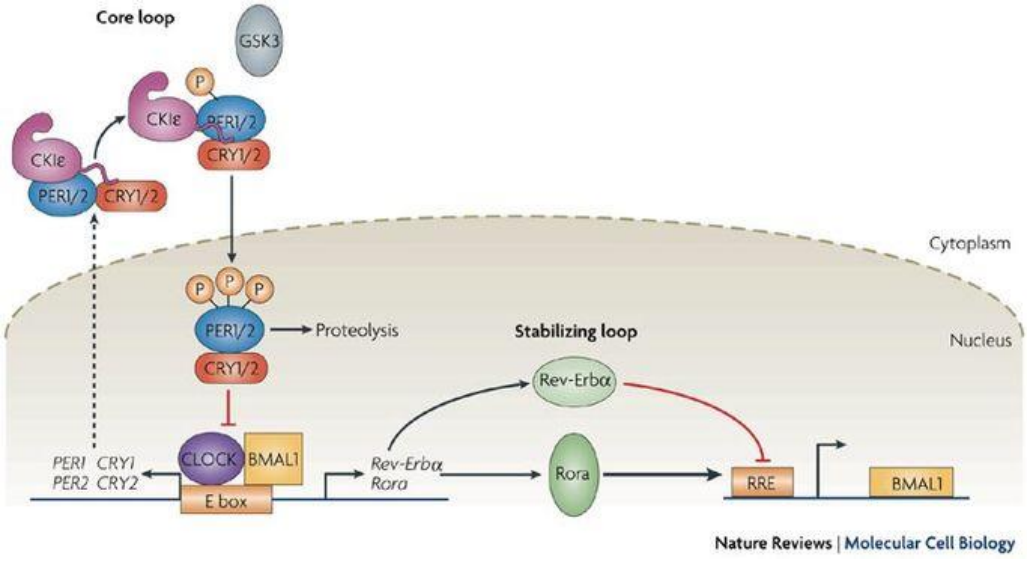

Figure 1.3 The schematic diagram of the TTFL in mammals. CLOCK and BMAL1 are the positive elements that drive expression of the negative regulators, PER1, PER2, CRY1 and CRY2. The PER and CRY proteins accumulate and form a complex and are phosphorylated by CKIε and glycogen synthase kinase-3 (GSK3). They then translocate to the nucleus to repress the positive regulator. At the end, the degradation of the PER and CRY proteins releases the repression of the transcription and allows the next cycle to start. The activator Rora and the inhibitor Rev-Erbα compose an additional stabilizing feedback loop, controls BMAL1 expression and reinforces the oscillations. P, phosphate. (Adapted from Gallego and Virshup, 2007)

1.2.4 Molecular circadian clock in cyanobacteria

It was believed that, in rapidly dividing cells (cell cycle significantly shorter than 24 hours), biological processes would not be coupled to a circadian oscillator (Cohen and Golden, 2015). In 1986, Huang and colleagues discovered a circadian rhythm of nitrogen fixation and amino acid uptake in *Synechococcus sp.* RF-1 (Chen et al., 1991; Huang et al., 1990). Since then the genetically tractable *Synechococcus elongatus* PCC 7942 has become a model organism for studying the molecular mechanism of the clock (Cohen and Golden, 2015).

The *kaiA*, *kaiB*, and *kaiC* genes are key genes in the oscillator of *S. elongatus*. The phosphorylation/dephosphorylation cycle caused by the dynamic interactions between these three proteins and conformation changes of the proteins are believed to be the core oscillator (Figure 1.4). KaiC is an autokinase, autophosphatase, and ATPase. The phosphorylation occurs at residues Ser431 and Thr432. (Nishiwaki et al., 2004; Xu et al., 2004). KaiC is a ring-shaped homohexamer whose monomer has CI and CII domains that shape the hexamer like two stacked doughnuts (Cohen and Golden, 2015). During the subjective daytime, KaiA binds to the non-phosphorylated KaiC on its C-terminus, promoting the autophosphorylation of KaiC. The phosphorylation of both sites stacks the CII rings on CI rings. The conformation change exposes the binding sites for KaiB. KaiB binds to the hyper-phosphorylated KaiC on its N-terminus, reactivating the autophosphatase activity of KaiC by sequestrating KaiA away from the C-terminus of KaiC. Therefore, in subjective night, the KaiC is auto-dephosphorylating and again the conformation change exposes the binding sites of KaiA for a new cycle (Chang et al., 2012). The KaiABC oscillator transmits the information to the output via a pathway consisting of SasA (*Synechococcus* adaptive sensor A) and RpaA (regulator of phycobilisome association A). SasA interacts with the N-terminus of KaiC in the same manner as KaiB. The binding induces the phosphorylation of SasA and phosphotransfer to the response regulator RpaA (Takai et al., 2006). RpaA is a DNA-binding

transcription factor when phosphorylated and binds directly to about 100 targets in the S. elongatus genome. The phosphorylated RpaA binds to the *kaiBC* promoter as well generating feedback to the core oscillator (Markson et al., 2013).

Although not considered as the core oscillator, the TTFL is nonetheless present in the cyanobacteria circadian clock. KaiA can positively regulate the expression of *kaiBC*, whereas KaiC is a negative regulator to its own promoter (Ishiura et al., 1998). However, none of the Kai proteins are DNA binding proteins. Hence the autoregulatory functions are indirect. This TTFL mechanism is not essential for the pacemaker in cyanobacteria because the KaiC phosphorylation cycles still can be detected in the test tube or when the TTFL is blocked in constant conditions with inhibitors (Tomita et al., 2005). Moreover, evidence showed that the TTFL is required under conditions of rapid growth to maintain robust circadian oscillations (Cohen and Golden, 2015).

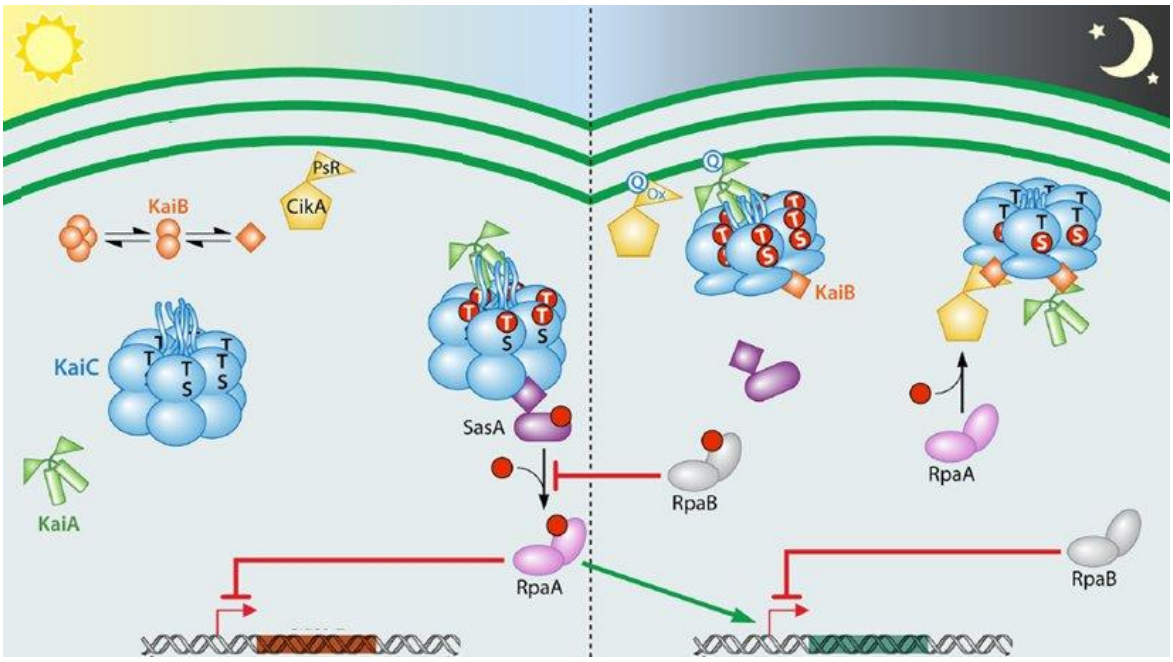

Figure 1.4 The schematic diagram of post-translational regulation of the circadian clock in cyanobacteria. The progression of the oscillator is shown (indicated by shading from sun to moon at the top). During the day (left panel), KaiA interacts with KaiC, promoting the phosphorylation of KaiC. Phosphorylation events are indicated by a red dot. SasA interacts with KaiC, promoting autophosphorylation of SasA and phosphotransfer to RpaA. RpaA-P accumulates over the day, regulating the expression of genes. At night (right panel), KaiA, KaiC, and CikA are all localized to the cell poles where fold-switched KaiB competes with SasA for binding to KaiC and sequesters KaiA away from the KaiC, promoting KaiC dephosphorylation through the night. CikA competes with KaiA for binding to fold-switched KaiB. The KaiBC complex promotes CikA's phosphatase activity toward RpaA. (Adapted from Cohen and Golden, 2015)

1.2.5 Molecular circadian clock in plants

Arabidopsis thaliana is the model organism used extensively in plant physiology and molecular biology research. Most studies of the plant circadian clock have considered *A. thaliana* in which the molecular mechanism underlying the circadian clock is best studied (Sanchez and Kay, 2016). In *A. thaliana*, and plants in general, the circadian clock comprises negative feedback loops regulated from transcriptionally to post-translationally, including post-transcriptional modification and protein turnover (Harmer, 2009). The molecular mechanism of the circadian oscillator can be portrayed based on the timing of the expression of morning-, daytime- and evening-phased genes (Figure 1.5). The TTFLs maintain proper timing of expression of each gene and their downstream targets throughout the day (Greenham and McClung, 2015).

The first molecular model of a circadian clock in plants was proposed in 2001. The TTFLs of *A. thaliana* consist of three genes: two MYB transcription factors, *CIRCADIAN CLOCK ASSOCIATED* 1 and *LATE ELONGATED HYPOCOTYL* (*CCA*1 and *LHY*, respectively), and *TIMING OF CAB EXPRESSION* 1 (*TOC*1) also known as *PSEUDO-RESPONSE REGULATOR* 1 (*PRR1*) (Alabadi et al., 2001). CCA1 and LHY mutually interact after being expressed in subjective morning and repress *TOC*1 expression. While *CCA*1 and *LHY* levels decrease at dusk, *TOC*1 starts being expressed and negatively regulates the transcription of *CCA*1 and *LHY* (Huang et al., 2012). An additional loop is formed by *PRR*9, *PRR*7, and *PRR*5 (members of the *PRR* gene family) that show partially redundant functions since they are homologs of *TOC*1 and repress *CCA*1 and *LHY* transcription (Sanchez and Kay, 2016). It is reported that PRR9 and PRR7 are induced by CCA1 and LHY. However, recent studies show that LHY or even TOC1 is a direct repressor of PRR9, PRR7, and PRR5 (Adams et al., 2015; Huang et al., 2012). PRR9 is also repressed by the "evening complex" (EC). The EC consists of the MYB-like transcription factor LUX ARRHYTHMO (LUX, also known as PHYTOCLOCK1), and EARLY FLOWERING 3 (ELF3) and ELF4,

two nuclear proteins with unknown biochemical function (Sanchez and Kay, 2016). The EC indirectly promotes the expression of CCA1 and LHY in turn repressing the EC components (Huang et al., 2012). A third loop was described comprising a morning-expressed group of genes, REVEILLE (RVE), homologs of CCA1 and LHY. RVE8 induces the transcription of afternoon and evening- phased genes: *PRR*5, *TOC*1, *LUX*, and *ELF*4. As a consequence, RVE8 is repressed by PRR9, PRR7, and PRR5 (Hsu et al., 2013).

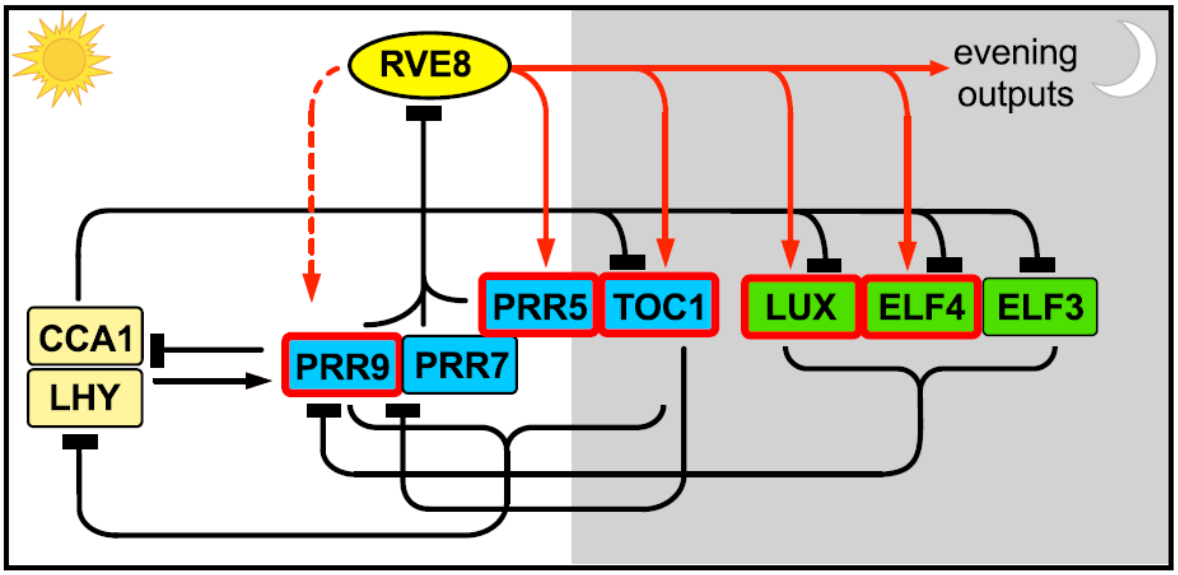

Figure 1.5 The schematic diagram of TTFLs in proposed clock model in *Arabidopsis thaliana*. The circadian time of higher activity level of each component is shown from daytime (left) to night (right). REVEILLE/CCA1/LHY family proteins (yellow) activate the expression of *PRR*5, *PRR*7 and *PRR*9; pseudo-response regulators (blue) repress the function of REVEILLE/CCA1/LHY family proteins; the evening complex components (green) repress PRRs inhibitory activity resulting in the activation of REVEILLE/CCA1/LHY family proteins. CCA1/LHY also regulate the expression of the evening complex components. RVE8 directly activates multiple evening-phased clock genes and that *RVE8* is indirectly regulated by TOC1, LUX and CCA1 through their regulation of *PRR5*, *PRR7* and *PRR9*. Only transcriptional regulation is shown. (Adapted from Hsu et al., 2013)

1.3 Molecular circadian clock in *Neurospora crassa*

1.3.1 *Neurospora crassa*

The filamentous fungus *Neurospora crassa* is one of the most thoroughly studied species. *N. crassa* is used as a model organism because of its simple requirements for culture and its haploid asexual life cycle that is convenient for genetic analysis. In the asexual part of the cycle, the hyphae from the germination and growth of an asexual spore (conidium) extends and branches to a mass of threads. In later development, the cross walls disappear in the hyphae so that a colony is a single cell containing numerous haploid nuclei. The nuclei in that hyphae can possess different genotypes, comprising a heterokaryon. A colony can produce millions of multinucleate macroconidia and uninucleate microconidia from aerial hyphae and the asexual cycle is repeated if they keep growing on a suitable medium (Davis, 2000).

Neurospora crassa is an exemplary heterothallic species that has two mating types. Mating can occur only between strains of opposite mating type (mat A and a, respectively). Once the parents come into contact, their cell walls and nuclei start fusing and then fruiting bodies called perithecia are formed containing diploid nuclei. Each diploid nucleus undergoes meiosis and develops to an ascus. The four products of a single meiosis undergo a mitosis that finally produce eight ascospore (sexual spores). The ascospores germinate and return to the asexual life cycle (Perkins and Davis, 2000).

Neurospora crassa is a great model system for studying the mechanism of circadian rhythms. The circadian rhythms of *Neurospora* first were reported in 1959 (Pittendrigh et al., 1959). However, the spore-formation rhythm is not overt in the wild type. The *band* mutation (also named *ras*-1^{bd}) is required to observe robust circadian output (Sargent et al., 1966). Asexual spore formation is controlled by the circadian clock in *Neurospora* with a period of 21.5 h (Dunlap et al., 2007), and this rhythm can be easily assayed on agar medium in race tubes, as a pattern of conidial regions called “bands” alternating with fungal mycelium called

"interbands" (Li et al., 2011). Since the mycelia need to differentiate and form aerial hyphae for conidial production while growing forward, the time between two peaks of bands can be calculated based on the distance between peaks and the growth rate (Baker et al., 2012). Because the differentiation is static once the growth front has passed and the banding pattern can be measured after an experiment is completed, no automated equipment is needed. This conidiation rhythm has been the standard assay in labs and all known clock genes were identified by observing changes in the conidiation rhythm. Moreover, the genetic and biochemical background is well-studied and a relatively large community is supporting the research. The genome is fully sequenced (Galagan et al., 2003) and annotated databases are available online (FungiDB, http://fungidb.org/fungidb/ and NCBI, https:// www.ncbi.nlm.nih.gov/). A near-complete knockout library was built up (Colot et al., 2006) and knockout strains are available from the Fungal Genetics Stock Center (FGSC).

1.3.2 FRQ-WCC oscillator

Decades ago, *Neurospora* clock mutants were isolated after mutagenesis of the wild-type (*bd*) strain with either the chemical mutagen N-methyl-N'-nitro-N-nitrosoguanidine (NG) or ultraviolet light. Seven mutants with altered circadian period lengths were mapped to a single locus called *Frq* (*Frequency*) (Feldman and Hoyle, 1973; Gardner and Feldman, 1980), located on the right arm of linkage group VII. Since the *frq* gene was cloned, more components have been found to regulate the circadian clock.

The popular model of the molecular mechanism in *Neurospora crassa* is a transcription/translation feedback loop as well (Figure 1.6). In this loop, the FRQ (FREQUENCY), WC-1 and WC-2 (White Collar 1 and 2) proteins are core elements. WC-1 and WC-2, GATA-family transcription factors with PAS (Per-Arnt-Sim) domains, are positive elements that form a heterodimeric complex named WCC (White Collar Complex) (Liu et al., 2003). WCC activates the transcription of the *frq* gene in the late subjective night (Baker et al., 2012). FRQ, the negative element, along with its binding partner FRH (FRQ-

interacting Helicase), inhibits the transcriptional activation of WCC in the nucleus, so consequently represses the expression of FRQ. The withdrawal of this repression is accomplished by phosphorylated FRQ recruiting the ubiquitin ligase FWD-1 (F-box/WD-40 repeat-containing protein) causing digestion of FRQ by the proteasome (He et al., 2003). The WCC then binds to the promoter of the *frq* gene again to reactivate the transcription. Since WCC also activates a number of clock-controlled genes not limited to the *frq* gene, this rhythmic activation-deactivation of the transcription is considered to drive the 24-hour rhythms in output, such as the conidiation rhythm (Guo and Liu, 2010).

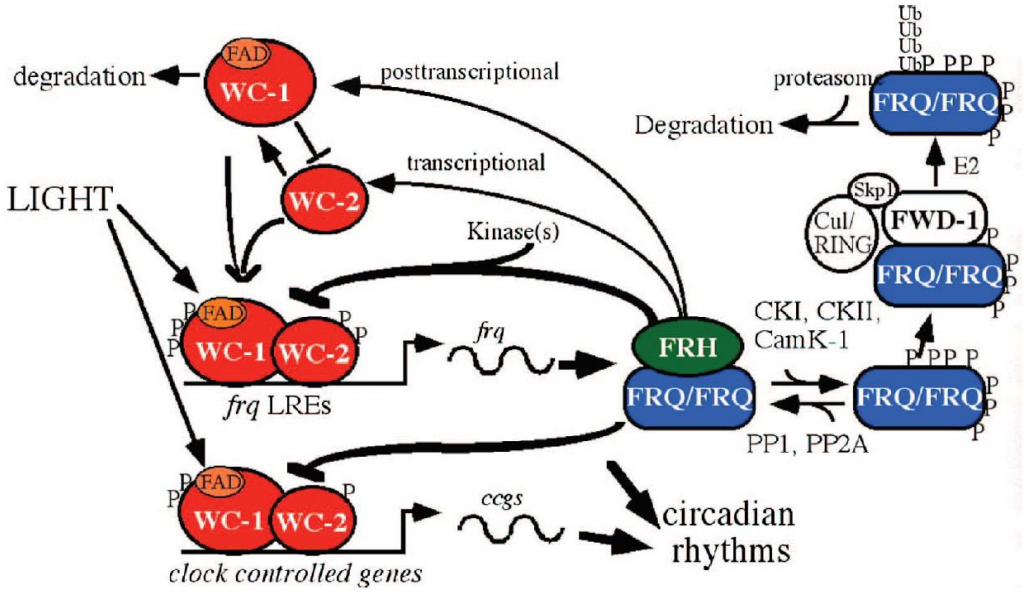

Figure 1.6 The schematic diagram of circadian clock regulation in *Neurospora crassa*. WC-1 is a blue-light photoreceptor and a transcription factor. With the interaction with WC-2, the WCC complex activates the transcription of *frq*. The FRQ homodimer along with the stabilizationer FRH are transported into the nucleus and repress the expression of both clock and clock-controlled genes activated by WCC. FRQ is being degraded when its expression is inhibited and the abundance of FRQ decreases. The transcription of the *frq* gene restarts after WCC is released from the repression and a new cycle initiates again. (Adapted from Liu and Bell-Pedersen, 2006)

1.3.3 FRQ-less oscillator

Although most of the research carried out on the circadian system in *Neurospora* is focused on the FRQ/WCC oscillator, it is known that a conidiation rhythm can be observed in the absence of a functional *frq* gene (Loros and Feldman, 1986; Merrow et al., 1999). Two null mutants have been found at the *frq* locus: frq^9, which has a point mutation expressing a truncated protein, and frq^{10}, which was constructed by targeted gene deletion (Aronson et al., 1994). Rhythms appear in *frq*-null mutants after the first few days of growth on the race tube, but the period is more variable than wild type and temperature compensation is defective (Aronson et al., 1994; Loros and Feldman, 1986). Calling null mutants of *frq*, *wc*-1 and *wc*-2 as "conditionally rhythmic" is more accurate than "arrhythmic", due to rhythmicity that can be induced by introducing more mutations or adding chemicals (Aronson et al., 1994; Lakin-Thomas, 2006; Lakin-Thomas and Brody, 2000; Lombardi et al., 2007; Merrow et al., 1999). Molecular rhythms can be seen in *frq*-null mutants, such as a rhythm in nitrate reductase (Christensen et al., 2004) or gene transcription of *ccg*-16 and levels of WC-1 protein (de Paula et al., 2006). Rhythmicity in the absence of the FRQ/WCC feedback loop must be driven by an oscillator called the FRQ-less oscillator (FLO), but the relationship between FRQ/WCC and FRQ-less oscillators has been discussed over the years, and the specific mechanism of FLO has not been understood so far (Li et al., 2011).

1.4 The *prd*-1 gene in *Neurospora*

1.4.1 Effects of the *prd*-1 mutation

As mentioned above several clock mutants in *Neurospora* have been identified as alleles of the *frq* gene. But one of the mutants, *frq*-5, was mapped to a position near the centromere on linkage group III (Feldman, 1982). It was renamed *prd*-1 (*period*-1) based on its effect on lengthening the period of the conidiation rhythm.

The *prd*-1 gene appears to play a key role in FRQ-less oscillators. The lipid-deficient strain *cel* sustains a long-period conidiation rhythm in the condition of low temperature or supplementation with unsaturated fatty acids when *frq* and *wc* -null mutations are introduced (Lakin-Thomas and Brody, 2000). The rhythm continues when the *prd*-1 mutation is introduced in *cel*, but the long-period rhythm is shortened, which suggests the *prd*-1 mutation blocks normal function of FLO (Lakin-Thomas and Brody, 1985).

The frq^{10} mutant is rhythmic when geraniol is added to the growth medium, and this system was used to assay the influence of *prd*-1 in FLO. The *prd*-1 mutants, having a long period in the frq^{+} background, lengthen the period in the frq^{10} background as well, suggesting that *prd*-1 is an important part of FLO (Lombardi et al., 2007).

1.4.2 Identification of the *prd*-1 gene

Our lab analyzed the rhythmicity of *prd*-1 in *chol*-1 frq^{10} strains using two conditions: 1) conidiation rhythms can be seen in *chol*-1 strains carrying *frq* and *wc* null mutants with limited choline. 2) Cycles of high temperature pulses can entrain the rhythms in *frq* and *wc* null mutants (Li and Lakin-Thomas, 2010). Previous work in our lab showed that *prd*-1 destroys the free-running FRQ-less rhythm in *chol*-1 and severely disrupts the heat-entrained FRQ-less rhythm in *chol*-1^{+} (Li and Lakin-Thomas, 2010).

Our lab has identified the *prd*-1 gene as NCU07839, and the product of it, PRD-1, is identified as a DEAD (Asp-Glu-Ala-Asp) box RNA helicase (Figure 1.7) (Adhvaryu et al.,

2016; Emerson et al., 2015). The DEAD-box RNA helicase family is conserved from yeast to human, involved in many processes of RNA metabolism, such as transcriptional regulation, splicing, nuclear export, ribosome biogenesis, translation and degradation (Linder and Jankowsky, 2011). Protein sequence similarity reveals that PRD-1 is homologous to the Dbp-2 ATP-dependent RNA helicase in yeast and the DDX5 DEAD-box RNA helicase in mammals that was found in the complex of proteins constituting the negative arm of the mammalian circadian feedback loop (Padmanabhan et al., 2012).

A single base substitution (G to A) occurs in the third intron of the *prd*-1 gene (Adhvaryu et al., 2016; Emerson et al., 2015). Sequencing of cDNA showed that the mutation affects splicing of the pre-mRNA, likely resulting in a premature stop codon (TAA) and a truncated PRD-1 protein which loses the C-terminal region, if the third intron cannot be spliced, despite the conserved DEAD-box domain and ATPase domain (Adhvaryu et al., 2016). It suggests that the C-terminal may be important for mediating the interactions with other proteins, especially those that are involved in circadian oscillators.

A constructed strain that introduced the wild-type *prd*-1 gene driven by a strong promoter *ccg*-1 inserted into *his*-3 locus successfully rescued the mutant phenotype (Adhvaryu et al., 2016; Emerson et al., 2015). This strain shows the normal phenotype which indicates sufficient amount of PRD-1 protein can neutralize the effect of the *prd*-1 mutant.

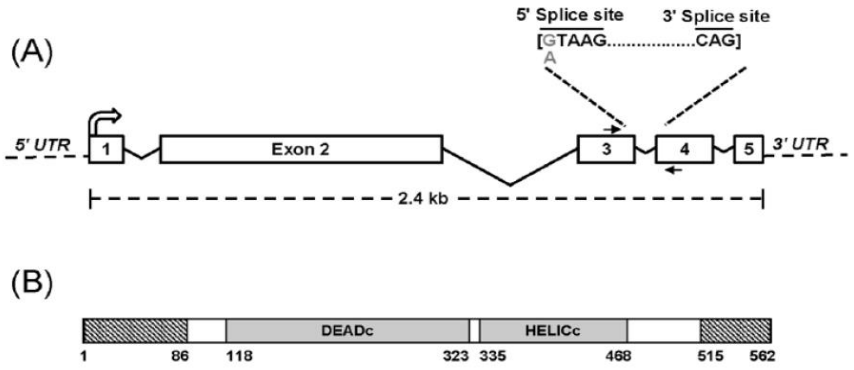

Figure 1.7 Organization of the *prd*-1 gene (A) and protein domains (B). (Adapted from Adhvaryu et al., 2016)

1.5 Objective of the thesis

Due to the tight association with the circadian rhythm, the *prd*-1 gene is hypothesized as an important component in the oscillatory mechanism. Despite the identification of the *prd*-1 gene encoding a DEAD-box RNA helicase, the function of it especially the one relating to the circadian clock is still ambiguous. My project is to study the function of the *prd*-1 gene in *Neurospora crassa*.

The *prd*-1 mutant has a slow-growth phenotype, and the knockout of this gene available from the FGSC is only a heterokaryon, suggesting that the *prd*-1 knockout is lethal. Nevertheless, attempts are still necessary to obtain a homokayotic *prd*-1 knockout strain, which is a valuable tool for understanding the function of *prd*-1.

Functions possessed by a gene are shown mainly through its expression product, therefore, studying the function of the PRD-1 protein will help us to expound the molecular mechanism of FLO in *Neurospora crassa*. Due to the unavailability of PRD-1 antibody, constructing a strain expressing FLAG-tagged PRD-1 is the prerequisite of experiments such as the examination of the rhythmicity of PRD-1 and Co-IP to find binding partners.

The phenotype of the *prd*-1 mutant is clock-relevant, but we know little about the *prd*-1 gene. If the *prd*-1 gene is clock-controlled, the PRD-1 protein and its mRNA should be rhythmic. Recently, it was published by another laboratory that the expression of PRD-1 and its mRNA is arrhythmic in wild type and light cannot induce changes of PRD-1 level (Emerson et al., 2015). In addition, it was proposed that different metabolic conditions may affect the expression of PRD-1, but abundance of PRD-1 was not assayed under different conditions. The research also did not test the expression of PRD-1 in *frq*-null strains, which is important to test if PRD-1 has a function associated with the FLO. I hypothesize that the expression of the *prd*-1 gene at mRNA or protein level may be different under different growth conditions or under the frq^{KO} background.

Although research showed that PRD-1 has no strong interactions with the positive and

negative elements in the FRQ-WCC oscillator (Emerson et al., 2015), whether the PRD-1 protein could bind to other proteins is still unclear. I presume that PRD-1 could interact with other proteins that have not been discovered to be correlated to the circadian clock yet. Whether the binding partners could affect the circadian rhythm needs deeper research. Immunoprecipitation followed by Mass Spectrometry to identify proteins interacting with PRD-1 should provide information about the function of PRD-1.

Last but not least, since the mutation causes the alteration of the sequence at C-terminal end, whether the C-terminus of PRD-1 is required for its function in the circadian clock needs to be determined. My hypothesis is that the function of the *prd*-1 gene would be dramatically altered or abolished if the C-terminus is deleted. The phenotype of the deleted strain could provide valuable clues about the function of the C-terminus of PRD-1.

Chapter 2 Essentiality of the *prd*-1 gene and its C-terminus

2.1 Introduction

The *prd*-1 gene has been identified as NCU07839 and abnormally spliced mRNA of *prd*-1 has been discovered by our lab. The mutated *prd*-1 gene resulted in the change of the phenotype. My presumption was that the *prd*-1 gene is a critical component in the circadian clock and the circadian rhythm is abolished without the *prd*-1 gene. Hence, obtaining an NCU07839^{KO} strain will be our first priority to understand its function.

However, in *Neurospora* even though it is haploid, one spore may possess more than one nuclei (Maheshwari, 1999). It is called a heterokaryon if a strain contains nuclei with different genotypes. To completely delete this gene in the cells, every copy of NCU07839 should be knocked out. In 2006, a consortium of labs constructed a library attempting to knock out every gene by a high through-put gene replacement method (Colot et al., 2006). In this library, we found that only a heterokaryotic NCU07839^{KO} strain is available, whose spores contain both wild type and knock-out nuclei. This implies that the deletion of the *prd*-1 gene results in the death of the cells. To ensure the essentiality of *prd*-1, we obtained this heterokaryon from FGSC and tried to isolate the NCU07839^{KO} nucleus.

Neurospora crassa produces relatively small numbers of uninucleate microconidia and very large numbers of multinucleate macroconidia in asexual vegetative life cycle. The environmental factors such as high humidity, low nutrition concentration, temperature and supplementary chemicals favor the formation of microconidia (Maheshwari, 1999). In practice, the microconidia preparation has been applied to obtain homokaryotic transformants for many years. Therefore, I planned to harvest microconidia to purify the *prd*-1^{KO} heterokaryon.

The point mutation in the *prd*-1 mutant causes alternative splicing at the 3'end of the mRNA, and the incorrectly spliced mRNAs could be translated to truncated proteins or

proteins with incorrect amino acid sequences at the C-terminus (Adhvaryu et al., 2016). The structural metamorphosis that may be caused by the mutated amino acid sequence may result in disfunction or a neomorph. I hypothesized that although the helicase domain of PRD-1 protein may be essential for survival, it may be the C-terminus of PRD-1 that makes a difference to the circadian rhythm. To verify this assumption, I planned to construct a strain that can only express the truncated PRD-1 protein whose C-terminus has been deleted. Therefore, I decided to do a gene replacement to knock a C-terminus deleted *prd*-1-FLAG cassette (*prd*-1ΔC-flag) into the genome and compare the phenotype with wildtype and the *prd*-1 mutant. In case the C-terminal deletion of *prd*-1 is lethal, I also planned to knock in a wild type *prd*-1 with FLAG as the control.

Two main pathways have been discovered in DNA repair that depend on DNA sequence homology: homologous recombination (HR) and nonhomologous end-joining (NHEJ). Homologous recombination is the most commonly applied and efficient method of gene replacement. HR occurs rarely in the wild-type *Neurospora crassa*. In 2004, the mutants named Δ*mus*-51 and Δ*mus*-52 were engineered to reduce the nonhomologous end-joining (Ninomiya et al., 2004). Vegetative growth, conidiation, and ascospore production were normal in homozygous crosses. The recombination of exogenous DNA into the genome is very high in those two strains, compared to 10 to 30% for the wild type (Ninomiya et al., 2004). After transformation, the *mus*-mutation needs to be removed to eliminate unknown effects. The *prd*-1 gene and *mus*-52 gene are localized in the same linkage group which cannot be efficiently segregated by crosses. Therefore, I used Δ*mus*-51 for the knock-in work.

The cutting-edge CRISPR/Cas9 technology has been proved to be effective for efficient gene editing in *Neurospora crassa* as well as other various organisms (DiCarlo et al., 2013; Fuller et al., 2015; Matsu-Ura et al., 2015; Tsarmpopoulos et al., 2016). Three plasmids with Cas9, guide RNA (gRNA) expression cassette, and knock-in cassette are transformed into the cell simultaneously. The Cas9 endonuclease can create a double-strand break guided by

the RNA targeting the desired region. The DNA repair pathways then are triggered and HR will occur with the presence of the knock-in DNA cassette containing homologous genomic sequence. The efficiency of this method has been demonstrated to be competitive to the method above which is accomplished by Δ*mus*-51/52 strains (Matsu-Ura et al., 2015). The advantage of the CRISPR gene editing method is that the transformation can be achieved in any recipient and the strain can be immediately used after transformation without the requirement of crossing. Hence, I also planned to introduce this method for the knock-in project.

The knock-in DNA cassette consists of at least four units: upstream homologous region (5' flank), designed sequence of replacement, selection marker and downstream homologous region (3' flank). To obtain a plasmid vector carrying this cassette, at least 5 restriction enzymes are required for the construction. It is reported that assembly PCR (overlapping PCR) could produce DNA fragments with complex content from hundreds of base pairs to 20 kb long (Bryksin and Matsumura, 2010; Shevchuk et al., 2004; Xiong et al., 2004; Yang et al., 2012). I planned to prepare the DNA segments in this way.

For the C-terminal deletion knock-in cassette, the upstream homologous region was designed as 1500 bp ending at the site of the mutation of the *prd*-1 gene. For the wild-type knock-in cassette, the upstream homologous region was designed as 1500 bp sequence before the end of the coding sequence. 10xGly, 3xFLAG and two stop codons were added thereafter to comprise the open reading frame. Antisense hygromycin resistance gene (*hph*) was inserted as the selection marker. The downstream homologous region was 1500 bp downstream of the *prd*-1 gene (Figure 7.1a). The whole knock-in DNA cassette was combined with a vector not homologous with the genome of *Neurospora*.

2.2 Materials and Methods

2.2.1 Strains

All the strains from lab stock will be identified using their stock number and simplified name. The characteristics of strains are displayed in parenthesis. The entire genotype of each strain is specified in Appendix A. #26 (*bd csp*-1 *chol*-1) was considered as wild type and a recipient of transformation. #567 (Δ*mus*-51, *his*-3) was also a recipient of transformation. The #518 strain to produce microconidia for fluorescence microscopy was obtained from the lab stock, a heterokaryon expressing RFP-VAM-3 and NCU05950-GFP. The *prd*-1^{KO} heterokaryotic strain was obtained from FGSC (FGSC#15506).

2.2.2 Microconidia purification

Methods were modified from the article (Ebbole, D., and M.S. Sachs, 1990). IAA-SC medium [0.1 X SC medium (Appendix B), 0.5% sucrose, 2% agar, 1 mM Na-iodoacetate] was added into slanted test tubes. Macroconidia were inoculated onto the medium and incubated at room temperature for 7-12 days. Microconidia were washed off with water and filtered through Millipore Durapore Millex 5 μm filters (Millipore). The numbers of microconidia were counted using hemocytometer. The microconidia suspension was mixed with sorbose plating medium [0.1% fructose, 0.1 % glucose, 2 % sorbose, 1X Vogel's salt (Appendix B), 2% Agar,] and poured into 100mm Petri plates. Colonies grown on sorbose plates were transferred to 2% glucose Vogel's agar medium for further tests. 200 μM hygromycin B was added into each medium when necessary.

To harvest the microconidia of the transformants, 20ml IAA-SC medium (0.1 X SC medium, 0.5% sucrose, 2% agar, 1 mM Na-iodoacetate) was poured in 100mm Petri plates. A sterile circular cellophane piece which is slightly larger than the plate was laid onto the medium. Spores were inoculated in the hole pierced at the centre of the cellophane. Plates were incubated upside down in a sealed box with humid atmosphere at room temperature for

7-12 days. All the mycelia and spores outside of agar were cleared up and the cellophane was peeled off before substituting a new lid. The plates were incubated at room temperature for another day and the microconidia were washed off from the agar surface with 2ml water. Diluted microconidia suspension was mixed with sorbose plating medium and poured into 100mm Petri dishes for colony growing.

2.2.3 Race tube assay

The growth medium was Vogel's minimal medium (Appendix B) with 0.5% maltose, 0.01% L-Arginine and 2% agar. Choline was added at 100 μM when indicated. Both medium and 30 cm glass tubes with cotton plugs (race tubes) were autoclaved at 121°C for 30 minutes. 6 mL medium was transferred into each race tube before solidification. Spores were inoculated on one side of the medium. The race tubes were placed in constant light (LL) at 30°C for one day and then transferred to constant darkness (DD) at 22°C. The growth front was marked every day under red safelight and the growth rate and period were calculated as previously described (Lakin-Thomas, 1998).

2.2.4 Spore PCR

Spore PCR was carried out using Terra™ PCR Direct Polymerase (Takara Bio Inc.). PCR conditions were set as recommended by the manufacturer.

To test the genotype of each microconidium from the *prd*-1^{KO} strain, primers targeting the knockout region (rc 5r prd-1KO and rc 3f prd-1KO) were used. The primers (NCU07839-2661-F and FLAG-R) were used to check the deletion region and FLAG. The primers (Primer-F11 and DownstreamNCU07839-R1) were used to assay whether the knock-in strains were homokaryons. Annealing temperature and extension duration varied with pairs of primers. The names of primers used for amplification will be annotated and the sequences of primers are listed in Appendix C.

2.2.5 DNA agarose gel electrophoresis

Agarose was dissolved in TAE buffer (40mM Tris, 20mM acetic acid, and 1mM EDTA) by microwaving. The agarose gel was mixed with 0.005% RedSafe™ Nucleic Acid Staining Solution (iNtRON Biotechnology) and poured into the cast with combs. DNA was loaded into the wells and electrophoresis was run in TAE buffer.

2.2.6 Regular PCR

DNA amplified from genomic DNA of *Neurospora* or from plasmid DNA was obtained by using Q5® High-Fidelity DNA Polymerase (NEB). PCR conditions were set as recommended by the manufacturer. Annealing temperature and extension duration varied with pairs of primers. The names of primers used for amplification will be annotated and the sequences of primers are listed in Appendix C.

2.2.7 Assembly PCR

Primers were designed to introduce overlaps to the ends of each DNA fragment. The overlaps of DNA fragments were about 50 bp long and shared similar Tm. After amplifying DNA fragments with overlaps by regular PCR, 50ng purified candidates as the templates were added into PCR reaction systems containing 0.5μM of the outer primers. Other components in the PCR reaction systems were added following the protocol of Q5® High-Fidelity DNA Polymerase. PCR conditions were set as recommended by the manufacturer. Annealing temperature was set as 60°C which was the designed Tm for the primers. The extension duration varied with the length of expected DNA fragments. Agarose gel electrophoresis was conducted to analyze the PCR products.

2.2.8 Techniques related to molecular cloning

PCR clean-up and DNA gel purification were done with Gel/PCR DNA Fragments Kit (Geneaid). Restriction enzyme digestion, ligation and bacteria (NEB® 10-beta Competent *E. coli*) transformation were executed following the protocols from the manufacturer. High-Speed Plasmid Mini Kit and Midiprep Plasmid DNA Kit (Geneaid) were utilized for the

plasmid extraction. Recombinant plasmids were sent to Sanger DNA sequencing service (Bio Basic Inc.) for sequencing and the results were aligned with the *N. crassa* database (FungiDB, http://fungidb.org/fungidb) in A Plasmid Editor (ApE, by M. Wayne Davis).

2.2.9 Transformation of *Neurospora*

The spores of transformation recipients were inoculated on 3ml Vogel's agar medium with 2% glucose in the slanted tubes and incubated for one week at room temperature. The contents in the slanted test tubes were transferred on 100ml Vogel's agar medium with 2% glucose in 1L flasks. 0.5mg/ml histidine was added in the media if necessary. The tissue in the flasks was scraped off and transferred into 50ml conical tubes. The spores were washed off with water by vortex. The spore suspension was filtered through four-layer cheesecloth and spin down at 3,000g at room temperature. The pellet was washed with water and spin down three more times. The pellet of spores was resuspended in an equal volume of 1M sorbitol. The resuspension of spores was stored at -80°C.

About 1 x 10^8 conidia was mixed with 10µg linearized plasmid DNA in 50 µl 1M sorbitol and incubated on ice for at least 15 min. The mixture was transferred into ice-cooled 2 mm electroporation cuvette and electroporated with the following parameters: voltage gradient: 7.5 kV/cm (1.5 kV in a 0.2 cm cuvette), capacitance: 25 µF, resistance: 600 ohms, using Gene Pulser® II Electroporation System (Bio-Rad). The transformed spores were resuspended with 1ml recovery medium (1x Vogel's salts, 1M sorbitol, 2% sorbose, 0.5% fructose, 0.5% glucose) immediately after the electroporation and incubated at room temperature with gentle rotation for 1hour. Transformed spores then were mixed with sorbose plating medium containing 1M sorbitol and poured into 100mm Petri dishes for colony growing. Other supplements (choline) were added into all types of medium when necessary.

2.2.10 Crossing

The female (mat A) was grown on 3ml synthetic crossing (SC) agar medium with supplements needed (choline or histidine). The male (mat a) was grown on Vogel's agar

medium with 2% glucose and supplements needed. After 5-7 days, the spores of the male were spread on the medium of the female and incubated at room temperature for 3-4 weeks. Individual ascospores were picked or separated into the Vogel's agar medium with 2% glucose and supplements needed for further tests.

Genotypes of multiple mutant strains were identified by various criteria: *ras*^{bd} by slower growth and banding phenotype, *csp-1* by failure of conidial separation, *chol-1* by slow growth without choline supplementation, *frq*^{10} by arrhythmic conidiation on high choline and presence of banding rhythms on zero choline in *chol-1* strains, and gene deletions by hygromycin resistance or by spore PCR with gene-specific primers to confirm gene replacement (Adhvaryu et al., 2016).

2.3 Results

A knockout strain would be a very useful tool for studying the function of PRD-1. However, only a heterokaryon knockout strain of the *prd*-1 gene is available from the FGSC, suggesting that *prd*-1 is an essential gene. After we received that knockout strain from FGSC, we tried to obtain a homokaryon strain by microspore purification.

2.3.1 Microconidia purification is effective to select homokaryons

The effectiveness of microconidia purification was my first concern. I tested the method by using a heterokaryon from our lab that has two types of nuclei: one carries RFP and the other carries GFP (Figure 2.1). The nuclei with GFP are a knockout of NCU05950 which is replaced by the *hph* (hygromycin resistant) gene. The nuclei with RFP do not have the *hph* gene. After harvesting microconidia, I plated 200 on the plates with hygromycin and 200 spores on plates without hygromycin. Under a fluorescence microscope I found that 139 colonies only expressing GFP could grow on the hygromycin plates, even though 3 heterokaryons expressing both RFP and GFP were found. On the plates without hygromycin, I found 76 colonies that only express GFP, 27 colonies that only express RFP and 28 colonies that are suspicious of being heterokaryons (Figure 2.1). These results demonstrate that microconidia purification can successfully generate colonies with a single type of nuclei.

2.3.2 The *prd*-1 gene is essential for *Neurospora crassa*

I next spread microconidia that were harvested from the *prd*-1 knockout heterokaryon strain. Based on the information from FGSC, the *hph* gene was introduced into the genome to knock out the *prd*-1 gene. As expected, only 2 colonies grew on the hygromycin plates and hundreds of colonies grew on the plates without hygromycin (Figure 2.1). To test their genotype, I ran spore PCR using the primers from both flanks of the transcript of the *prd*-1 gene (refer to 2.2.4). The DNA gel showed that the heterokaryotic *prd*-1 knockout strain obtained from FGSC has two sorts of nuclei and colonies from microconidia have only one

type of nuclei. For the colonies selected by hygromycin, a very faint band of wild-type *prd*-1 gene can be observed, indicating that they may still be heterokaryons with only a few wild-type nuclei present under the drug selective pressure (Figure 2.2). To further check whether they are homokaryons, I grew them on race tubes without hygromycin and did spore PCR of spores from both ends of the tubes. Spore PCR showed that the number of wild-type nuclei increased and both colonies are heterokaryons (Figure 2.3). The growth rates of those two colonies were same as wild-type on the race tubes.

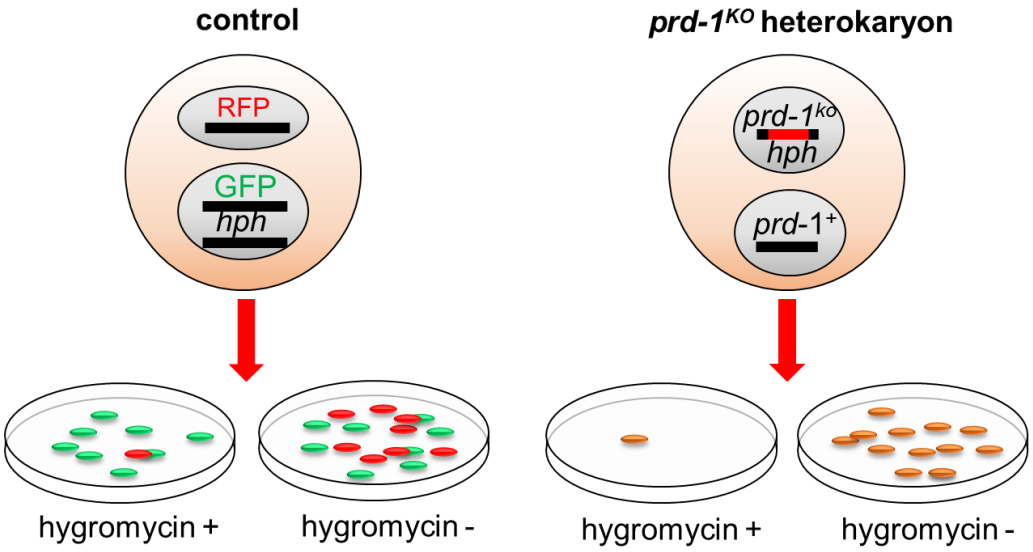

Figure 2.1 Schematic results of sorbose plates with/without hygromycin selection. The single nucleus is isolated from heterokaryons by microconidia purification. Normally one microconidium forms one colony on the sorbose plate but two microconidia may form one colony when they are too close.

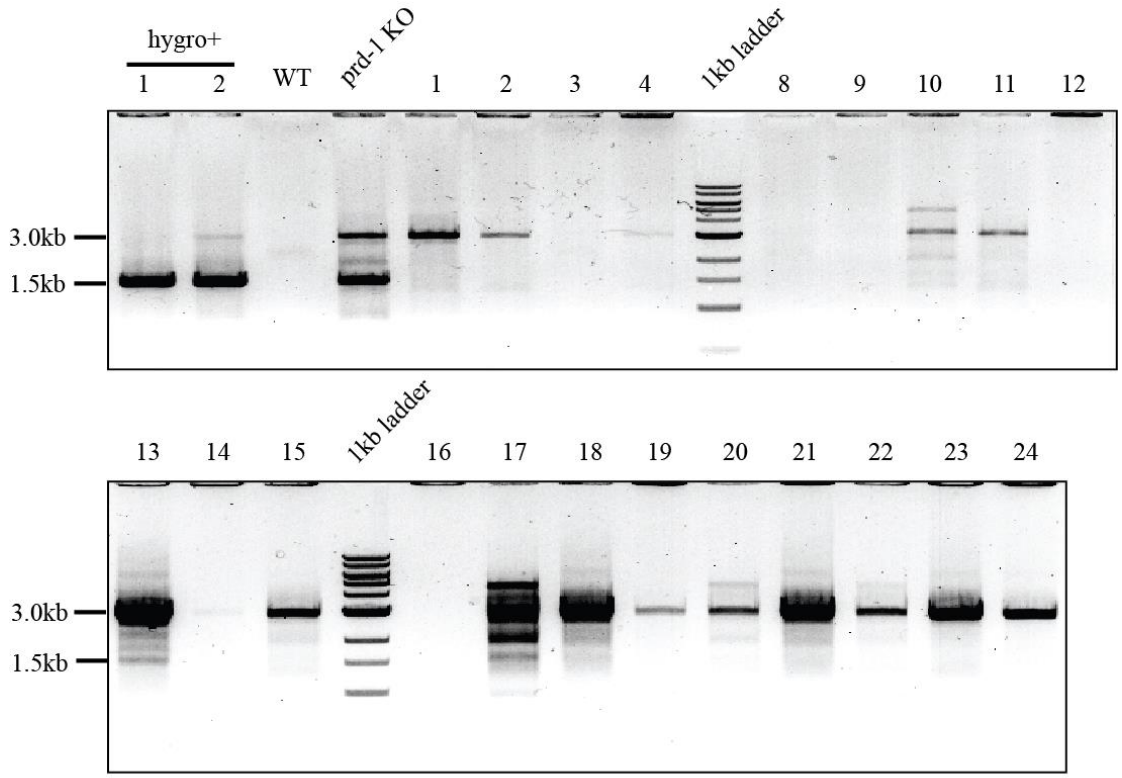

Figure 2.2 Result of *prd*-1^{KO} spore PCR after microconidia purification. In the knockout strain, *prd*-1 is replaced by *hph* (hygromycin resistant gene). No.1-24 are colonies grown on the sorbose plates without hygromycin B. Hygro^{+} #1, 2 are colonies selected by hygromycin B. Target bands should be 3kb for *prd-1* gene and 1.5kb for *hph* gene.

Figure 2.3 Result of spore PCR from both ends of race tube. #1, 2 are colonies selected by

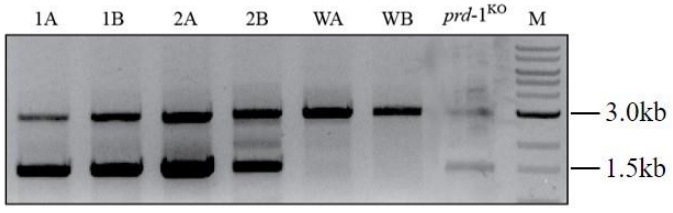

hygromycin B after microspore purification. A represents spores that are from the beginning of race tube and B represents spores from the end of race tube. W means wild-type strain (#259 Oak Ridge). M represents 1kb ladder (GeneDirex).

2.3.3 The failure to construct knock-in DNA cassette by assembly PCR

I planned to amplify the DNA cassette by assembly PCR and then ligate it into a blunt-end vector. I first attempted to assemble the four units in one reaction (Figure 2.4a). I also failed to assemble DNA fragments two by two. The assembly PCR did not work with these long DNA fragments when I used a gradient of annealing temperature. Then I designed primers to dissect every large piece into ~500bp small segments, and then assembled them all at once or two by two (Figure 2.4b). Frustratingly, I could ligate two 500bp DNA by overlapping PCR, but I failed to use 1kb segments to ligate anymore (Figure 2.4 c, d). In short, assembly PCR could not ligate large fragments (>1kb) even though the PCR conditions were optimized.

2.3.4 The construction of knock-in DNA cassette and guide RNA expression plasmid by restriction endonucleases

I turned to design the construction with restriction enzymes due to the failure of assembly PCR. Considering the low efficiency of ligating five pieces at once, I planned to build two subclones first and then ligate two DNA fragments together which are amplified from the subclones (Figure 2.5). The subclone 1 carried the 5'flank and the sequence of replacement (pBM61-*ccg*-*prd*-1ΔC-FLAG; pBM61-*ccg*-*prd*-1-FLAG was made in Chapter 3), and subclone 2 contains the selection marker and the 3'flank (pJET-*hph*-3'flank). The C-terminus deleted *prd*-1 gene as 5'flank was amplified by PCR. The digested PCR product was ligated into the plasmid (pBM61-*ccg*-*prd*-1-FLAG) from lab stock. The subclone 2 was made by inserting *hph* and 3'flank into the backbone of a plasmid (pJET-native-*prd*-1) from lab stock. The *hph* gene is amplified from pCSN44 which was obtained from FGSC. For the final construct (pJET-*prd*-1ΔC-FLAG-KI, pJET-*prd*-1-FLAG-KI), SbfI and XbaI were introduced to the ends of the 5'flank+Gly-FLAG and the subclone 2. The digested purified DNA pieces

were ligated accordingly and transformed into bacteria. The recombinants were confirmed by the size via digestion (Figure 2.6 a, b, c, d) and by the sequencing results.

Plasmids expressing Cas9 and gRNA were bought from Addgene. The gRNA sequence needed to be substituted by a sequence in *prd*-1. 20bp sequence was chosen as guide RNA which is in the 3' UTR close to the stop codon in the *prd*-1 gene and it showed high specificity compared to the whole genome. The substitution sequence was synthesized by Bio Basic Inc. and inserted into the gRNA expression plasmid by NheI and KpnI. The recombinants were confirmed by the size via digestion (Figure 2.6e) and by the sequencing results.

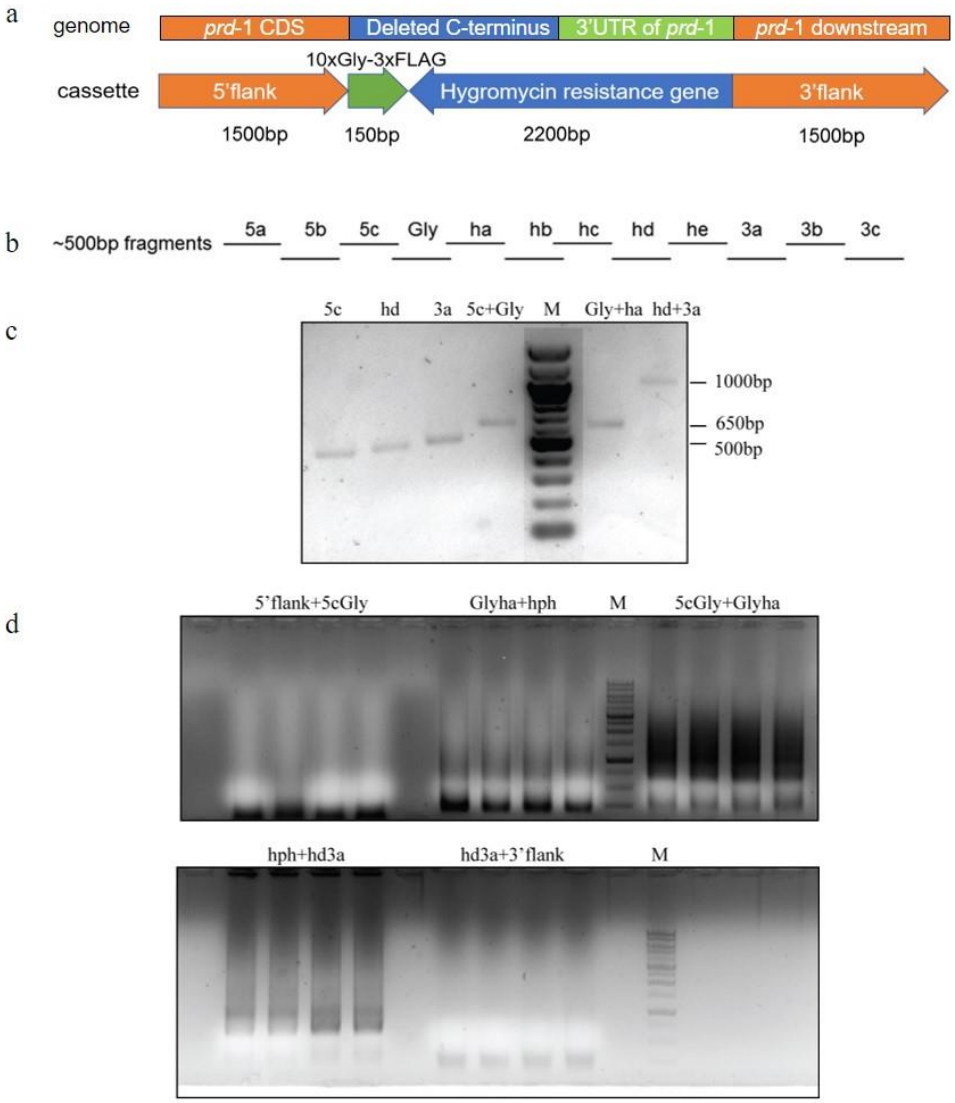

Figure 2.4 The construction of knock-in DNA cassette by assembly PCR. a) The design of knock-in cassette. Primers for amplifying each fragment: NCU07839-1662-F & NCU07839-3161+Gly-R, NCU07839-3161+Gly-F & Flag+TtrpC-R, Flag+TtrpC-F & PtrpC+downstreamNCU07839-R, PtrpC+downstreamNCU07839-F & Downstream NCU07839-R, from left to right, respectively. b) The design of small fragments for assembly PCR. Primers for amplifying each fragment from left to right are listed in the Table 7.1. c) Assembly PCR results of small fragment assembly (<500bp). M: 100bp DNA ladder d). Assembly PCR of large fragment assembly (>500bp). M: 1kb DNA ladder.

Table 2.1 Primers used for the amplification of fragments in Figure 2.4b

DNA fragment	Forward Primer	Reverse Primer
5'flank a	NCU07839-1600-F	NCU07839-2259-R
5'flank b	NCU07839-2181-F	NCU07839-2733-R
5'flank c	NCU07839-2661-F	NCU07839-3161+Gly-R
10xGly-3xFLAG	NCU07839-3161+Gly-F	Flag+T trpC-R
hph a	Flag+T trpC-F	T trpC-R1
hph b	T trpC- F1	Hph-R1
hph c	Hph-F1	Hph-R2
hph d	Hph-F2	Hph-R3
hph e	Hph-F3	PtrpC+downstreamNCU07839-R
3'flank a	PtrpC+downstreamNCU07839-F	Downstream NCU07839-R1
3'flank b	Downstream NCU07839-F1	Downstream NCU07839-R2
3'flank c	Downstream NCU07839-F2	Downstream NCU07839-R3

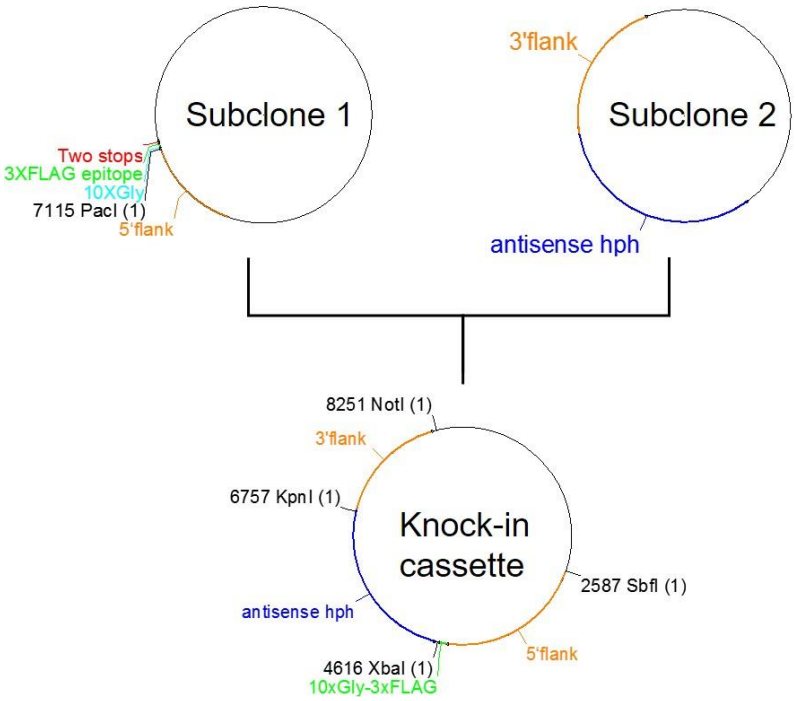

Figure. 2.5 Schematic graph of the construction of plasmids carrying knock-in cassette.

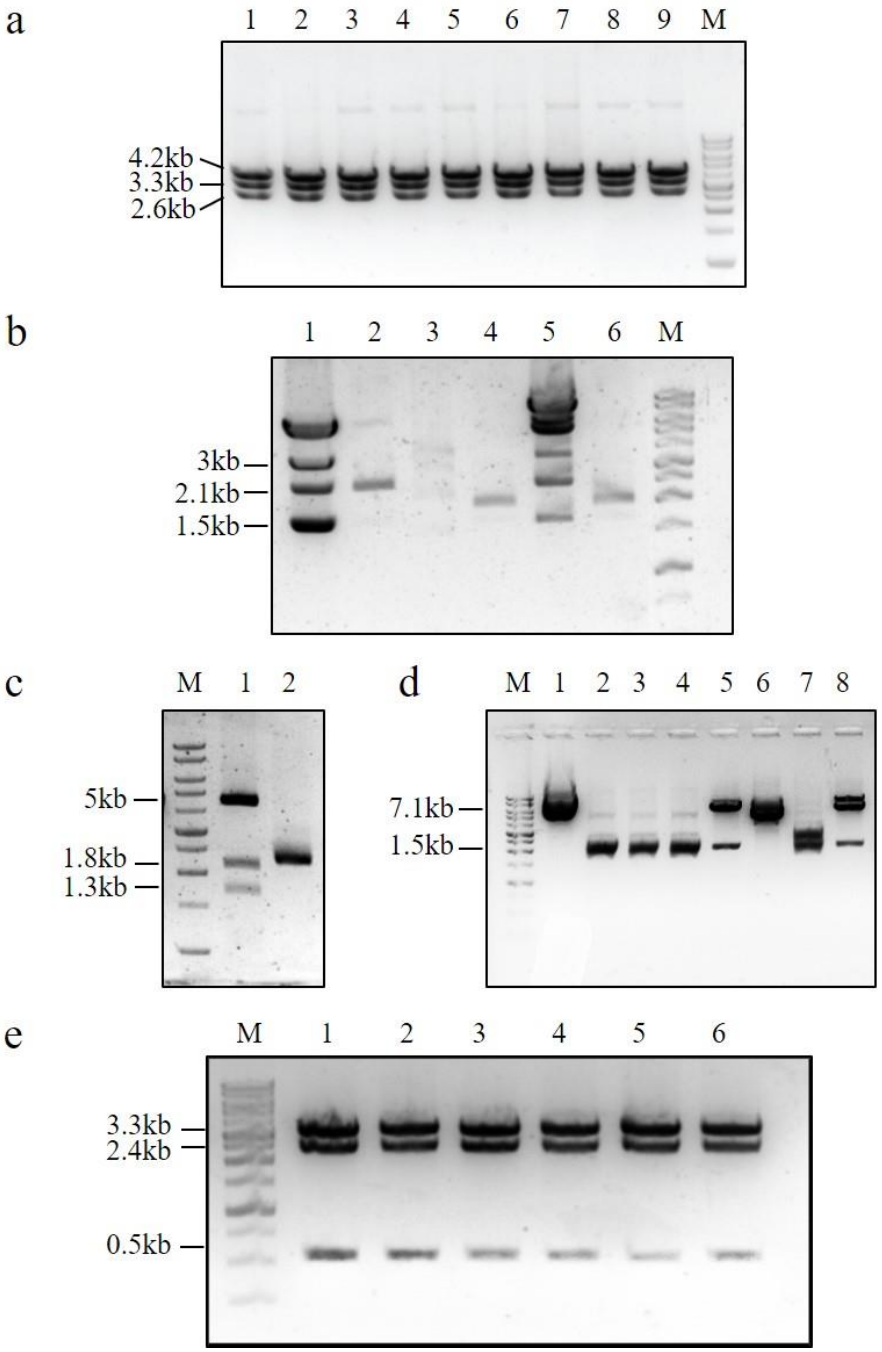

Figure 2.6 DNA gel pictures of digested plasmids. Expected bands are annotated beside each picture. a) pBM61-*ccg-prd*-1ΔC-FLAG. b) pJET-*hph*-3'flank. c). pJET- *prd*-1ΔC-FLAG-KI. d) pJET- *prd*-1-FLAG-KI. e) gRNA expression plasmid.

2.3.5 The construction of knock-in transformants

2.3.5.1 Knock-in of Δ*mus*-51 strain

15μg of plasmid carrying the knock-in DNA cassette was linearized and electroporated into the Δ*mus*-51 strain (#567). Colonies grown on sorbose plating medium with hygromycin were transferred to individual test tubes with 1ml 2% glucose Vogel's agar medium. Spore PCR was done to check the deleted region with primers (NCU07839-2661-F and FLAG-R). The gel picture showed that the designed sequence was successfully integrated onto the genome (Figure 2.7a).

2.3.5.2 Knock-in of wild type strain by CRISPR gene editing

Once all the plasmids were obtained, three plasmids were co-transformed into the macrospores of a wild type (#26) at the same time. One plasmid expresses the guide RNA, one expresses the Cas9 protein to cleave the *prd*-1 gene, and the knock-in plasmid would be integrated into the genome via the HR pathway. Colonies grown on the sorbose medium with hygromycin were transferred to individual test tubes with 1ml 2% glucose Vogel's agar medium. Spore PCRs were done to check the deleted region and to check whether the colonies were heterokaryons (Primer-F11 and DownstreamNCU07839-R1). The gel picture showed that the designed sequence was successfully integrated onto the genome and that all the colonies were heterokaryons (Figure 2.7b).

2.3.6 The essentiality of C-terminus of the *prd*-1 gene

To observe the phenotype of the *prd*-1ΔC-flag strain, the mutation Δ*mus*-51 needed to be eliminated to minimize the unknown effects and the untransformed nuclei carrying the wild type *prd*-1 gene needed to be removed to prevent the rescue of phenotype. Meanwhile, the *bd* mutation needed to be introduced to show overt circadian rhythms. Therefore, I crossed the transformants with #26 to select the homokaryotic *bd chol*-1 *prd*-1ΔC-flag strain.

Progenies were isolated on sorbose plating medium and the numbers of colonies on both media with/without hygromycin selection were counted (Figure 2.8a). Genetic analysis

showed the possible proportion of the ascospores that could grow on the media when at least one out of 2 or 3 nuclei was transformed in each conidium. The results of the control (*prd*-1^{+}-flag knock-in) corresponded to the expectation of 'viable'.

However, the results of the C-terminal deletion strains met the expectation of 'lethal'. Spore PCR was used to examine the colonies grown on the hygromycin medium. Consistent with the expectation, most of the progenies from the control transformation were homokaryons; all the progenies from the C-terminus deleted *prd*-1 strains were heterokaryons suggesting that the spores could not survive with only the truncated *prd*-1 gene (Figure 2.8b).

The homokaryotic *prd*-1^{+}-flag knock-in strains were grown on race tubes and the phenotypes were close to the wild type (Figure 2.9). These data validated my design of the knock-in cassette and the methods utilized.

For the transformants obtained using CRISPR gene editing, they underwent both microconidia purification and a cross to collect homokaryons. I failed to select homokaryons of either the control or deletion strains from microconidia by PCR. The numbers of colonies that grew on the media with/without hygromycin selection were corresponding to our theoretical genetic analysis and the results confirmed that the *prd*-1^{+}-flag knock-in strains were viable and the *prd*-1ΔC-flag knock-in is lethal (Figure 2.10a). However, a homokaryon of the control transformants could not be found by spore PCR regardless that the C-terminus deleted *prd*-1 strains were all heterokaryons (Figure 2.10b). These results demonstrated that the method of CRISPR gene editing needed to be optimized.

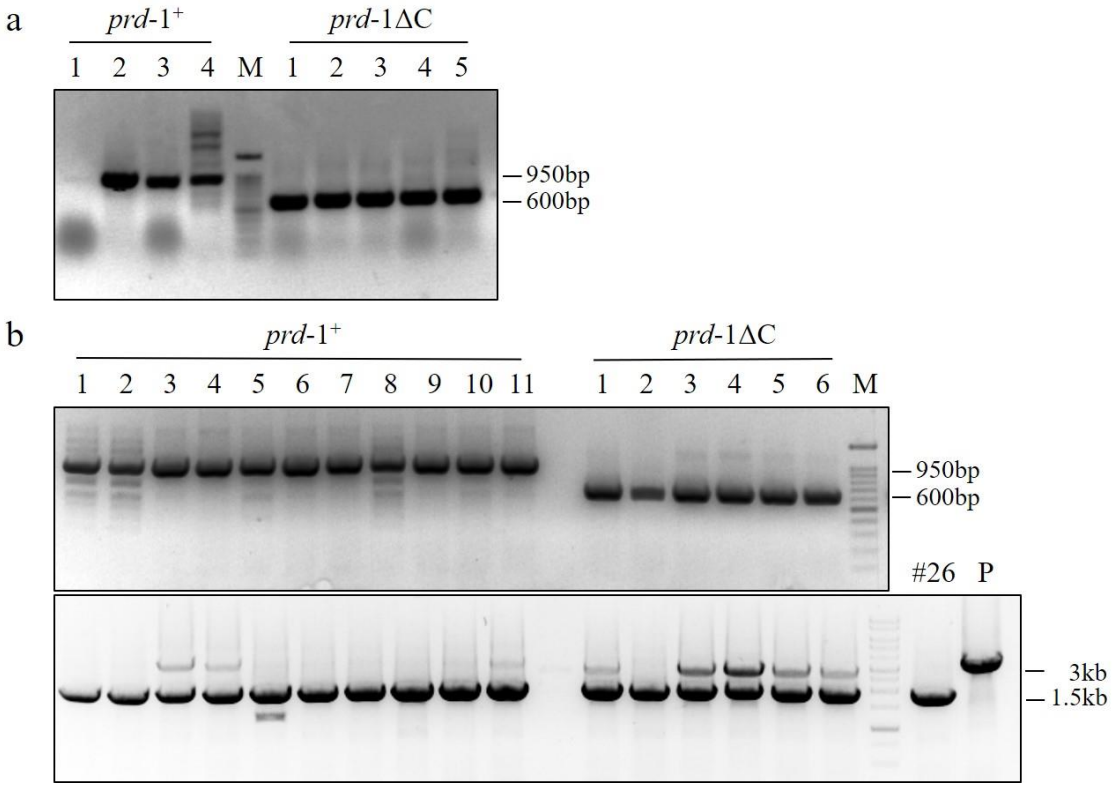

Figure 2.7 Spore PCR of the knock-in transformants. Expected bands are labeled beside each picture. a) The DNA was knocked into #567. M: 100bp ladder. b) The DNA was knocked into #26 triggered by CRISPR gene editing. The deletion region and the FLAG tag check (upper), deleted bands is 600bp; The heterokaryon check (lower), the replaced genomic sequence should be about 3kb. M: DNA ladder. P: pJET- *prd*-1-FLAG-KI.

a

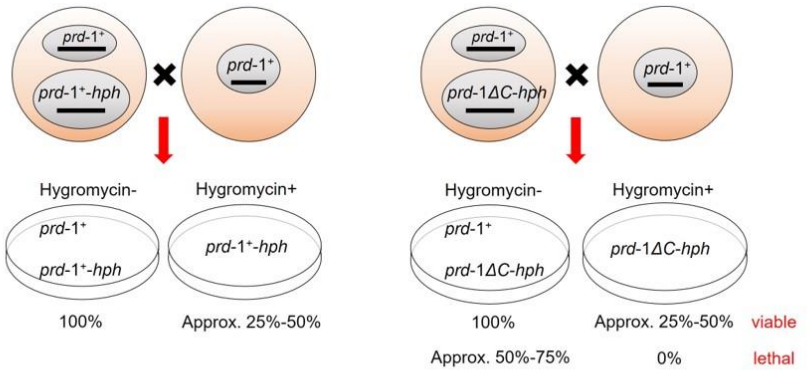

	hygromycin-	hygromycin+	ratio
Cross 1	430	271	0.63
Cross 2	386	222	0.57
Cross 3	305	128	0.42
Total	1121	621	0.55

	hygromycin-	hygromycin+	ratio
Cross 1	144	0	0
Cross 2	497	9*	0.02
Cross 3	403	12*	0.03
Total	1044	21*	0.02

b

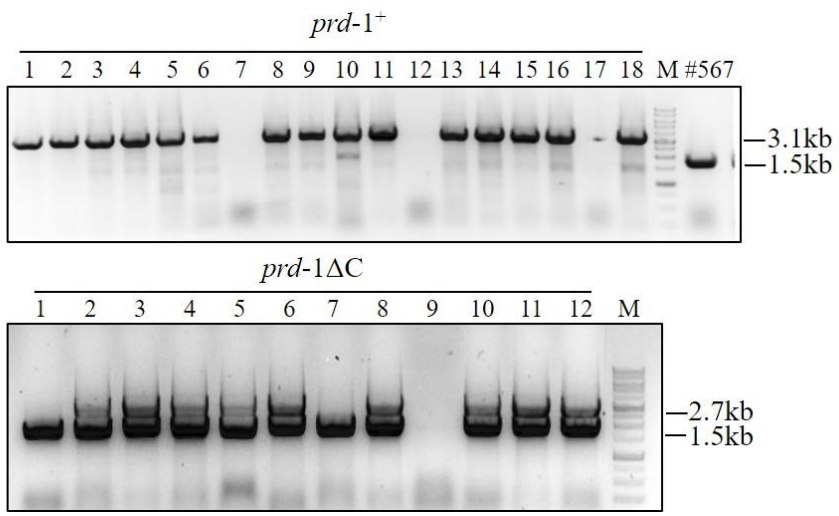

Figure 2.8 The purification of homokaryotic knock-in transformants of #567 (Δ*mus*-51). a) The diagram of the cross to #26. The proportions of the ascospores that could germinate on each medium in theory are shown. The numbers of colonies on the plates are shown. *: the colonies were identified as heterokaryons. b) Spore PCR to check the heterokaryons. Expected bands are labeled. Transformed *prd*-1^{+}: 3.1kb; Untransformed *prd*-1^{+}: 1.5kb; Transformed *prd*-1ΔC: 2.7kb. M: 1kb ladder.

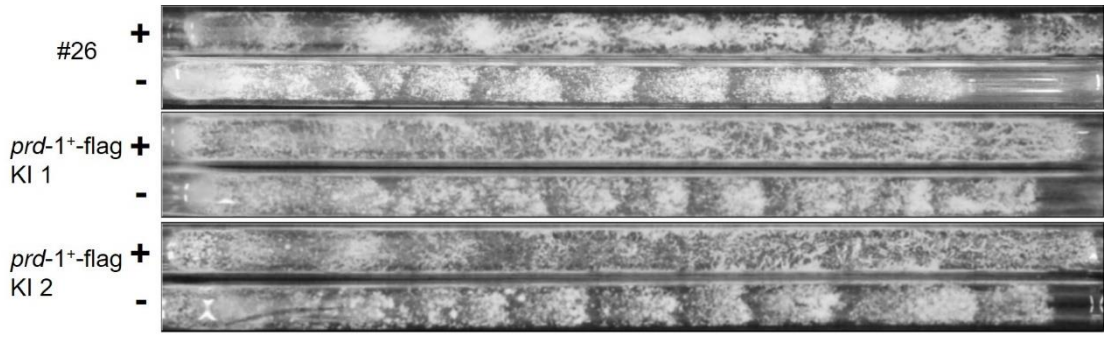

Figure 2.9 The race tubes of selected *prd*-1^{+}-flag homokaryons. The strains were incubated on Vogel's agar medium with 0.5% maltose, 0.17% L-arginine and 100μM choline (+) or without choline (-) at 22°C, DD.

a

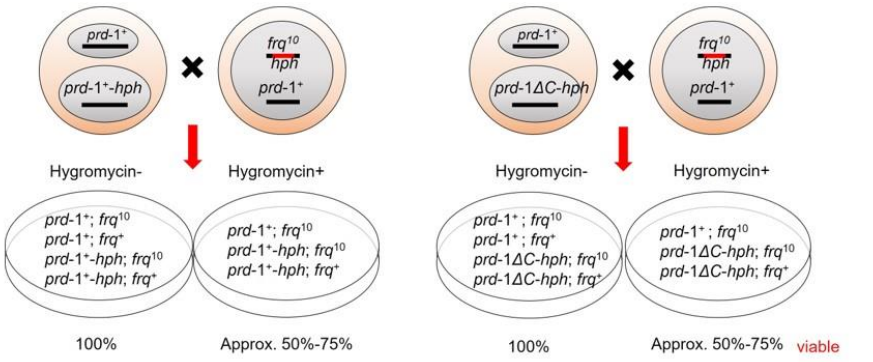

	hygromycin-	hygromycin+	ratio
Cross 1	85	68	0.8
Cross 2	414	288	0.7
Cross 3	304	240	0.8
Total	803	596	0.74

	hygromycin-	hygromycin+	ratio
Cross 1	613	317	0.51
Cross 2	483	262	0.54
Cross 3	243	146	0.60
Total	1339	725	0.54

b

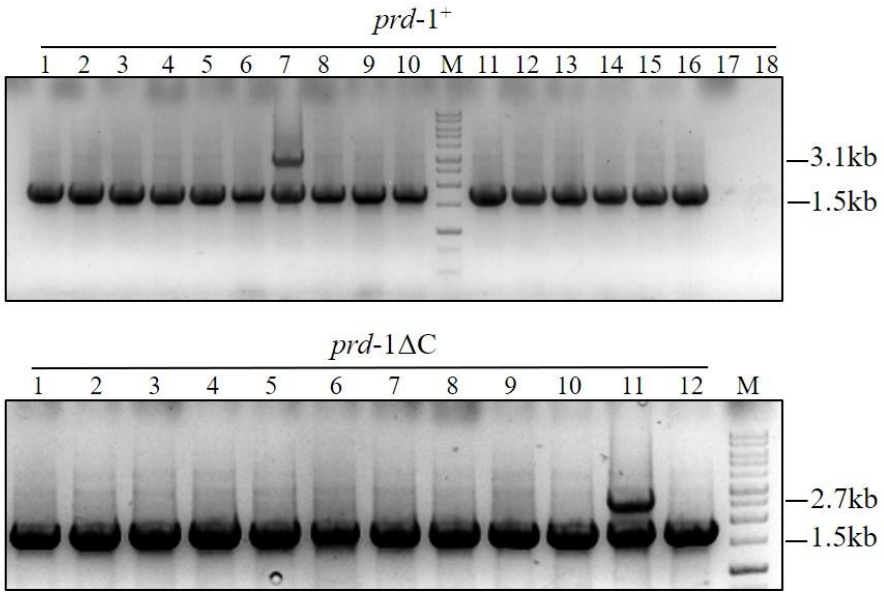

Figure 2.10 The purification of homokaryotic knock-in transformants of #26 triggered by CRISPR gene editing. a) The diagram of the cross to #149 (*bd frq*^{10} *his*-3, mat A). The proportions of the ascospores that could germinate on each medium in theory are shown. The numbers of colonies on the plates are shown. b) Spore PCR to check the heterokaryons. Expected bands are labeled. Transformed *prd*-1^{+}: 3.1kb; Untransformed *prd*-1^{+}: 1.5kb; Transformed *prd*-1ΔC: 2.7kb. M: 1kb ladder.

2.4 Conclusion

The effective separation of GFP/RFP expressing nuclei as the control illustrated the validity of microconidia purification. Although heterokaryons were found on the plates, it is possibly due to some macrospores getting through the filter or incidences that two microconidia may merge to one colony by chance.

The attempt to isolate *prd*-1^{KO} homokaryons failed, showing that replacing *prd*-1 with *hph* causes the death of *Neurospora*. On the hygromycin plates, since the growth of microconidia is inhibited rather than killed, the wild-type microconidia will germinate. If a *prd*-1^{KO} microconidium is close enough to the wild-type one, they will merge and share the functional *prd*-1 and *hph* gene. This heterokaryon subsequently is able to grow on the hygromycin plates. The heterokaryotic genotype of the colonies from hygromycin plates confirmed it. Surprisingly, from the results of spore PCR, in selected heterokaryons, wild-type nuclei compose an extremely small proportion of total nuclei, which still is enough to sustain the viability of the microconidia. In conclusion, *prd*-1 is an essential gene of *Neurospora crassa*. A small amount of PRD-1 protein may be sufficient for its function, or perhaps the expression of *prd*-1 is highly effective to produce sufficient amount of PRD-1 from a few copies of the gene.

In this chapter, the designed DNA sequence was knocked into the genome successfully and heterokaryotic transformants were viable. Once I tried to isolate homokaryons, the C-terminal deletion of the *prd*-1 gene caused inviability but the wild-type *prd*-1 knock-in strains were acquired through crosses. As a conclusion, the C-terminus of the PRD-1 protein is indispensable for its normal function, but whether the normal function is associated with the circadian clock requires deeper investigation.

I also attempted to introduce assembly PCR and CRISPR gene editing methods to my experimental work to construct the knock-in DNA cassette and knock-in strains respectively, along with conventional methods that were applied to *Neurospora crassa* for many years.

The canonical methods worked perfectly whereas the new methods need further troubleshooting and optimization. The assembly PCR cannot give products when long DNA pieces were the unit of assembly. The CRISPR gene editing successfully triggered the DNA repairing pathway and the knock-in cassette was integrated into the genome. However, the failure to purify the *prd*-1^{+}-flag knock-in strains implies that some off-target effects occurred during the DNA damaging and DNA repairing processes which might generate some lethal mutation or multiple copies of wild-type *prd*-1 gene in one nucleus since the NHEJ pathway is still functional in WT.

Chapter 3 Rhythmicity of the *prd*-1 gene

3.1 Introduction

The *prd*-1 gene has been considered as a component in the FLO to regulate the circadian rhythm based on the phenotype of the mutant. Typically, the key proteins such as FRQ, PER-1 and CRY controlling circadian clocks have a rhythmic expression level in a constant environment (Baker et al., 2012; Takahashi, 2017; Tataroglu and Emery, 2015). Conversely, if the expression level of PRD-1 is rhythmic, it is more probable that PRD-1 plays a direct role in regulating the circadian clock. To examine the expression level of a protein, a common method is by Western blotting with proteins extracted at different time points over two or three days (Baker et al., 2012; Cheng et al., 2005). A reliable antibody is required for the immunodetection. Since no antibody of PRD-1 is available, it is more practicable to tag the protein with an epitope (FLAG/GFP) for Western Blotting.

Moreover, studying the interactions between PRD-1 and other proteins will make an important contribution to understanding the function of PRD-1. The known function of the binding partners could give us clear guidance on discovering the function of PRD-1. Co-immunoprecipitation is a standard way to purify proteins that interact with proteins of interest (Cheng et al., 2005). Mass spectrometry will identify the pulled-down proteins. The Co-IP/MS experiment needs a solid binding between the protein complex and antibody on the beads. M2 Anti-FLAG Affinity Gel has been successfully applied for IP in many labs (Honda and Selker, 2009; Yang et al., 2006). Hence, constructing a strain expressing FLAG-tagged PRD-1 protein is very useful for studying the PRD-1 protein.

PRD-1 has been shown to be a nuclear protein (Adhvaryu et al., 2016). The N-terminus of PRD-1 is considered to include a nuclear localization signal (NLS) by DELTA-BLAST (Domain Enhanced Lookup Time Accelerated BLAST) in the NCBI website. Tagging the FLAG at N-terminus may block the transportation of the PRD-1 protein into the nuclei. The

C-terminus of PRD-1 may have a function since mutation of the C-terminus of PRD-1 results in the alteration of phenotype. Thus, a relatively smaller tag would probably cause less effect on the normal function of the protein. Tagging the FLAG at the C-terminus is extensively applied in many publications. Based on my assessment of the risks of linking the tag to either terminus, I decided to attach FLAG to the C-terminus of PRD-1.

Since *prd*-1 is an essential gene and a low amount of the *prd*-1 gene is sufficient for its function (Chapter 2), it is difficult to know whether the *prd*-1 gene has a strong promoter. To get clear results for Co-IP, higher expression is preferred. The common strong promoter we use in our lab is the *ccg*-1 promoter, which is demonstrated to be effective by previous work. The native promoter of the *prd*-1 gene is also required for determining whether the *prd*-1 gene is normally rhythmically expressed. Therefore, I planned to construct two strains expressing PRD-1-FLAG driven by either the *ccg*-1 promoter or the native promoter (*ccg*-*prd*-1-flag and native-*prd*-1-flag).

Inserting the expression cassette at the *his*-3 locus by the HR (homologous recombination) is the routine transformation used in *Neurospora* to express FLAG-tagged proteins (Emerson et al., 2015; Honda and Selker, 2009). The recipient carries a mutated *his*-3 gene in which a point mutation was found in the 3' coding sequence. The *his*-3 mutant requires exogenous histidine for growth. The expression cassette is comprised by three regions: the 5'flank, the insert sequence and the 3'flank. The 5'flank of the cassette is a wild-type *his*-3 gene with the 5' sequence deleted, and the 3'flank of the cassette is homologous to the downstream 3'flank of the *his*-3 gene. During the HR, the *his*-3 gene between the 5' and 3' flank will be replaced by the expression cassette and the function of the *his*-3 gene is repaired. Only the *his*-3^{-} spores whose *his*-3 gene is successfully repaired with exogenous plasmid DNA can grow without additional histidine. Owing to the lethal effect of *prd*-1^{KO}, I can only transform an expression cassette into the *his*-3 locus of the strains with *prd*-1^{+} or *prd*-1 mutant background. As a result, more than one copy of *prd*-1 is functioning, which

means that the phenotype of transformants may not be exactly the same as the wild type because of the possible influence caused by higher dosage of PRD-1. Therefore, I will choose transformants with the phenotype close to the wild type for subsequent experiments.

Rhythmic behavior is a reflection of the rhythmicity of molecular machinery. Since the *prd*-1 mutant has an altered phenotype, it is presumed that PRD-1 may regulate the circadian clock. Many proteins that are believed to control the circadian clock are rhythmically expressed in both protein level and mRNA level (Dunlap, 1999; Panda et al., 2002). Thus, the rhythmicity of the expression of the *prd*-1 gene may give some clues about whether it is directly involved in the molecular clock. Rhythmic expression is an important trait of the clock genes; however, a significant portion of total transcripts are also expressed circadian rhythmically (Reddy et al., 2006). The *prd*-1 gene may also be a clock-controlled gene which affects the output of the rhythms that are downstream of the molecular clock if the expression of *prd*-1 is rhythmic. In either way understanding the rhythmicity of the expression of *prd*-1 is very helpful to narrow down the range of its possible functions.

In 2015, Emerson et al published their work on examining the expression of *prd*-1 (Emerson et al., 2015). They traced the luciferase activity which is driven by the promoter of *prd*-1 and concluded that the promoter of *prd*-1 cannot produce a rhythmic expression of luciferase. They also collected samples every four hours over two days and detected the expression of PRD-1 tagged by V5. The Western blotting results showed no evidence that the PRD-1-V5 is rhythmically expressed. However, these results are not sufficient to demonstrate the expression of *prd*-1 is not rhythmic. There are two objections to their conclusions. The first point is that the *prd*-1 mRNA was not assayed. The *prd*-1 mutation causes abnormal splicing of the mRNA of *prd*-1 which happens after transcription. Even though the activity of the promoter of *prd*-1 is not rhythmic, it is not clear if the pre-mRNA is rhythmically regulated by other processes such as splicing or degradation resulting in the rhythmic expression of *prd*-1 mRNA. Only by assaying the mRNA expression level can this

be elucidated. The second one is that the PRD-1 was not assayed under physiological growth conditions. The paper claimed that the glucose concentration alters the period of the *prd*-1 mutant and the PRD-1-GFP relocalized to the cytoplasm in starvation conditions, which suggested that the carbon supply influences the function of PRD-1. However, they grew the samples for the circadian time course in a fixed volume of liquid medium over a few days and extracted protein from them for the Western blotting. The concentration of glucose is decreasing while the tissue is growing so that some of the samples must be starved when harvesting. In this case the expression of PRD-1-V5 does not represent the situation of normal growth. For these reasons, we conducted experiments to detect the expression level of *prd*-1 mRNA and PRD-1-FLAG of samples that grow on solid agar medium, in order to assure constant glucose supply while growing and simulate the natural mode of growth of *Neurospora crassa*.

The period of every strain is determined on the race tubes which contains Vogel's medium with 0.5% maltose, 0.17% arginine and 2% agar. As mentioned above, the expression of *prd*-1 may be influenced by carbon sources. Hence, to make sure the period on plates is consistent with that on the race tubes we decided to grow the fungus on the same medium.

One of the features of the endogenous circadian clock is that the rhythm is maintained without any zeitgebers (time giver). After removing the light, the expression of light-regulated genes will change. Only the genes involved in or controlled by the molecular clock will keep being expressed rhythmically even if the light has been removed for a certain time. Hence, samples are collected after one circadian cycle has passed in the dark.

3.2 Materials and Methods

3.2.1 Strains

All the strains from lab stock will be identified using their stock number and simplified name. The characteristics of strains are displayed in parenthesis. The entire genotype of each strain is specified in Appendix A. All the strains analyzed in this chapter carry *bd csp*-1 *chol*-1 mutations except #438, a strain was obtained from FGSC (FGSC#10377) expressing FLAG-Pcna, used as the positive control in Western Blotting.

3.2.2 Race tube assay

Refer to 2.2.3.

3.2.3 Protein extraction

Conidia were inoculated in 1 ml Vogel's medium with 2% glucose into each well of 24-well microtiter plates and incubated in LL (constant light) at 30°C for 36 hours (or 22°C for 3 days) until mycelial disks formed. Mycelia were collected by transferring disks onto wet filter paper in a Buchner funnel on a vacuum flask using aspirator for vacuum. Disks were washed with distilled water and each disk was put in a microcentrifuge tube with a hole poked in the top with a needle. Samples were frozen in liquid N_2 and store at -80°C. The frozen tissue was ground in liquid-nitrogen-cooled mortar and the powder was transferred to microcentrifuge tubes on ice. The volume of powder was estimated and an equal volume of protein extraction buffer PEB (50 mM Tris pH 6.8, 2% SDS, 10% Glycerol, 5 mM EDTA-Na_2, 1μg/ml Leupeptin, 1μg/ml Pepstatin A, 1mM PMSF) was added. The mixture was vortexed vigorously and boiled for 5min. The tubes were centrifuged at 25°C, 12,000g for 10 min. The supernatant was removed to new tubes for DC protein assay (BioRad) as instructed by the manufacturer. The calculated protein was measured to 20 μg and PEB was added to 10 μl. Protein samples were boiled and loaded onto SDS-PAGE gel with equal volume (10 μl) of 2X loading buffer (0.125 M Tris-HCl pH 6.8, 4% SDS, 10% 2-

mercaptoethanol, 10% glycerol, 0.004% bromphenol blue).

3.2.4 Nuclei isolation

The mycelia were grown in 100ml Vogel's medium with 2% glucose in 500ml flasks at 25°C for three days. Tissue (5-6g) was harvested and washed in double distilled water by filtration. The tissue was frozen and ground in liquid nitrogen until very fine powder using mortar and pestle. The powder was homogenized with pestles in 9 mL of Buffer A (1M sorbitol, 7% Ficoll-400, 20% glycerol, 5mM Mg acetate, 5mM EGTA, 3mM $CaCl_2$, 3mM DTT, 50mM Tris-HCl, pH 7.5) and incubated on ice for 5min. 18 mL of buffer B (10% glycerol, 5mM $Mg(AC)_2$, 5mM EGTA, 25mM Tris-HCl, pH 7.5) was added slowly with stirring. The homogenate was layered (using pipette to make it flow slowly along the wall of a 50ml tube) onto 5ml Buffer C (1.85ml Buffer A+3.15ml Buffer B) and centrifuged at 3,000g for 7min at 4°C to remove cell debris. The resulting supernatants were removed and carefully layered onto 5ml buffer D (1M sucrose, 10% glycerol, 5mM Mg acetate, 1mM DTT, 25mM Tris-HCl, pH 7.5) in 40ml centrifuge tubes. The tubes were centrifuged at 9,400g for 15min at 4°C to pellet the nuclei. The supernatant (keep it as cytoplasmic fraction) was removed and the nuclei were suspended with 1ml Buffer E (25% glycerol, 5mM Mg acetate, 3mM DTT, 0.1mM EDTA, 25mM Tris-HCl, pH 7.5). The resuspension was stored at -80°C. All buffers contained protease inhibitors 1μM leupeptin, 1μM pepstatin A and 50μM PMSF. Proteins were then extracted following the SDS extraction protocol (3.2.3).

3.2.5 Western blotting and immunodetection

Proteins were separated by 12% Acrylamide/Bis SDS-PAGE (Appendix B) in running buffer (25 mM Tris, 192 mM glycine, 0.1% SDS) at 50 mA per gel for about 45 minutes. Proteins were transferred to PVDF membrane (Immobilon-P, Millipore) as instructed by the manufacturer. Membranes were blocked in blocking buffer (10 mM Tris, pH 7.5, 150 mM NaCl, 0.05% Tween 20, 0.5% skim milk powder, 0.5% BSA) for 60 min and incubated with anti-FLAG® M2 antibody (Sigma-aldrich) in blocking buffer for 1 hour at room temperature.

After three washes with TBST (10 mM Tris, pH 7.5, 150 mM NaCl, 0.05% Tween 20), the tagged proteins were detected using horseradish-peroxidase-conjugated (HRP) secondary antibodies and Immobilon ECL reagents (Millipore) as instructed by the manufacturer.

3.2.6 Genomic DNA extraction

Conidia were inoculated in 1 ml Vogel's medium with 2% glucose into each well of 24-well microtiter plates and incubated in LL (constant light) at 30°C for 36 hours (or 22°C for 3 days) until mycelial disks formed. Mycelia were collected by transferring disks onto wet filter paper in a Buchner funnel on a vacuum flask using aspirator for vacuum. Disks were washed with distilled water and each disk was put in a microcentrifuge tube with a hole poked in the top with a needle. Samples were frozen in liquid N_2 and store at -80°C. The frozen tissue was ground in liquid-nitrogen-cooled mortar and the powder was transferred to microcentrifuge tubes with 600µl of DNA extraction buffer (100mM Tris-HCl pH 8.0, 50mM EDTA, 1% SDS) and proteinase K on ice. The tubes were vortexed and incubated at 65°C for 60 min. The cell debris was removed by centrifuging at 14,000g, 4°C for 5min. The supernatant was incubated at 37°C for 60 min with 5µl RNase solution (10mM Tris pH 8.0, 50% glycerol, 10mg/ml RNase) and 200µl of 7.5M ammonium acetate. The mixture was cooled on ice for 5 min and mixed with 500µl chloroform. The tubes were centrifuged at 14,000g, 4°C for 5min. The supernatant was mixed with 650µl isopropanol and centrifuged at 14,000g, 4°C for 15 min. The pellet was washed with 1 ml 70% ethanol and centrifuged at 7,500g, 4°C for 5 minutes. The supernatant was removed and he pellet was dried on the sterile bench. The DNA was dissolved with proper amount of double distilled water and the concentration was measured by NanoDrop™ 2000/2000c Spectrophotometer (ThermoFisher).

3.2.7 Regular PCR

Refer to 2.2.6.

3.2.8 Techniques related to molecular cloning

Refer to 2.2.8.

3.2.9 Transformation of *Neurospora*

Refer to 2.2.9.

3.2.10 Spore PCR

Refer to 2.2.4.

3.2.11 Microconidia preparation

Refer to 2.2.2.

3.2.12 Crossing

Refer to 2.2.10.

3.2.13 Culture and harvest of time courses

Strains were grown on the surface of cellophane on Vogel's medium (Appendix B) with 0.5% maltose, 0.01% L-Arginine, 2% agar and 100μM choline in 150 mm Petri plates. To begin with, the spores from the lab stocks were inoculated on a starting plate containing the same medium without cellophane pieces laid on the medium and incubated at 30°C LL for two days. Agar plugs were made by plugging the wider end of the Pasteur pipette into the agar medium at the growth front and the plugs were transferred onto the cellophane surface to the edge of the plates. The mycelia of each strain for the inoculation onto each plate came from one starting plate. The inoculated cellophane plates first were incubated in LL at 30°C and then transferred to DD at 22°C. To collect samples every four hours over 48 hours after the transfer to DD, the time points for the transferring and harvesting were scheduled as Table 3.1. The growth fronts of mycelia were scraped off from the cellophane surface using 10 mm-wide spatulas in the dark under the red safe-light and frozen in microcentrifuge tubes with liquid nitrogen.

Table 3.1 The schedule for sampling every 4 hours between 24-72 hours after transferring into dark. H stands for the harvesting time. Inoc represents inoculation time.

Sample	Hours in LL at 30°	Hours in DD at 22°	Total hours of growth	Mon 2 pm	Mon 6 pm	Mon 10 pm	Tues 10 am	Tues 10 pm	Wed 10 am	Thurs 10 am	Thurs 2 pm	Thurs 6 pm
A	24	24	48				Inoc		22°DD	H		
B	24	28	52				Inoc		22°DD		H	
C	24	32	56				Inoc		22°DD			H
D	12	36	48				Inoc	22°DD		H		
E	12	40	52				Inoc	22°DD			H	
F	12	44	56				Inoc	22°DD				H
G	16	48	64		Inoc		22°DD			H		
H	16	52	68		Inoc		22°DD				H	
I	16	56	72		Inoc		22°DD					H
J	4	60	64		Inoc	22°DD				H		
K	4	64	68		Inoc	22°DD					H	
L	4	68	72		Inoc	22°DD						H
M	4	72	76	Inoc	22°DD							H

3.2.14 Coomassie blue staining

The membrane was washed in distilled water for 10 min and rinsed in 100% methanol for 1 min until it is totally wet (transparent). The membrane was then incubated with Coomassie blue solution (0.1% Coomassie R-250, 50% methanol, 10% acetic acid) for a few minutes until bands were visible. The stained membrane was washed in destaining buffer (50% methanol, 10% acetic acid) until bands were clear.

3.2.15 Digoxigenin (DIG)-conjugated DNA probe

The DIG-labeled hybridization probe was generated by PCR using the primers (NCU07839-1423-F, NCU07839-1636-R), PCR DIG Probe Synthesis Mix (Roche) and Q5 High-Fidelity DNA Polymerase (NEB). PCR conditions were set following the instructions of the manufacturers. The purity of the synthesized probe was tested by agarose gel electrophoresis and the concentration was measured by NanoDrop 2000 (ThermoFisher).

3.2.16 RNA extraction

Frozen mycelia were ground to powder using a mortar and a pestle that were pre-cooled with liquid nitrogen. The powder was quickly transferred into microcentrifuge tubes containing 1ml ice-cold TRI Reagent® (Molecular Research Center, Inc.). Homogenate was vortexed and incubated at room temperature for at least 5min. 0.2 ml of chloroform was added to the homogenate and mixed by shaking vigorously for 15 seconds. The mixture was incubated at room temperature for 15 minutes then centrifuged at 12,000g for 15 min at 4°C. The supernatant was removed into 0.5ml isopropanol and the mixture was incubated at room temperature for 5-10 min. The RNA is precipitated by centrifugation at 12,000g for 8 minutes at 4°C. The RNA pellet was washed with 1 ml of 75% ethanol by vortex and resettled by centrifuging at 7,500g for 5 minutes at 4°C. After the RNA pellet was air-dried, the RNA was dissolved with various amount of Diethylpyrocarbonate (DEPC) -treated water to bring OD260 to about 1. The concentration was calculated by UV spectroscopy. An aliquot of 40µg RNA was mixed with 10% volume of 3M sodium acetate and 2 volumes of 95% ethanol and incubated at -80°C overnight for complete precipitation. The RNA was pelleted at 12,000g at 4°C and washed with 100µl 75% ethanol. The air-dried RNA pellet was dissolved in 5µl water + 20µl denaturation cocktail (1X MOPS, 50% formamide, 2.2 M formaldehyde, 0.5 mM EDTA, 4%glycerol, 0.04% bromophenol blue) and incubated at 75°C for 5 min. Samples were cooled on ice for RNA gel electrophoresis.

3.2.17 Northern blotting and immunodetection

The RNA was separated on 1.2% agarose MOPS gel with 5% formaldehyde and 1x RedSafe (iNtRON Biotechnology). The RNA gel was photographed under the UV light and then the RNA was transferred and crosslinked onto BrightStar®-Plus Nylon membranes (Ambion) as instructed by the manufacturer. The membrane was hybridized with 0.1ng/ml DIG-labeled probe in 10ml ULTRAhyb® Hybridization Buffer (Ambion) as instructed. The chemiluminescence was detected using DIG High Prime DNA Labeling and Detection Starter Kit II (Roche) and CDP-star® from Brightstar® Biodetect Kit (Ambion). The signal

was immunodetected by Anti-DIG Fab-AP with 6 minutes' exposure.

3.2.18 Data analysis and statistics

The chemiluminescence signal was captured and analyzed by MicroChemi Imaging System (DNR). The Coomassie blue stained membrane was scanned by the scanner (EPSON). The RNA gel was photographed by FluorChem FC2 Imaging System (Alpha Innotech). The mean grey values of the bands included by a box with constant dimensions were measured using ImageJ (version 1.51, NIH). The brightness of each band was determined by subtracting the brightness of the background. The relative expression level of protein was the ratio of the measurements of chemiluminescence to the measurements of Coomassie blue staining. The relative expression level of RNA was the ratio of the measurements of chemiluminescence to the measurements of RedSafe staining on the gel photographs. The average relative expression level is normalized as 1. One-way ANOVA (analysis of variance) and student's T-test were executed by Microsoft Excel 2016.

3.3 Results

3.3.1 Preliminary test of PRD-1-FLAG strains from lab stock

Former lab members constructed *his*-3^{+}::P$_{ccg\text{-}1}$/P$_{prd\text{-}1}$::*prd*-1^{+}::flag/gfp transformants and I needed make sure that the strains met the criteria: correct genotype; wild-type phenotype; and high expression level of tagged proteins.

To begin with, I tested the phenotype (race tubes) and genotype (spore PCR) of the candidate strains. Only #507 (*ccg-prd*-1-flag) showed a well-rescued phenotype and the phenotype of #519 (native-*prd*-1-flag) looks close to wild-type (Table 3.1). Spore PCR using primers from the *his*-3 locus showed that expression cassettes have been transformed into the genome successfully (Figure 3.1). Regardless of their correct genotypes, I abandoned those strains with incorrect phenotype and utilized only #507 and #519 for following experiments.

As mentioned above, immunoprecipitation is a key step to find proteins that interact with PRD-1. It is known that the PRD-1 protein is a nuclear protein and the abundance may be low compared with total protein abundance. The *ccg*-1 promoter is assumed to be a strong promoter that could drive higher production of the protein than the native promoter of *prd*-1. Therefore, I planned to isolate nuclear proteins from #507 first to obtain a high concentration of FLAG-tagged PRD-1 protein. Because our lab had not done immunoprecipitation or nuclei isolation before, I needed to verify the method and test its efficiency.

Table 3.2 The results (Mean ± SE, n=5) of race tube analysis to test the phenotype. #26, #260 are controls. All other strains also carry the *chol*-1 and *prd*-1 mutations.

strain	condition	period (hour)	growth rate (mm/hour)
#26 (*chol*-1)	100μM choline	22.2±0.12	1.34±0.04
	No choline	63.0±5.74	0.5±0.02
#260 (*chol*-1 *prd*-1)	100μM choline	24.6±0.13	0.77±0.01
	No choline	126.3±16.86	0.40±0.02
#480 (*ccg-prd*-1-gfp)	100μM choline	24.9±0.1	1.0±0.01
	No choline	82.5±2.65	0.43±0.01
#490 (native *prd*-1)	100μM choline	19.8±0.29	1.18±0.01
	No choline	arrhythmic	0.58±0.01
#506 (*ccg-prd*-flag)	100μM choline	23.5±0.12	1.06±0.02
	No choline	69.4±1.81	0.46±0.01
#507 (*ccg-prd*-flag)	100μM choline	22.2±0.02	1.17±0.01
	No choline	66.4±6.75	0.46±0.02
#519 (native *prd*-1-flag)	100μM choline	21.8±0.34	0.96±0.01
	No choline	60.0±2.66	0.47±0.01

Typically, SDS protein extraction buffer is used to extract total proteins in a harsh way, but IP buffer extracts protein in a gentle manner to protect protein-protein interactions with less concentrated detergent. The nuclear protein may not be extracted by IP buffer thoroughly due to the low capability to disrupt the nuclear envelope. Moreover, whether the components in nuclei isolation buffer could affect the extraction or protein binding needed to be examined as well. Therefore, I ran proteins extracted from #1 (WT) and #507 (*ccg-prd*-1-flag) by three different buffers (without doing nuclei isolation) on SDS-PAGE gel. A positive control (#438) which came from a strain expressing a FLAG-tagged protein irrelevant to *prd*-1 was also loaded. The FLAG tag was detected by Anti-FLAG M2 antibody.

I obtained similar results from different extraction buffers and both strains (Figure. 3.2). PRD-1 has a size of 61 kDa. Weak bands at about 63kDa can be observed from the membrane. Different buffers seem not to be different when extracting proteins. However, the brightness of bands from #1 and #507 is much lower than that from the positive control. It may be explained by low abundance of PRD-1.

Next, I tried to isolate the nuclei and extract concentrated nuclear protein with IP buffer. The nuclear protein was concentrated after nuclei isolation since a brighter band showed up at the right position. Yet no significant difference could be seen between #1 and #507, suggesting that what I acquired may just be concentrated non-specific bands (Figure 3.3).

The FLAG-tagged strain did not show a positive result, which indicates that the PRD-1-FLAG protein is not expressed efficiently. In fact, it is implied in my first result because the picture was obtained after 7 minutes' exposure whereas the positive control showed a very strong signal with only a 40-second exposure.

Why couldn't the successfully transformed strain express FLAG-tagged protein? A doubt was raised that something was wrong at the tag region. We have two tags that are commonly used in the lab – FLAG and GFP. In case those transformants with tagged PRD-1 protein have the wrong tag or no tag in the genome, I tested the genomic DNA of all PRD-1-FLAG

transformants in lab stocks by PCR with primers (NCU07839-3136-F, pBM61-1) accurately targeting the tag region. Surprisingly, all *prd*-1-flag transformants which have the *ccg-1* promoter are in fact GFP-tagged strains, and transformants which have the *prd*-1 promoter are FLAG-tagged strains (Figure 3.4). However, I double-checked the sequence of the *prd*-1 promoter which was transformed by the former student and found it is hundreds of base pairs shorter than the one in the database (FungiDB). Hence, all the FLAG-tagged strains in lab stock are unqualified for future experiments.

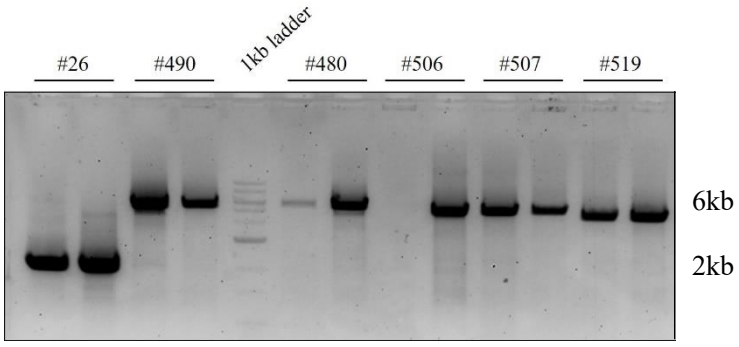

Figure 3.1 Spore PCR results of some prd-1 transformants in Table 3.1. Two replicates of each strain were loaded. The sizes of target bands are 2kb (WT) and 5~6kb (transformed).

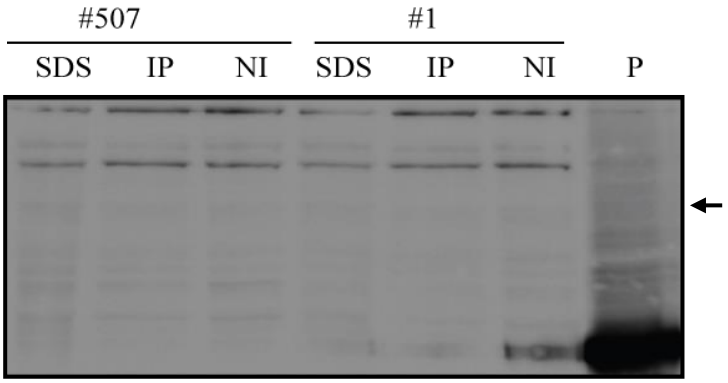

Figure 3.2 Western Blotting results by Anti-FLAG M2 antibody (7 min exposure). Arrow indicates where PRD-1 protein should be. Protein extracted by different protein extraction buffers: SDS, immunoprecipitation (IP) and nuclei isolation (NI) buffer. P: positive control.

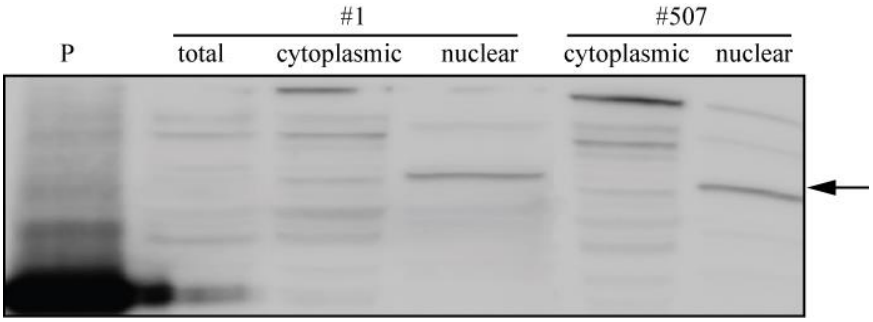

Figure 3.3 Western Blotting results by Anti-FLAG M2 antibody (7 min exposure). Arrow indicates where PRD-1 protein should be. Protein extracted after nuclei isolation. P: positive control.

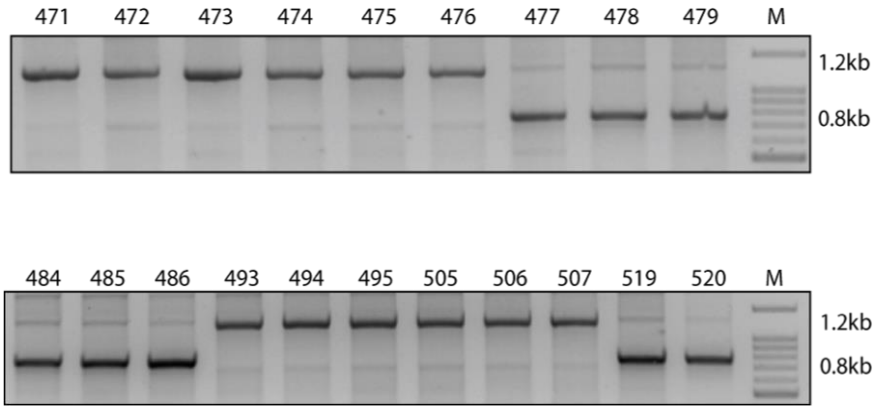

Figure 3.4 PCR of genomic DNA to test epitope tag. #471-476, #493-507: *ccg* promoter; #477-479, #484-486, #519-520: native promoter. GFP tag (1.2kb) is larger than FLAG tag (0.8kb).

3.3.2 Construction of *ccg-prd*-1-flag plasmid

The test above demonstrated that the GFP-tagged strains with the *ccg* promoter were mistakenly labelled as FLAG-tagged strains. As a result, I needed to construct a *ccg-prd*-1-flag plasmid targeting the *his*-3 locus to construct the corresponding *N. crassa* strain. To achieve this, I introduced SpeI and PacI sites to both ends of *prd*-1 coding sequence by PCR (PacI-NCU07839-3503-R, SpeI-NCU07839-1040-F) and then ligated the digested DNA segments to the plasmid (Figure 3.5). The backbone is digested from pCCG-C-Gly-3XFLAG obtained from FGSC. Both colony PCR and plasmid digestion tests gave the expected result (Figure 3.6). The first round of sequencing failed and the second round of sequencing using a new set of longer primers confirmed that one of my clones has the correct sequence.

3.3.3 Construction of native-*prd*-1-flag plasmid

Although the *ccg*-1 promoter may lead to a better expression of PRD-1, it is more persuasive if our results are collected from strains with Flag-tagged protein driven by the native promoter. It is also necessary to use native promoter for measuring the normal expression levels of the PRD-1 protein. When I was analyzing the incorrect transformants, I found that the 'native promoter' of the plasmid that was used for the transformation was missing a section of sequence at the 5' upstream region, when compared with the sequence data from FungiDB.org. Therefore, I planned to construct a new plasmid with the entire native promoter and upstream region.

My initial strategy was to attach the segment of missing sequence to the incorrect plasmid by NotI and XbaI (Figure 3.7). The colony PCR of the bacteria transformed by the ligated plasmid showed only #2, 5 had correct but very faint bands (Figure 3.8). I extracted plasmids from those colonies and did restriction enzyme tests which failed because the XbaI is *dam* methylation sensitive and the cutting site happened to be blocked by methylation. Since no more suitable cutting sites can be used to identify the insert, I had to give up this strategy.

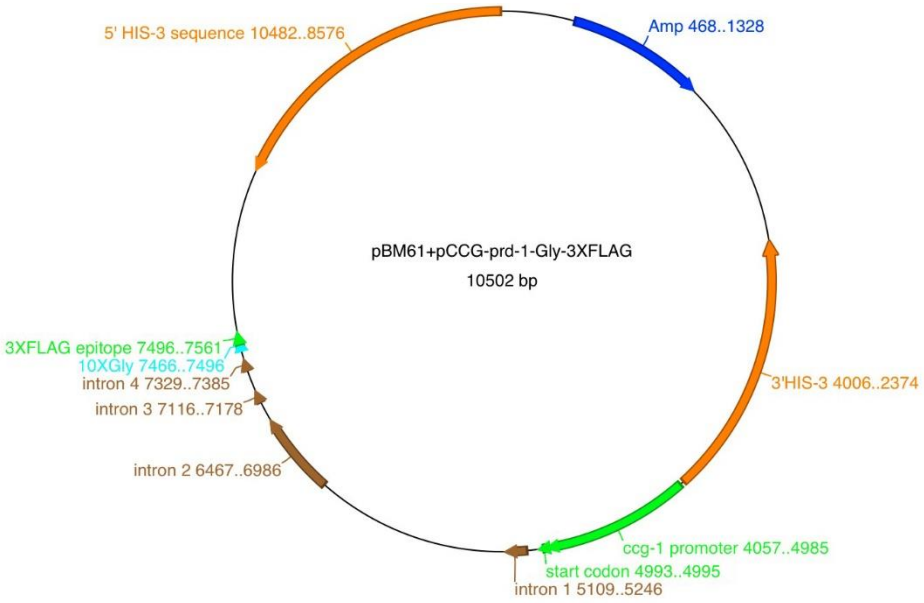

Figure 3.5 Plasmid map of pBM61-ccg-*prd*-1-flag**.**

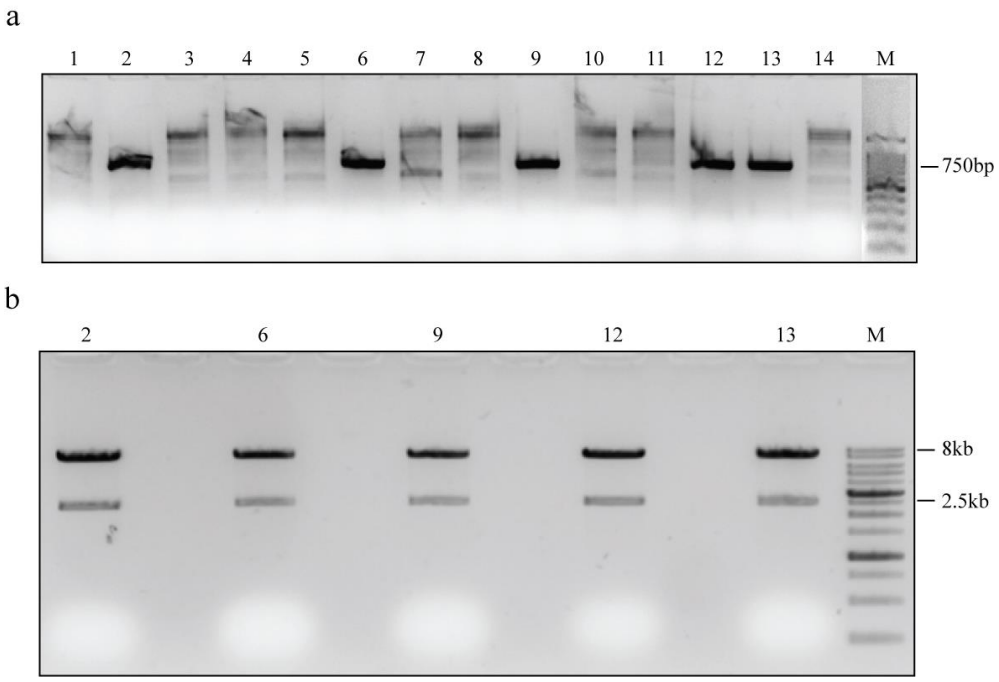

Figure 3.6 Construction of pBM61-ccg-*prd*-1-flag. Expected bands are annotated beside the pictures. a) Colony PCR to select transformed *E. coli* cells. Primers: native-prd-1 up-F (Not I), native-prd-1 up-R (Xba I). b) Restriction enzyme digestion (SpeI and PacI) of colonies from a).

My second strategy was to insert the whole cassette: native promoter and *prd*-1 wild-type gene without the stop codon, into an original backbone plasmid with the *his-3* gene and the sequence of FLAG (pCCG-C-Gly-3XFLAG) (Figure 3.7). I amplified the insert fragment from wild-type genomic DNA by PCR with Not I and Pac I sites introduced (native-prd-1 up-F (Not I), PacI-NCU07839-3503-R). After digestion by NotI and PacI, the purified insert and backbone fragments were ligated and transformed into 10-beta *E. coli* competent cells. For the first trial, I failed to obtain colonies that could grow in the liquid LB medium. For the second and third trial, I obtained a total of 15 colonies that were discovered to be the parent vector. Considering that the backbone plasmid may not be thoroughly digested and super-coiled uncut plasmid will run at the same position on the gel with the cut backbone fragment, I cannot separate them by gel purification. Thus, for the fourth trial, I did a two-step digestion for both fragments, and as a result, the colonies were not backbone plasmid even though still not what I wanted (Figure 3.9). When the fifth trial also failed, I was advised that NotI cannot digest PCR products completely if the cutting sites are located at the end of DNA and I should do subcloning to ligate fragments into T-vectors or blunt-end vectors. The insert was cloned into pJET (Thermofisher) successfully (Figure 3.10). For the sixth trial, I ligated the purified digested fragments from both the subclone and the backbone plasmid. I found that all the colonies were pJET-native-*prd*-1 subclones. Due to the fact that the size of the pJET vector is similar to the insert, in order to separate them, I digested the subclones with BspHI to cut up the vector.

Finally, I harvested my anticipated plasmid on the seventh trial (Figure 3.11) and sent it for sequencing. Unfortunately, two base pairs (C and T) were found missing in the CT-repetitive region in the first intron of the *prd*-1 gene. Is this plasmid acceptable? RT-PCR of the *prd*-1 mutant showed that the mutated *prd*-1 gene can be spliced alternatively which leads to the aberrant phenotype (Adhvaryu et al., 2016). Thus, no error is acceptable in the plasmid even in an intron. Sequence errors may come from the genomic DNA as the template of the

amplified insert or via PCR. Therefore, I amplified a small region which contains the first intron of the *prd*-1 gene from both transformed bacteria and WT strains. Sequencing results revealed that the sequence of our WT strains in our lab is identical to the sequence from the database. As a consequence, I should reconstruct the plasmid.

I amplified the *prd*-1 transcript from the sequenced genomic DNA, and then ligated it into the blunt-end vector pJET (Thermofisher) (Figure 3.12a). I sent the subclones for sequencing to make sure that the sequence of pJET-native-*prd*-1 was not mutated. Purification of the NotI/PacI-digested subclone and backbone plasmid was then followed by the ligation. Eventually, I selected and sequenced a correct plasmid from dozens of colonies after several transformations (Figure 3.12 b and c).

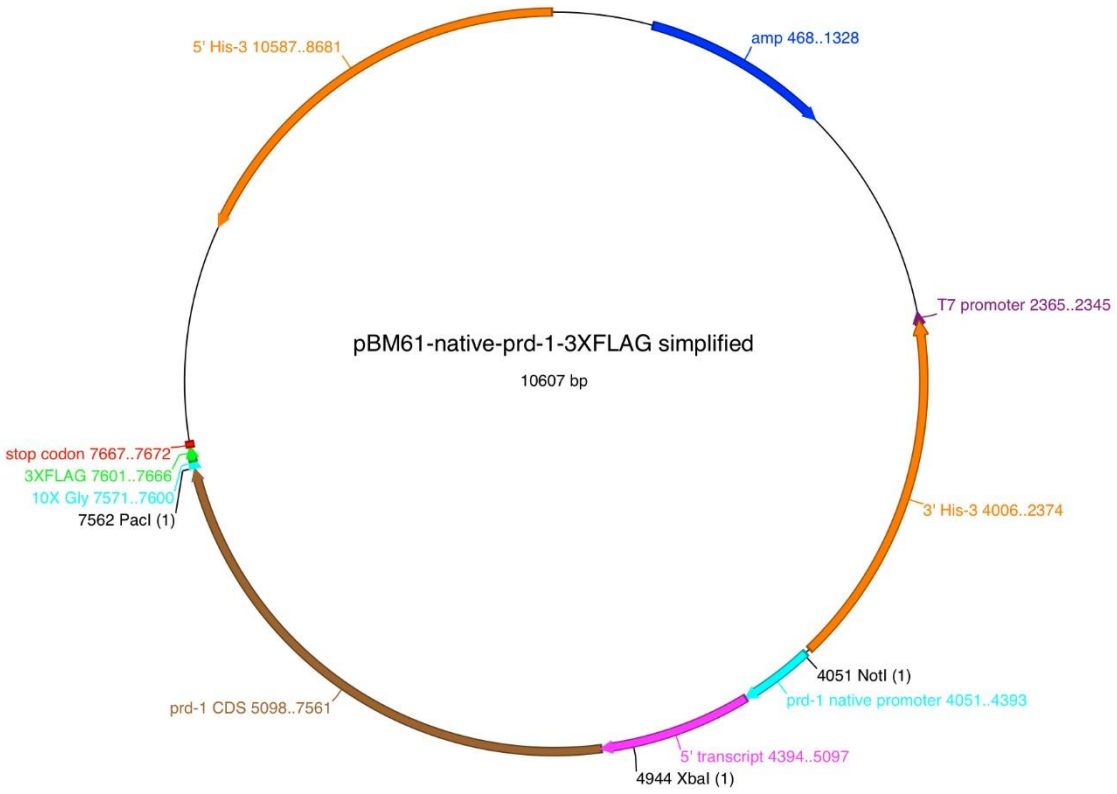

Figure 3.7 Plasmid map of pBM61-native-*prd*-1-flag.

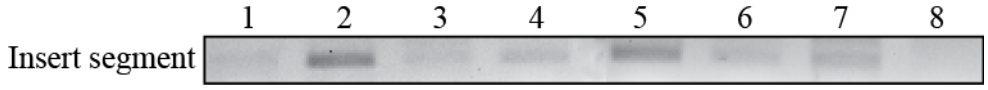

Figure 3.8 Colony PCR result of native-*prd*-1-flag plasmids with primers used for amplifying insert DNA segment.

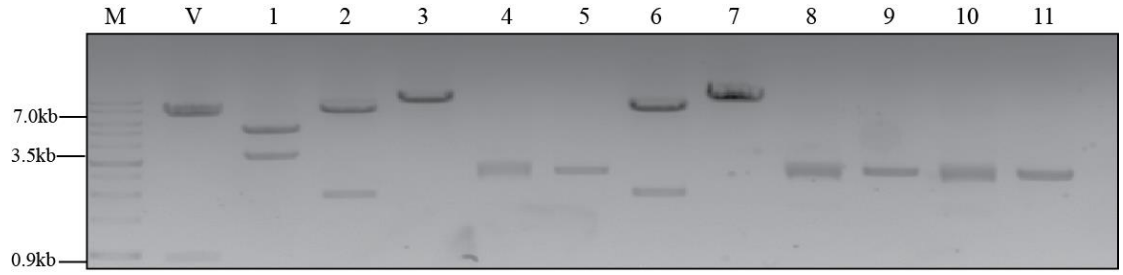

Figure 3.9 Restriction enzyme test of native-*prd*-1-flag transformants. Before the ligation, two-step digestion was carried out to remove parent vector pCCG-Gly-FLAG. The correct plasmid should produce two bands 7.0kb and 3.5kb. M: 1kb DNA ladder; V: parent vector.

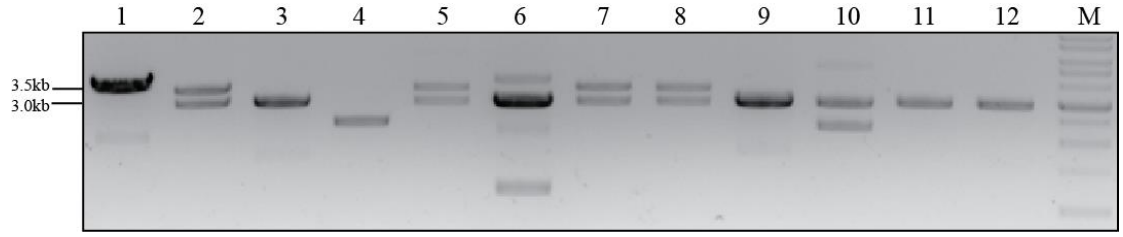

Figure 3.10 Restriction enzyme test of pJET-native-*prd*-1 subclones. The size of backbone fragment is 3.0kb and insert fragment is 3.5kb.

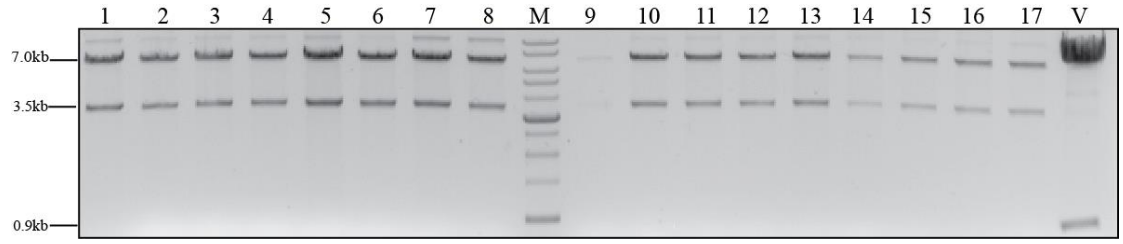

Figure 3.11 Restriction enzyme test of pBM61-native-*prd*-1-flag transformants. The 3.5kb DNA fragment is inserted into vector successfully. V stands for backbone vector pCCG-Gly-FLAG

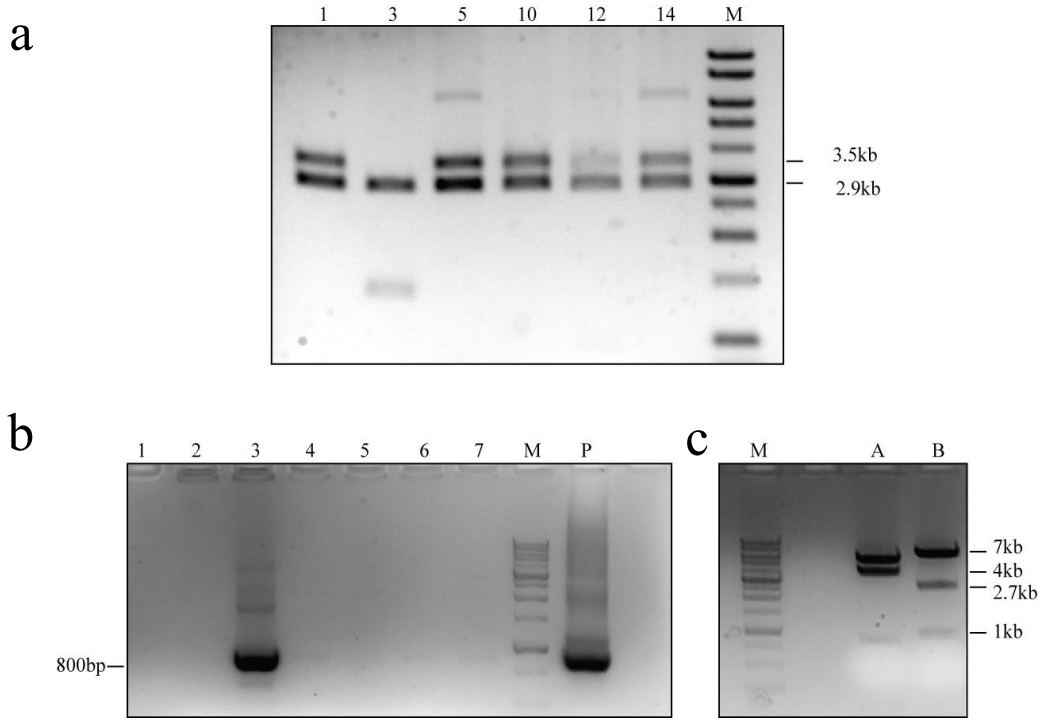

Figure 3.12 Construction of native-*prd*-1-FLAG. Expected bands are annotated beside the pictures. a) Restriction enzyme digestion (NotI and PacI) of putative pJet-native-*prd*-1 plasmids from selected colonies. #1,5,10,14 have correct bands. b) PCR of native-*prd*-1-FLAG *E. coli* colonies using the primers native-prd-1 up-F (Not I) and native-prd-1 up-R (Xba I). P: pJET-native-*prd*-1. c) Restriction enzyme digestions of pBM61-native-*prd*-1-FLAG #3. M: 1kb ladder. A: NdeI, NotI and XbaI. expected bands: 5.7kb, 4kb, 0.9kb. B: HindIII. Expected bands: 6.9kb, 2.7kb, 1kb.

3.3.4 Construction of transformants expressing FLAG-tagged PRD-1

Once the plasmids were obtained, the next step was transformations of *Neurospora*. The plasmids have a *his*-3 targeting region which is a partial sequence of the *his*-3 gene. The transformed spores will no longer be histidine deficient and untransformed spores will not grow on the medium without histidine. However, as the recipient, macrospores possess more than one nucleus. Indeed, only a few nuclei will be transformed. Therefore, I needed to isolate homokaryotic strains whose nuclei all carry the transformed genome. Two methods are commonly used for homokaryon purification - microconidia isolation and crossing.

3.3.4.1 *Ccg-prd*-1-flag

I transformed the *ccg-prd*-1-flag plasmid into macrospores of a *his*-3 mutant #274 (histidine-requiring strain) after the midi preparation of the plasmid. I transformed linearized highly concentrated plasmid into fresh spores and obtained dozens of colonies. Subsequently, spore PCR showed that all of them were heterokaryons (having both transformed and untransformed nuclei). To obtain homokaryons, I chose three colonies which had highest portion of transformed nuclei for microconidia purification. Two microconidia purifications failed to isolate homokaryons. Meanwhile, since we are interested in the FRQ-less oscillator, I also started to cross the heterokaryons with a frq^{10} strain to get strains with the *frq* knockout background. Ascospores showed a very low germination ratio so that only three ascospores germinated out of 100 picks. A more efficient way to select homokaryons is to pour thousands of ascospores on the sorbose medium in the Petri plates to isolate colonies, even though pouring 200 ascospores in one plate may result in heterokaryons. I identified 3 homokaryons from 50 colonies by spore PCR (Figure 3.13a), and then I ran a race tube test (Table 3.2) and a hygromycin test to determine their genotype. Finally, I obtained two homokaryons such that one has the frq^{+} background (#586) and the other has the frq^{KO} background (#587) (Figure 3.13b).

3.3.4.2 Native-*prd*-1-flag

I transformed the native-*prd*-1-flag plasmid into two recipient strains #274 (*prd*-1^{+}) and #310 (*prd*-1^{-}). For the transformants with WT background, I proceeded with microconidia purification and attained one homokaryon (#588) as shown by spore PCR (Figure 3.13d). For the transformants with *prd*-1 background, I obtained a homokaryotic transformant with *prd*-1 mutation background directly from transformation (Figure 3.13c). The phenotype of the strains were analyzed by the race tube assay (Table 3.2).

Table 3.3 The results (Mean ± SE, n=3) of race tube analysis to test the phenotype. #26, #80 are controls. All other strains also carry the *chol*-1 mutations.

strain	condition	period (hour)	growth rate (mm/hour)
#26 (*chol*-1)	100μM choline	21.3±0.06	1.41±0.01
	No choline	47.1±2.11	0.46±0.02
#80 (*chol*-1 *frq*^{KO})	100μM choline	arrhythmic	1.40±0.002
	No choline	53.3±1.65	0.48±0.01
#586 (*ccg-prd*-1-flag)	100μM choline	26.8±0.92	0.98±0.02
	No choline	59.2.5±8.66	0.45±0.02
#587 (*ccg-prd*-1-flag *frq*^{KO})	100μM choline	arrhythmic	1.23±0.01
	No choline	45.0±2.38	0.51±0.01
#588 (native-*prd*-1-flag)	100μM choline	22.3±0.06	1.1±0.02
	No choline	51.88±4.96	0.45±0.02
#589 (native-*prd*-1-flag *prd*-1^{-})	100μM choline	20.6±0.02	1.28±0.03
	No choline	56.0±2.68	0.56±0.02

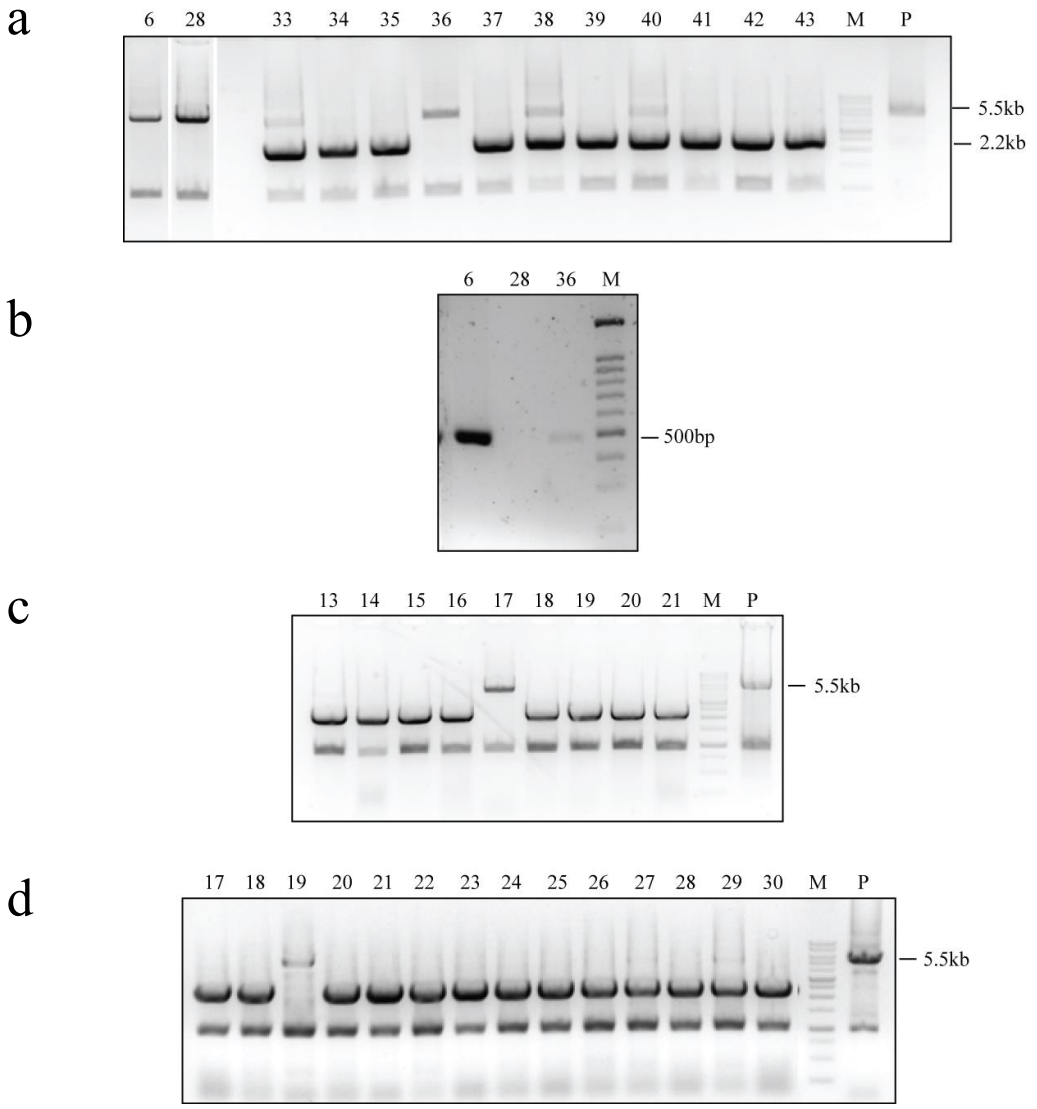

Figure 3.13 Construction of transformants expressing FLAG-tagged PRD-1. a) Spore PCR of *ccg-prd*-1-FLAG crossing progenies using primers targeting *his*-3 locus (His3-F1 and His-3R2) to select homokaryons. Transformed nuclei shows a 5.5kb band. b) Spore PCR of homokaryons from a) using *frq* primers targeting *frq* locus. Wild type *frq* shows a 500bp band. #6: frq^{+}, #28: frq^{10}, #36: *frq* heterokaryon. c) Spore PCR of native-*prd*-1-FLAG transformants with the *prd*-1 mutant background using primers targeting *his*-3 locus (His3-F1 and His-3R2). Transformed nuclei shows a 5.5kb band. d) Spore PCR of colonies from microconidia purification of native-*prd*-1-FLAG transformants with *prd*-1^{+} backgound using primers targeting *his*-3 locus (His3-F1 and His-3R2).

3.3.5 The rhythmicity of the *prd*-1 mRNA

3.3.5.1 The generation and efficiency test of DIG-labeled DNA probe

To detect the mRNA of the *prd*-1 gene by Northern blotting, a DIG-labeled probe has to be specifically targeting the transcript of *prd*-1. Avoiding any potential alternative splicing at the C-terminus, I chose a ~200nt probe from the N terminus of the *prd*-1 gene excluding the introns (see the sequence in Appendix D). The probe was aligned with the whole genome of *Neurospora crassa* showing that the probe sequence is highly specific.

Since the DIG-labeled dNTP will impact the amplification, the production of a DIG-labeled probe is not as high as a normal PCR product. Additionally, the probe cannot be purified by gel purification. Therefore, I needed to optimize PCR conditions to ensure that no non-specific products are amplified. I amplified unlabeled probe with different annealing temperatures and different templates. The agarose gel electrophoresis showed a single bright band that was amplified from plasmid DNA annealing at 66°C (Figure 3.14a). When using DIG-labeled dNTP mixture, the size of the PCR product appeared to be significantly larger than the unlabeled DNA fragment (Figure 3.14b). According to the DIG-labeling Kit instructions, the labeled probe migrates slower on the agarose gel. Thus, I believe I have amplified the correct DIG-labeled probe.

To test the efficiency of this probe, I prepared RNA from both wild type and the *prd*-1 mutant on both liquid and solid media. I tried 1ng of DIG-labeled probe to hybridize with 40μg of total RNA. Northern blotting demonstrated that 1ng of my probe is sufficient for the detection and the *prd*-1 mutant has a higher expression level of *prd*-1 mRNA (Figure 3.15). No significant difference of the chemiluminescence can be seen between agar plates and liquid medium.

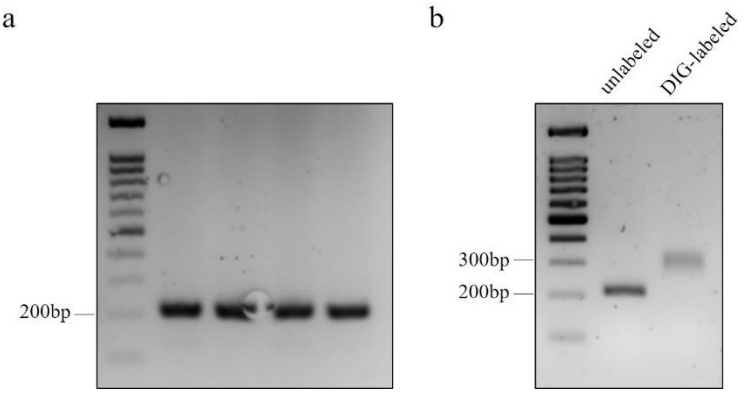

Figure 3.14 DNA probes in the 1.5% agarose gel. a) unlabeled probe is amplified from plasmids under the following PCR conditions: 98°C 30sec, 66°C 30sec, 72°C 30sec for 32 cycles. Four replicates were run on the gel. b) Both unlabeled and labeled probes are amplified under the same PCR conditions. The labeled probe has a slower migration rate.

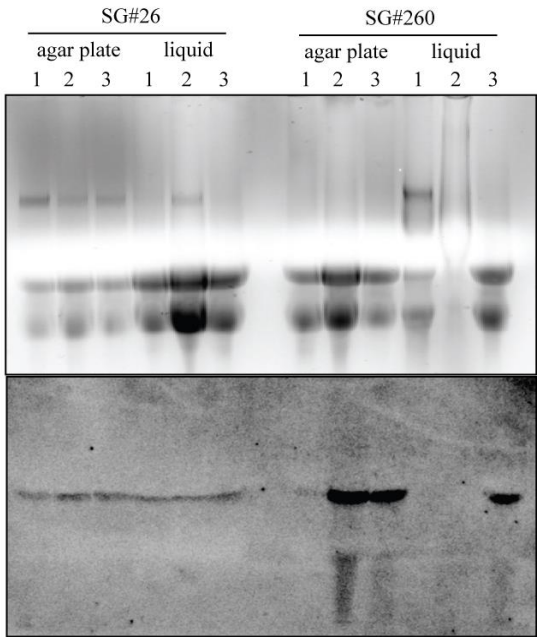

Figure 3.15 Agarose gel (upper panel) and Northern blot (lower panel) of 40µg total RNA of WT (#26) and *prd*-1 mutant (#260) from solid or liquid culture. Three replicates of each sample are loaded on the gel.

3.3.5.2 The expression of the *prd*-1 mRNA is not circadianly rhythmic

Once the probe was verified, I prepared samples for the time course. To assay the expression level of wild-type mRNA of *prd*-1, I chose #26 (*prd*-1^{+}) for subsequent experiments.

I collected 13 samples every 4 hours from 24 hours to 72 hours after the plates were transferred into constant dark at 22°C. 40μg total RNA of each sample was loaded on the RNA gel and Northern blotting was carried out. I conducted the experiments five times and I used the last four results for quantification because of uneven loading in the first trial.

On the gel, the amount of 28S rRNA is roughly twice as much as 18S rRNA and both have clear bands (Figure 3.16a) indicating that the RNA sample was not degraded. When comparing the membrane with RNA gel, the signal is mainly located at the position of 28S rRNA.

Using compiled data of four independent trials, Figure 3.16b shows that the expression levels of *prd*-1 mRNA fluctuate slightly but not rhythmically. Particularly, a period about 24 hours cannot been observed. The standard errors are relatively high compared to the means. ANOVA reveals that no significant difference of expression level exists among 13 time points. Therefore, the expression of *prd*-1 mRNA is not circadianly rhythmic.

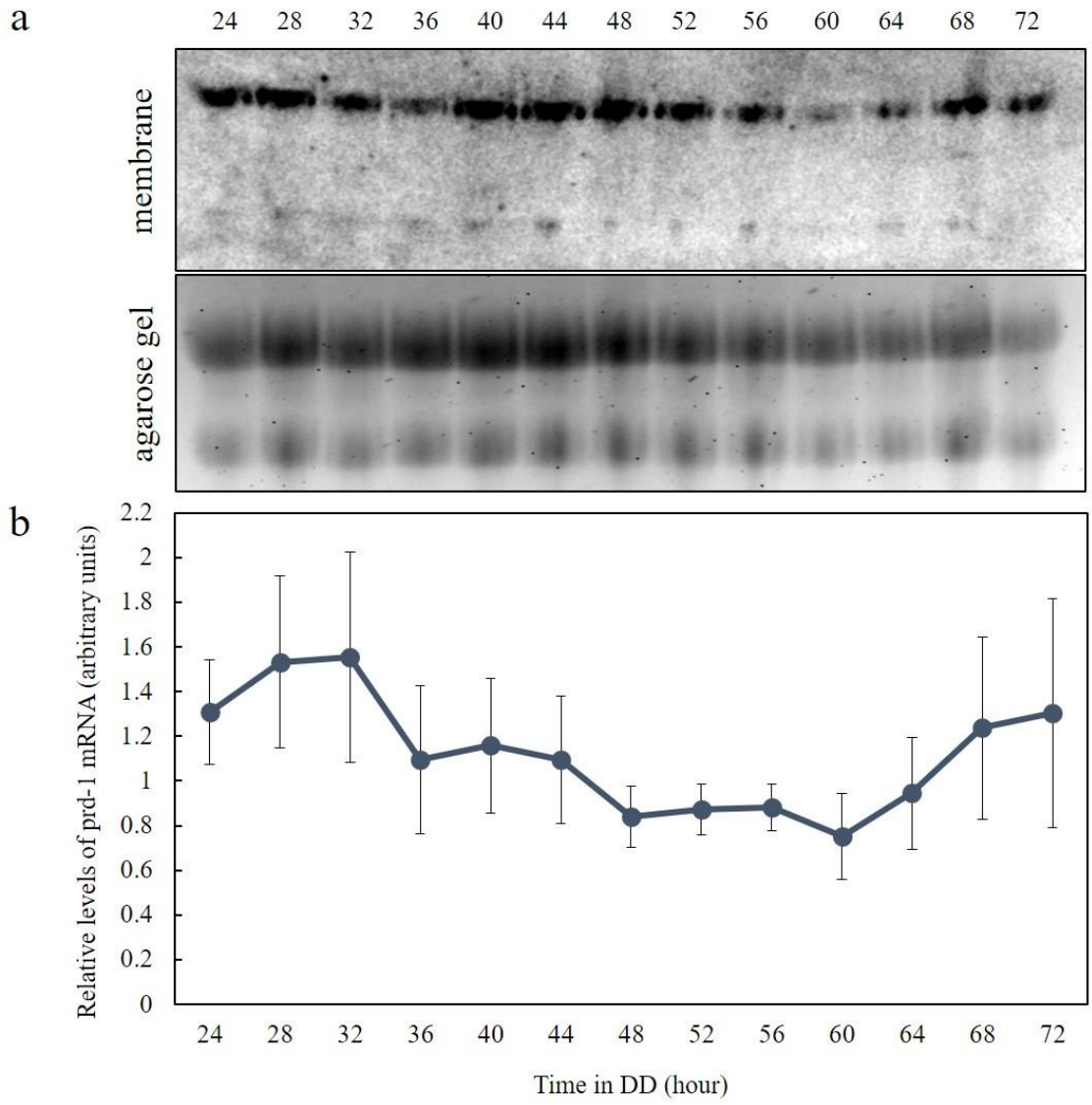

Figure 3.16 The results of circadian time course of the *prd*-1 mRNA. a) Representative picture of immunodetected membrane and RNA gel. b) Relative expression levels of the mRNA of *prd*-1 over 48 hours. Mean ± SE is shown (n=4). P= 0.7571 (one-way ANOVA).

3.3.6 The rhythmicity of PRD-1

3.3.6.1 Preliminary test of #588 (native-*prd*-1-flag)

As mentioned in 3.3, 4 strains expressing PRD-1-FLAG were confirmed to be qualified for subsequent experiments. Initially, I needed to check the expression level of the tagged protein. I grew the fungus in constant light in liquid medium at 25°C. I extracted protein and ran Western blotting with M2 Anti-FLAG antibody. The results implied that all transformed strains have a high expression level of tagged protein (Figure 3.17).

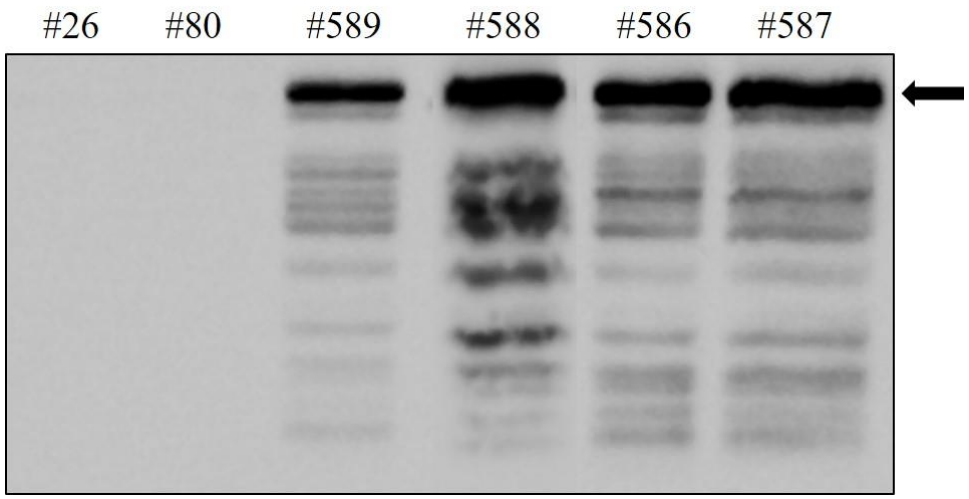

Figure 3.17 Western blotting results using Anti-FLAG M2 antibody (Exposure time 1 min). The arrow indicates where PRD-1-FLAG should be. #26: WT; #80: *frq*10; #586: *ccg*-1-*prd*-1-FLAG; #587: *ccg*-1-*prd*-1-FLAG, *frq*10; #588: native-*prd*-1-FLAG; #589: native-*prd*-1-FLAG, *prd*-1^{-}.

3.3.6.2 The expression of PRD-1-FLAG is not circadianly rhythmic

Once the expression of PRD-1 was confirmed, I prepared samples for the time course. Since #588 expresses the PRD-1-FLAG driven by the native promoter, the results from it should be more accurate than the results from the strains containing the *ccg*-1 promoter. To study the rhythmicity of PRD-1, I chose #588 for subsequent Western blotting.

I collected 13 samples every 4 hours from 24 hours to 72 hours after the plates were transferred into constant dark at 22°C. I conducted the experiments five times and I used all five results for quantification.

From the chemiluminescence (Figure 3.18a), we cannot observe rhythmic expression of FLAG-tagged PRD-1. However, the integrated results from all five trials displayed fluctuations (Figure 3.18b). The analysis of variance confirmed that the PRD-1 expression level at 13 time points are significantly dissimilar (P=0.03). When comparing the peaks and troughs, significant differences presented between 24h and 32h, 32h and 44h, 48h and 60h. It seems to implicate a period about 16 hours to 20 hours. The peaks have only 1.5-2 fold expression above the troughs which is not a dramatic expression level. Hence, the expression level of PRD-1 does fluctuate to some extent, yet it is not circadianly rhythmic.

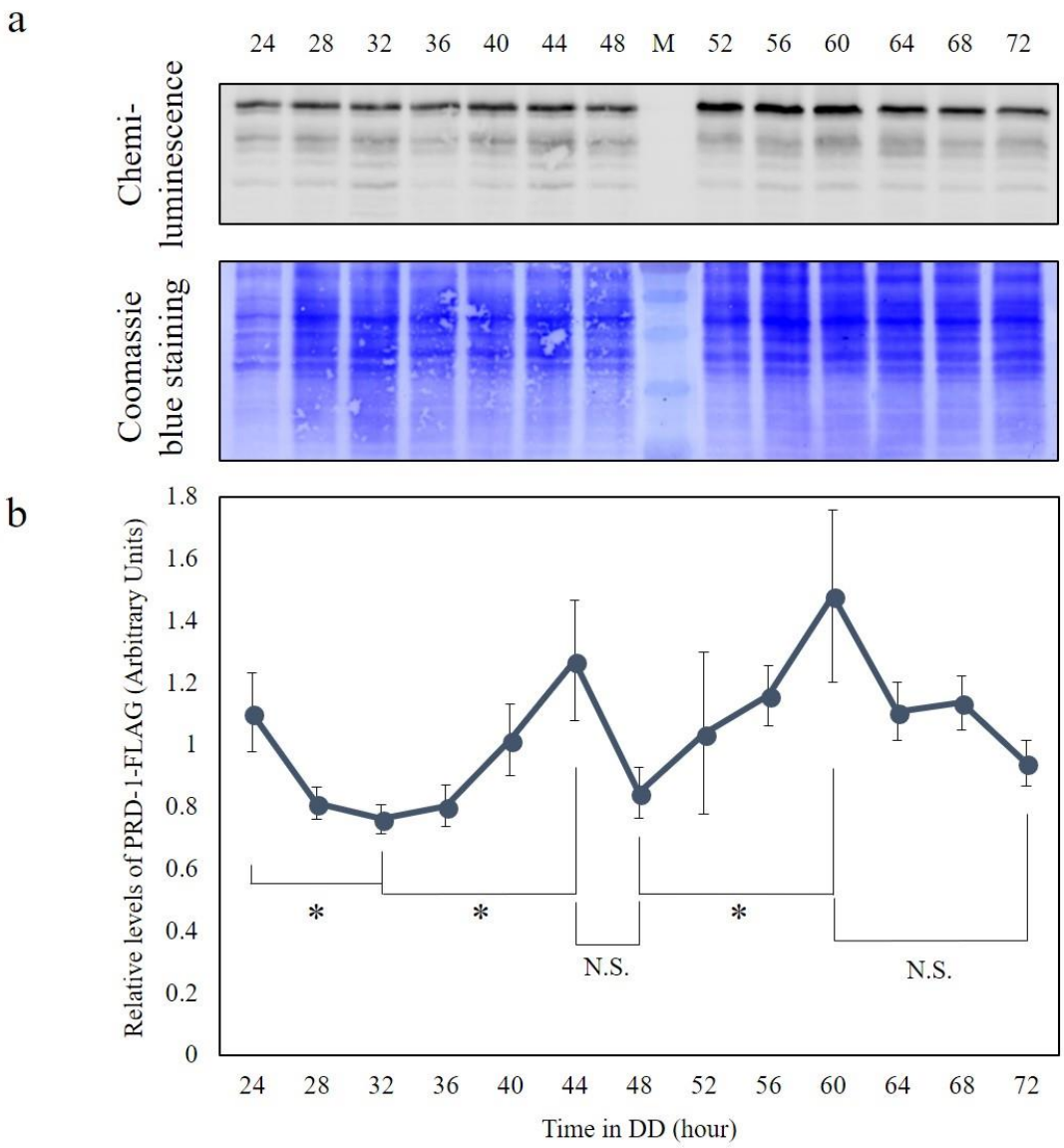

Figure 3.18 The results of circadian time course to assay PRD-1-FLAG. a) Representative picture of immunodetected membrane and Coomassie blue stained membrane. M: BLUeye Pre-stained Protein Ladder (GeneDireX). Five bands of the ladder are shown (from top to bottom, about 75, 63, 48, 35, 25kDa) b) Relative expression levels of PRD-1-FLAG over 48 hours. Mean±SEM are shown (n=5). *: $P<0.05$ (student's T test). N.S.: not significant $P>0.05$ (student's T test). $P= 0.03$ (one-way ANOVA).

3.4 Conclusion

When I attempted to detect the expression of PRD-1-FLAG extracted from strains constructed by previous lab members, the Western blot showed that no difference could be detected between WT and *ccg-prd*-1-flag transformants. Further analysis of the DNA sequences revealed that the former strains are not appropriate for Western blot and IP. Hence, I constructed the plasmids containing the *prd*-1-flag expression cassette and transformed them into *Neurospora crassa*. Homokaryons were obtained by microconidia or ascospores.

The *prd*-1 mutant expresses only a small proportion of normally spliced mRNA and the phenotype is altered. This may imply that the dosage of PRD-1 influences the phenotype. Since the transformants have more than one copy of *prd*-1, either wild-type or mutant, the phenotype might be altered. The period and growth rate of the transformants are slightly different from the WT strain on race tubes, which is consistent with our hypothesis.

In this chapter, the rhythmicity of the expression level of the *prd*-1 gene was examined. Samples of WT and PRD-1-FLAG-expressing strains were collected from 24^{th} hour to 72^{nd} hour after transfer into constant dark. The mRNA of *prd*-1 was detected by DIG-conjugated DNA probe utilizing Northern blotting. The PRD-1-FLAG was detected by Anti-FLAG antibody using Western blotting.

The data demonstrated that the mRNA and the protein of *prd*-1both are not expressed in the pattern of a circadian rhythm. In spite of some fluctuation of *prd*-1 mRNA, the variation is relatively high at each time point. The ANOVA showed that no significant difference exists during 48 hours. As for the protein level, regardless of a significant change between peaks and troughs, the durations of the oscillation are more like 16 hours which is different from the period of the free-running rhythm, 22 hours (Table 3.2) (Figure 3.19).

In summary, the *prd*-1 gene is unlikely to be a component of or directly controlled by the circadian clock in *Neurospora crassa*.

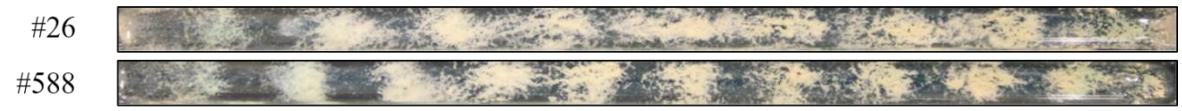

Figure 3.19 Representative picture of the race tubes of wild type (#26) and native-*prd*-1-flag strain (#588). The strains were grown on the same medium as the one used in the time courses. The race tubes were incubated at 30°C, LL for 1day and then at 22°C, DD for about 10 days.

Chapter 4 Interacting partners of PRD-1

4.1 Introduction

Co-Immunoprecipitation (Co-IP) is a key step to identify proteins that interact with PRD-1. PRD-1 is homologous to the DEAD-box RNA helicase family. The function of RNA helicases is extremely various (Linder and Jankowsky, 2011). It is difficult to determine what roles PRD-1 is playing by simply referring to the functions of RNA helicases. Identifying the binding partners of PRD-1 will offer clear guidance to understand the function of PRD-1. Another DEAD-box RNA helicase FRH (FRQ- binding RNA helicase) is found to regulate the TTFL in *N. crassa* by binding to FRQ (Cheng et al., 2005). The PRD-1 protein may also interact with the components that are involved in the circadian clock. Thus, I planned to pull down the proteins binding to PRD-1 and analyze them by MS (Mass Spectrometry).

In Chapter 3, I constructed the strains expressing PRD-1-FLAG driven by the native promoter and #588 is appropriate for Co-IP. To acquire more significant results from MS, a high abundance of PRD-1-FLAG is preferred. It is known that the PRD-1 protein is a nuclear protein (Adhvaryu et al., 2016). The abundance of this nuclear protein may be low compared with total protein abundance. Nuclei isolation may be required to obtain a high concentration of FLAG-tagged PRD-1 protein. It is reported that the PRD-1-GFP protein is transported to the cytoplasm when the cells are starving (Emerson et al., 2015). To identify the nuclear binding partners of PRD-1, samples have to be harvested when the glucose has not been depleted in the medium. Therefore, tissues will be grown in a high volume of medium for only 24 hours.

4.2 Materials and Methods

4.2.1 Strains and cell culture

All the strains from lab stock will be identified using their stock number and simplified

name. The characteristics of strains are displayed in parenthesis. The entire genotype of each strain is specified in Appendix A. #26 (*bd csp*-1 *chol*-1) was considered as wild type. The FLAG-tagged PRD-1 protein was extracted from #588 (*bd csp*-1 *chol*-1 *his*-3^{+}::native-*prd*-1-flag). #444 (*bd csp*-1 *chol*-1 NCU05950^{KO} *his*-3^{+}::NCU05950-flag) was treated as a control in Co-IP and MS.

For the IP experiments that were followed by Western blotting, fresh conidia were inoculated in 1ml Vogel's liquid medium with 2% glucose in a 24-well plate at 25°C for three days and harvested when mycelia mat was formed. For Co-IP, fresh conidia were cultured on 3ml Vogel's agar medium with 2% glucose in stock tubes. After 7days, mycelia of the whole test tube were transferred to 100 ml Vogel's liquid medium with 2% glucose on a rotating shaker at 130 rpm for 24 hours at 25°C, LL. Fresh mycelia were harvested by washing with water and filtration, then frozen in liquid nitrogen, and stored at -80°C.

4.2.2 Nuclei isolation and protein extraction

Refer to 3.2.3 and 3.2.4.

4.2.3 Co-IP for Western blotting

Frozen tissue was ground in liquid nitrogen in mortar and pestle. The powder then was mixed with ice-cold IP extraction buffer (50mM HEPES pH 7.4, 150mM NaCl, 1mM EDTA, 0.02% (v/v) NP40, 10% (v/v) Glycerol, 1µg/ml Leupeptin, 1µg/ml Pepstatin A, 1mM PMSF) by inversion and incubated for 5 min at 4°C. Cell debris was pelleted at 15,000g for 15min at 4°C. The supernatant was kept as total IP extract. The pellet was resuspended in SDS protein extraction buffer (50 mM Tris pH 6.8, 2% SDS, 10% Glycerol, 5 mM EDTA, 1µg/ml Leupeptin, 1µg/ml Pepstatin A, 1mM PMSF) and boiled for 5 min. The supernatant from boiled tubes was kept as indissoluble proteins after centrifugation at 12,000g for 10 min for examining extraction efficiency. The concentration of protein samples was measured with DC protein Assay (BioRad). 50µl Sepharose® 4B beads (Sigma-Aldrich) were washed with 1ml IP extraction buffer and pelleted at 500g, 4°C five times. 10µl Anti-FLAG M2 Affinity

Gel (Sigma-Aldrich) was washed with 1ml IP extraction buffer at 500g at 4°C twice and incubated with 1ml 0.1M glycine-HCL pH3.5 for 10 min. The gel was washed with 1mL IP extraction buffer three more times at 500g at 4°C. The pre-washed unconjugated resin was mixed with 1 mg protein of IP extract and incubated on a rotating shaker at about 12rpm at 4°C for 1hour. Incubated unconjugated resin was centrifuged at 750g for 1min at 4°C and the supernatant (kept as Input) was mixed with glycine-incubated M2 Affinity Gel. The mixture was incubated on a rotator overnight at 4°C. The affinity gel was precipitated by centrifugation at 750g, 1 min at 4°C. The supernatant was kept as Post-IP for capture efficiency examination. The affinity gel was washed three times with 1ml IP extraction buffer and boiled with 20µl SDS protein extraction buffer. The affinity gel was pelleted down at 750 g, 25°C and the supernatant was kept as IP-pulldown.

4.2.4 Western blotting

Refer to 3.2.5

4.2.5 SDS-PAGE gel staining

The SDS-PAGE gel was incubated with the staining solution (10% $(NH_4)_2SO_4$, 10% H3PO4, 20% methanol, 0.12% Coomassie brilliant blue G-250) on a rotating platform at 20 rpm overnight. The stained gel was washed in double distilled water until the bands were clear. The gel was briefly dried and scanned by a scanner.

4.2.6 Co-IP and Mass Spectrometry

The Co-IP method is similar to 5.2.3. 10mg proteins in 5ml IP extraction buffer from total IP extract were pre-cleared by 50µl pre-washed Sepharose beads in 5ml microcentrifuge tubes at 4°C for 1 hour. The supernatant was incubated with 10µl Anti-FLAG Affinity Gel overnight on a rotator at 4°C. The affinity gel was precipitated at 750g for 1 min at 4°C and washed with 1ml ice-cold IP extraction buffer three times. The gel then was rinsed with FLAG-rinsing buffer (50mM NH_4HCO_3 pH 8, 75mM KCl, 2mM EDTA) twice and stored at

-80°C. Frozen beads were sent to SPARC Biocentre (Hospital for Sick Children, Toronto, Canada) for the C18 column cleaning, ammonium hydroxide elution, trypsin digestion and LC-MS analysis. Four trials conducted by the optimized protocol were analyzed.

4.2.7 Data analysis

The results of MS were acquired in Scaffold software (Proteome Software, Inc). The sequences of peptides were aligned to NCBI *Neurospora crassa OR74A* protein database. The existence probability of chosen proteins for analysis were above 95%. Two methods were applied to select interacting proteins of PRD-1. First, proteins that had more than 3 appearances and had aggregated total spectrum counts which were at least twofold that of both controls were selected. In the second method, if the abundance of a protein from #588 was at least two times the abundance of one of the controls in a single experiment, the protein was assigned one valid count. Proteins that have more than 6 out of maximum 8 valid counts were selected.

4.3 Results

4.3.1 Nuclei isolation is not necessary for IP

In Chapter 3, #588 was shown to express sufficient PRD-1-FLAG for the immunodetection. Typically, SDS protein extraction buffer is used to extract as much protein as possible, but IP buffer extracts protein in a gentle manner to protect protein-protein interactions. Whether the IP buffer could extract sufficient amount of PRD-1-FLAG needed to be examined. Similarly, whether nuclei isolation could concentrate the PRD-1 protein needed to be analyzed. Therefore, I extracted proteins of #26 and #588 with IP buffer from both whole cell lysate and isolated nuclei pellets. The Western blotting results showed that the IP buffer was able to extract proteins from #588 but not thoroughly because a notable amount of PRD-1-FLAG could be extracted by SDS protein extraction buffer from the debris

(Figure 4.1). However, PRD-1-FLAG was not significantly concentrated after nuclei isolation, whereas the non-specific binding proteins were concentrated in nuclear extract of #26. This suggested that the nuclei isolation is not a necessary step before IP.

4.3.2 Capture efficiency of Anti-FLAG M2 Affinity Gel

Next, I tested the efficiency of M2 Anti-FLAG Affinity Gel binding to the PRD-1-FLAG protein. I prewashed the lysate with Sepharose beads to eliminate non-specific binding proteins. Prewashed sample (input) was incubated with M2 Anti-FLAG Affinity Gel overnight and washed with IP buffer. I boiled the beads with SDS buffer to elute proteins and loaded them on SDS-PAGE gel. The Western blot of #588 showed that unconjugated agarose beads did not substantially reduce the abundance of PRD-1-FLAG and 10µl affinity gel could pull down almost all the tagged PRD-1 protein (Figure 4.2a). Meanwhile, the non-specific binding proteins were enriched in the pulled-down proteins of wild type (#26).

I also stained the SDS-PAGE gel with Coomassie brilliant blue G-250 and tried to observe the pulled-down proteins from 10mg of total extract on the gel. The stained gel showed that proteins from the affinity gel were dramatically less than the input and several clear bands could be seen (Figure 4.2b). However, no isolated band could be observed at the putative position of PRD-1-FLAG based on the molecular weight marker.

The results demonstrated that the methods I used were functioning and the samples were acceptable for MS.

4.3.3 Candidates of PRD-1 binding partners

The pulled-down proteins binding on M2 Anti-FLAG Affinity Gel were sent to the SPARC Biocentre for MS analysis. The sample from #26 (WT) was used as the negative control. The sample from #444 (NCU05950-FLAG) was used as a control. Two methods were applied to select enriched proteins as described in 4.2.7. The lists from both selection methods are highly matched: 37 and 31 proteins were selected from the two methods and 29 of them appeared in both lists. The complete information of overlapped enriched proteins is

listed in Appendix E. In the candidate list, most of the binding proteins of PRD-1 are the proteins associating with ribosomes.

Proteins that are highly enriched (10 fold or more) in my sample are listed in Table 4.1. All the binding proteins were ribosomal proteins. Among these 10 candidates, 3 came from the small subunit and 7 came from the large subunit. 40S ribosomal protein S6 had the highest total count.

Table 4.1 List of candidates binding to PRD-1. Total spectrum counts of each protein from four independent trials are aggregated. Proteins from #588 that are 10-fold or more enriched compared to both controls are shown.

Gene Name	Identified Proteins	Total Spectrum Counts			Ratio of Enrichment	
		WT	NCU05950-FLAG	PRD-1-FLAG	PRD-1-FLAG/WT	PRD-1-FLAG/NCU05950-FLAG
NCU08502	40S ribosomal protein S6	1	4	69	69	17.25
NCU04779	60S ribosomal protein L8	6	6	63	10.5	10.5
NCU06843	60S ribosomal protein L3	1	4	47	47	11.75
NCU07829	60S ribosomal protein L7	0	1	44	∞	44
NCU00258	40S ribosomal protein S7	0	1	39	∞	39
NCU02707	60S ribosomal protein L6	0	2	35	∞	17.5
NCU00294	60S ribosomal protein L10a	0	1	31	∞	31
NCU02181	40S ribosomal protein S4	0	1	26	∞	26
NCU08389	60S ribosomal protein L20	0	2	21	∞	10.5
NCU01827	60S ribosomal protein L27	0	1	13	∞	13

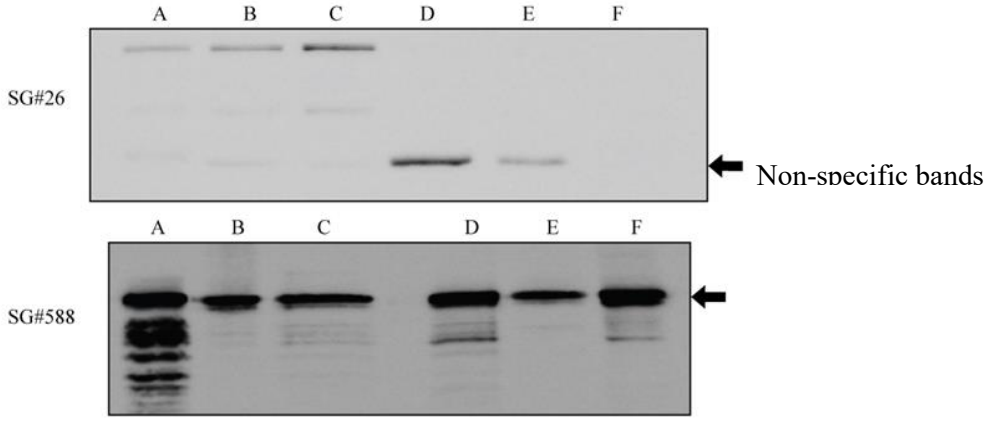

Figure 4.1 Western blotting results detected by Anti-FLAG antibody. 20μg protein was loaded on each lane. Arrows indicate where PRD-1 protein should be. Proteins of #26 (WT) and #588 (native-*prd*-1-flag) were extracted under different conditions. A: Total protein extracted by SDS buffer; B: Total protein extracted by IP buffer; C: supernatant of nuclei isolation (regarded as cytoplasmic protein); D: nuclear protein extracted by SDS buffer from isolated nuclei; E: nuclear protein extracted by IP buffer from isolated nuclei; F: remaining nuclear protein after IP buffer extraction extracted by SDS buffer.

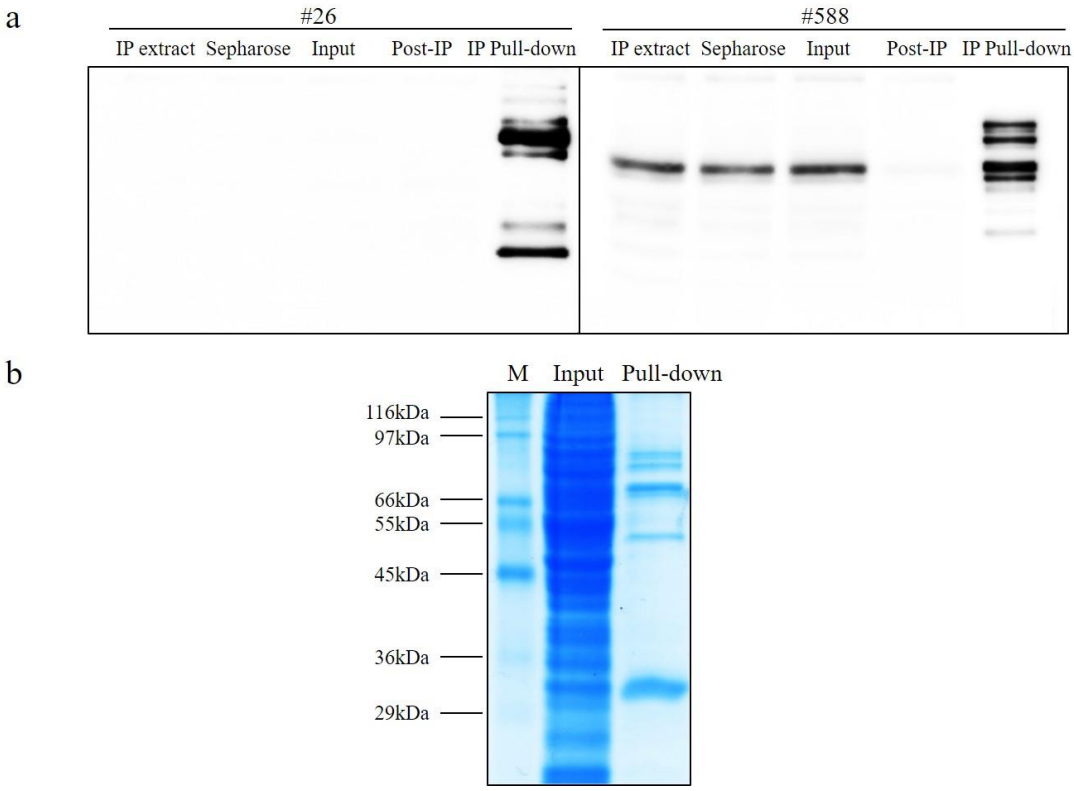

Figure 4.2 IP capture efficiency assay. a) Western blotting results detected by M2 Anti-FLAG antibody. 20µg IP extract protein, 20µg protein binding to Sepharose beads, 20µg Input protein, 20µl Post-IP supernatant and 20µl IP-pulldown protein from #26 (WT) and #588 (native-*prd*-1-flag) were loaded. b) Coomassie brilliant blue stained SDS-PAGE gel. 20µl wide range SigmaMarker (M), 20µl Input, all pulled-down proteins were loaded on the gel.

4.4 Conclusion

In this chapter, I conducted experiments for Co-IP and MS analysis to discover the interacting partners of PRD-1. The IP buffer is satisfactory for immunoprecipitation regardless of the relatively low extraction efficiency. The nuclei isolation is not a necessary step prior to Co-IP since PRD-1-FLAG was not highly concentrated in nuclear extract, even though the nuclear protein was enriched. I sampled from every step in Co-IP and found that the pre-clear step with Sepharose beads did not substantially decrease the concentration of PRD-1-FLAG and the M2 Anti-FLAG Affinity Gel could pull down most of the FLAG-tagged proteins.

Once the methods were validated, experimental samples with controls were sent for MS analysis. Based on objective standards, enriched proteins were selected. At the top of the list were ribosomal proteins from both subunits. Most of the candidate binding partners were ribosomal proteins. These results suggested that the PRD-1 protein may be one of the essential components in the ribosome and it may influence the phenotype by affecting ribosome biogenesis.

Chapter 5 Growth responses under different conditions

5.1 Introduction

The *prd*-1 mutant grows slower than wild type, suggesting that the *prd*-1 gene may regulate the growth of *Neurospora*. It is possible that the abnormal circadian rhythm of the *prd*-1 mutant is a response to mis-regulated growth. Evidence on the association between nutrient sensing and the circadian rhythms is emerging. The altered growth response of the *prd*-1 mutant to different nutrients may reveal the function of PRD-1 in metabolic regulation which could account for the abnormal circadian rhythm. Therefore, I planned to assay the growth response of *prd*-1 mutant on different media, attempting to discover hints for the function of the *prd*-1 gene.

5.1.1 The association between glucose concentration and the *prd*-1 gene.

Emerson's paper showed that the phenotype of the *prd*-1 mutant is altered in media with different carbon availability (Emerson et al., 2015). The period of *prd*-1^{-} shortened with decreasing glucose concentration from 1% to 0% whereas the wild type persisted with the normal period. They also reported that PRD-GFP will relocalize to the cytoplasm after starvation. These suggest that the *prd*-1 gene may function differently when the glucose concentration is changed. Hence, the *prd*-1 mutant by altering some of the functions of wild-type PRD-1 may cause a different growth response to the same medium.

5.1.2 The association between amino acids and the *prd*-1 gene.

The *prd*-1 mutant abolished the FRQ-less rhythm and the *prd*-1 gene is considered as a component of FLO. UV90, another gene that affects FLO, is found to be involved in the TOR pathway, which is crucial for nutrient sensing. Both glutamine and leucine stimulate TOR activity in mammals and yeast, with glutamine being the preferred nitrogen source for yeast (Stracka et al., 2014). In *N. crassa*, glutamine is also the preferred amino acid nitrogen source for growth. Glutamine is a nitrogen donor and a pivotal compound as a repressor of nitrogen

catabolism (Calderon and Mora, 1989). Arginine is another prominent nitrogen source in *N. crassa*. Large amounts of arginine are stored in the vacuole, and released when nitrogen is depleted (Davis and Weiss, 1988). I therefore chose to assay the effects of three amino acids: glutamine (Gln), arginine (Arg) and leucine (Leu).

5.1.3 The measurement of growth rate and growth limit

The growth of organisms can be affected by many environmental factors in many aspects. Two general parameters are commonly used to assess the growth: the growth rate and the growth limit. Typically, the growth curve is an S-shaped curve which could be defined by these two parameters. *Neurospora crassa* also displays the S-shaped growth curve. However, the growth curve varies with different culturing methods. To evaluate the growth response of *Neurospora* with different nutrient sources, the standard growth curve needs to be determined first under standard growing conditions. The growth curves with different nutrient sources will be compared to the standard curve.

The *prd*-1 mutant has a slower growth rate, thus has a distinct standard growth curve to the wild type. It is not feasible to detect the growth rate at every time point, but the average growth rate can be calculated through a division of the growth by the time required to reach that growth. It is difficult to track the exact time needed for the maximum growth under every condition and harvest the cells at the precise time. Hence, I planned to sample a time point at which the 50% maximum growth is reached on the standard curve to represent the growth rate. I also planned to sample a time point at which the maximum growth is reached on the standard curve to represent the growth limit.

5.2 Materials and Methods

5.2.1 Strains

#4 was considered as the wild-type strain and #170 was a *prd*-1 mutant strain. Both strains carried the *bd* mutation.

5.2.2 Culture

The Vogel's liquid medium contains ammonium nitrate (NH_4NO_3) as the only nitrogen supply. Different amount of glucose (0.125%-1%) or different amino acids (50mM Gln, Arg, Leu) were added into the liquid medium. For the media in which the amino acids are the only nitrogen source, the amino acids were added to Vogel's liquid medium without NH_4NO_3. 1000 fresh macrospores were inoculated into in 1ml liquid medium in 24-well plates and grown at 25°C with constant light.

5.2.3 The measurement of dry weight

The 1.5mL microcentrifuge tubes (Progene) were pre-dried at 80°C for two days and the weight of tubes was measured. The mycelia were collected through filtration and washed with double distilled water. Washed mycelia were then transferred into pre-dried tubes and desiccated at 80°C for two days and the weight of tubes containing dried tissues was measured. The dry weight of *Neurospora crassa* was the difference between these two measurements.

5.3 Results

5.3.1 The determination of the standard growth curve

Spores were inoculated to 1ml standard liquid medium (1% glucose Vogel's medium) and mycelia mats were harvested every 24 hours to track the growth curve. The samples were desiccated immediately for 2 days after harvesting. The growth curve of 6 days' growth is shown (Figure 5.1).

Both curves are 'S" shape. It took wild type about 2 days or the *prd*-1 mutant nearly 5 days to reach the growing plateau. The growth limit is about 4mg of WT and about 5mg of the *prd*-1 mutant. The growth rate at exponential stage looks similar. Referring to the standard curve, the time points to harvest half maximum growth that are on the midpoint of the ascent curve are about 36th hour for WT and about 90th hour for the *prd*-1 mutant. The time points to represent the growth limit at the stationary phase are around 52nd hour for WT and around 108th hour for the *prd*-1 mutant.

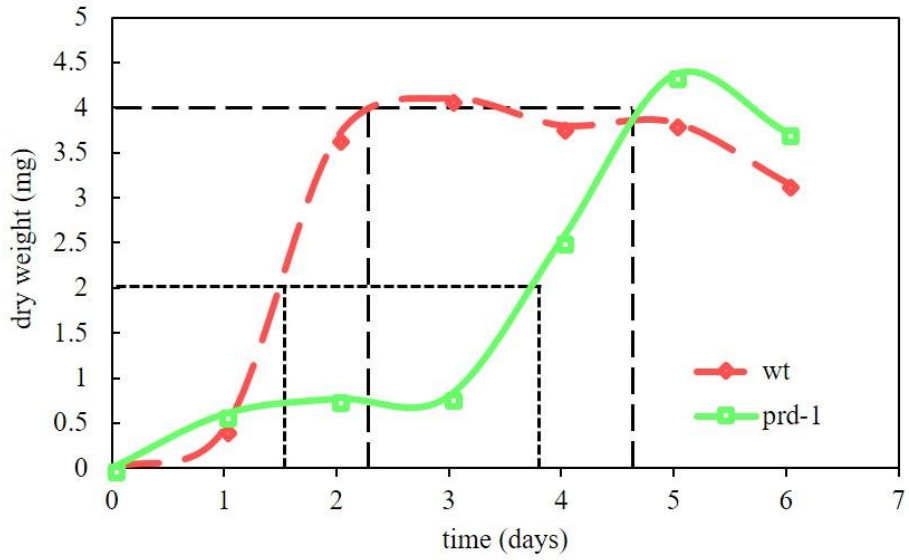

Figure 5.1 The standard growth curve in 1% glucose Vogel's medium. The dashed lines showed the half/maximum growth to determine the harvesting time points for subsequent experiments.

5.3.2 The growth response to glucose concentration gradient

The dry weights of mycelia grown in media with a gradient of glucose concentration were measured (Figure 5.2). I found that WT and the *prd*-1 mutant had parallel responses when glucose concentration decreased. The *prd*-1 mutant seems to be able to transform more glucose to mycelia even though the differences are not significant (P>0.05). The growth reached maximum when they were harvested at 36th hour with 0.25% and 0.125% glucose. Since the growth stopped when the glucose is used up, the data considered as half maximum growth cannot be analyzed.

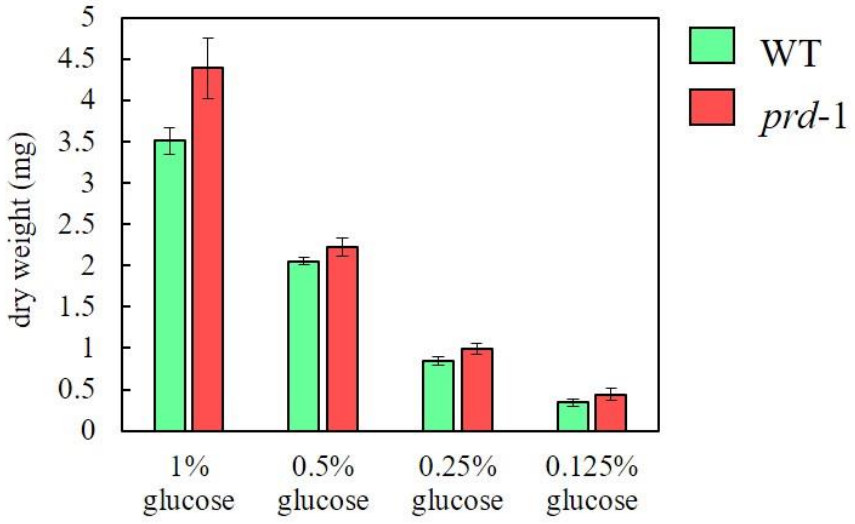

Figure 5.2 The maximum growth in Vogel's media with a gradient of glucose concentration. Samples were collected at 50th hour (WT, green) and 108th hour (*prd*-1^{-}, red). Means of dry weight ± SEM are shown. Data from three independent experiments were analyzed.

5.3.3 The growth response to amino acids

Intriguingly, when different amino acids were supplied in the Vogel's media with 1% glucose, different responses were seen (Figure 5.3).

In WT, when NH_4NO_3 was present, extra glutamine and arginine had no effect for the growth limit nor growth rate, whereas leucine suppressed the growth dramatically. When amino acids were the only nitrogen resource, glutamine and leucine cannot be assimilated efficiently and leucine scarcely can be used for growth; arginine maintained the normal growth limit but decreased the growth rate.

As for the *prd*-1 mutant, when NH_4NO_3 was present, glutamine promoted the growth slightly whereas arginine inhibited the growth in both aspects; unlike WT, leucine generated no effect on either growth limit or growth rate. When NH_4NO_3 was absent, glutamine inhibited the growth limit but not growth rate; arginine inhibited the growth at both levels; leucine also inhibited the growth to the same extent as arginine.

The trends can be observed directly in Figure 5.4. The growth curves of both strains were simulated based on collected data. In the standard condition (NH_4NO_3), the curve of *prd*-1$^-$ can be considered as stretched in the X-axis and slightly elevated in the Y-axis compared to WT (portrayed in green). With glutamine in the medium, the growth curve of *prd*-1$^-$ can be generated from the curve of WT the same way as described in the standard condition. However, with arginine in the medium, the curve of *prd*-1$^-$ is suppressed in the Y-axis compared to WT. With leucine, the curve of *prd*-1$^-$ is dramatically elevated in the Y-axis compared to WT. These data demonstrate that the *prd*-1 mutant responds differently with arginine and leucine present in the medium.

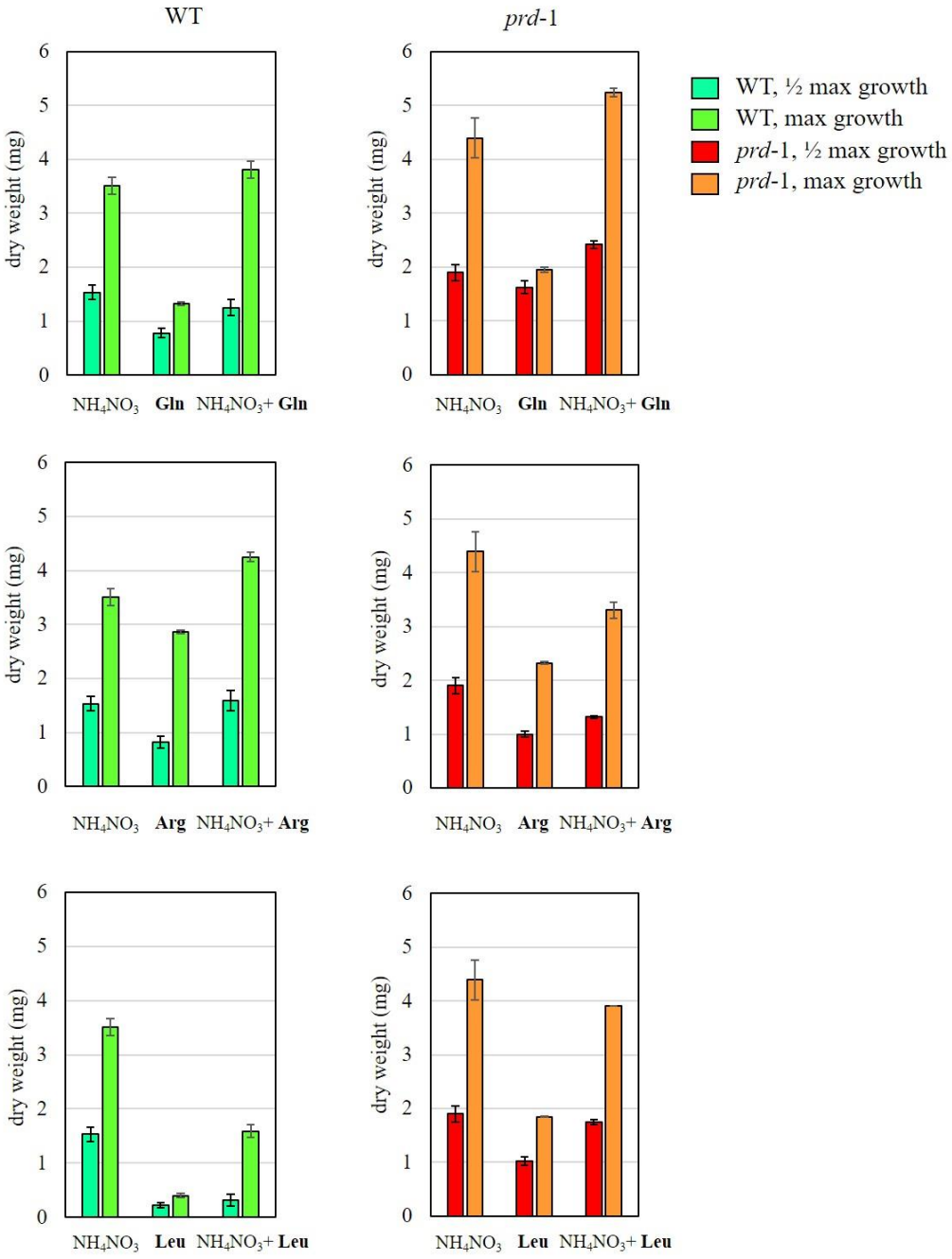

Figure 5.3 The growth in Vogel's media with 50mM amino acids. Samples of half maximum growth (darker left bars) were collected at 36th hour (WT, green, left panel) and 90th hour (*prd*-1^{-}, red, right panel). Samples of maximum growth (brighter right bars) were collected at 50th hour (WT, green, left panel) and 108th hour (*prd*-1^{-}, red, right panel). Means of dry weight ± SEM are shown. Data from three independent experiments were analyzed.

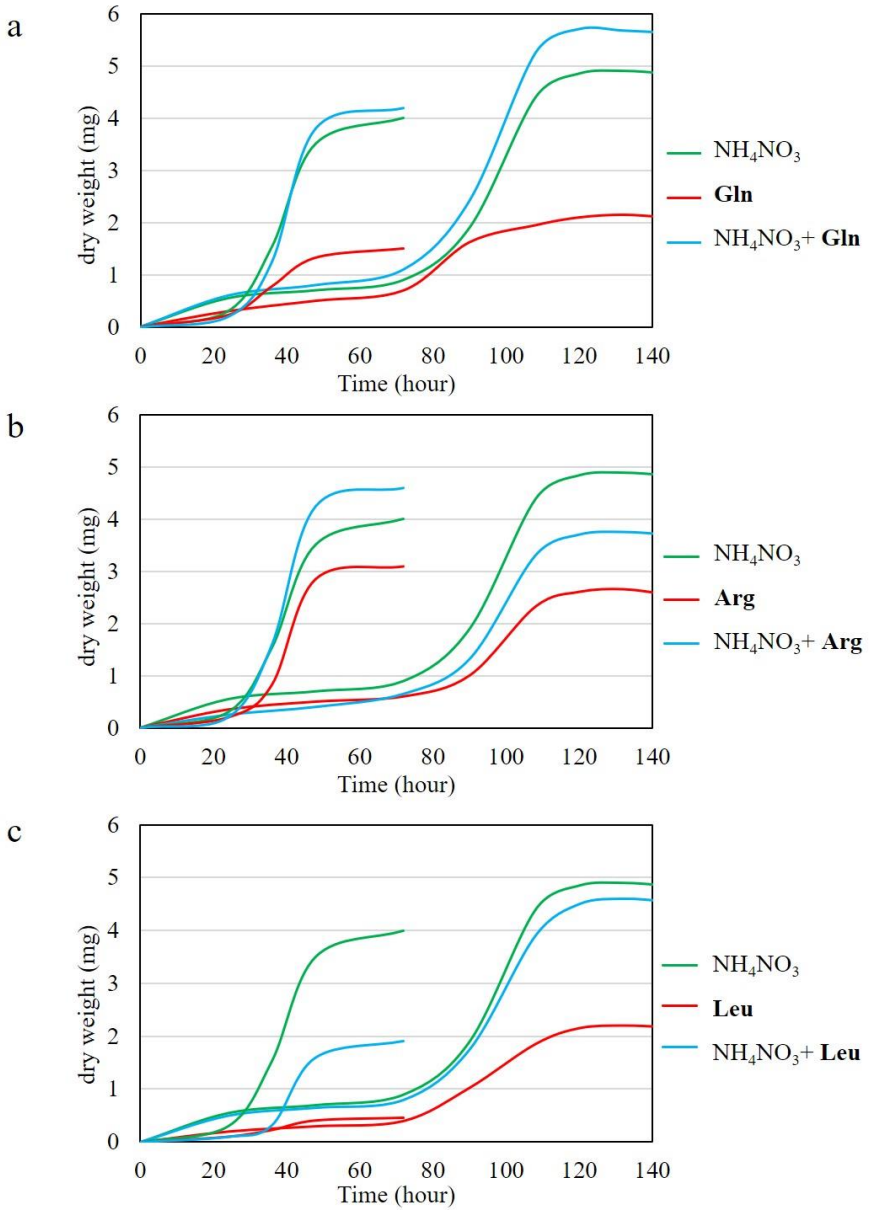

Figure 5.4 Simulated growth curves of WT (0-72h) and *prd*-1^{-} (0-140h) strains in Vogel's liquid media with 1% glucose and 50mM glutamine (a), arginine (b) and leucine (c). The curves were smooth fit lines of scatter plots generated by Microsoft Excel based on the data collected in Figure 6.3 and Figure 6.1

5.4 Conclusion

In this chapter, I attempted to examine whether the *prd*-1 mutant impacts nutrient sensing which could influence the growth pattern and the circadian rhythms. Dry weight of the mycelia harvested at two time points for each strain was measured based on the standard curves.

In the media with a gradient of glucose concentration, the growth pattern of the *prd*-1 mutant behaved the same as the wild type. This result suggests that the *prd*-1 gene does not function in the glucose-sensing pathway. The relocalization of PRD-1-GFP and the change of period under different abundances of glucose may be the downstream responses to the altered growth.

In the media with different amino acids, the *prd*-1 mutant displayed distinct growth patterns to those of wild type. When NH_4NO_3 was present, both strains behaved alike with extra glutamine; however, they reacted conversely with extra arginine and leucine. When the amino acids are the sole nitrogen source, the wild type cannot utilize glutamine and leucine efficiently but does use arginine for the standard growth. The *prd*-1 mutant, intriguingly, showed a similar assimilation efficiency on all three amino acids regardless of faster growth rate with glutamine.

These data suggest that the *prd*-1 mutation affects nutrient-sensing or metabolic pathways of *N. crassa* resulting in different growth responses.

Chapter 6 Discussion

The *prd*-1 mutant was found to lengthen the period of the circadian rhythm and to reduce the growth rate. Most of the work on the circadian clock in *Neurospora crassa* has been conducted involving the *frq* gene which is considered as the core regulator in the circadian oscillator, but how the *prd*-1 mutant affects the circadian rhythm was poorly understood. When the FRQ-WCC oscillator is disabled, rhythms can still be observed, which suggests that a FRQ-less oscillator exists. The *prd*-1 mutant also disrupts the FRQ-less rhythm. Therefore, studying the function of the *prd*-1 gene helps us to understand the mechanism of circadian rhythm regulation.

Although the *prd*-1 gene has been identified as a homologue of DEAD-box RNA helicases, there is still limited information to clarify in which biological processes the *prd*-1 gene is involved. Building on previous research, in my project I tried to obtain a *prd*-1 knock-out strain; I constructed strains expressing FLAG-tagged PRD-1 protein and assayed the rhythmicity of its expression; I performed co-IP to pull down the proteins binding to PRD-1 and identified them by MS analysis; I examined the growth response of the *prd*-1 mutant to different glucose concentrations and amino acids; and I attempted to construct the C-terminus deleted *prd*-1 strain. The results of these various experiments outlined an approximate profile of the function of *prd*-1.

6.1 Lethality of *prd*-1^{KO}

The failure to purify the *prd*-1^{KO} homokaryon indicated that *prd*-1 is an essential gene for survival. The PRD-1 protein consists of 4 domains: N-terminus, DEAD/DEAH box domain, helicase domain and C-terminus. The absence of all four domains in the *prd*-1^{KO} resulted in the lethality. However, more than one DEAD-box RNA helicase is expressed in the cell, especially FRH, one that is not essential but affects the circadian rhythm by binding to FRQ. The helicase activity of FRH is not required for its function in the circadian clock

(Cheng et al., 2005). This implies that the DEAD-box and the helicase domain may be dispensable and the N- or C-terminus has effects that may be crucial for the clock function. The C-terminus is the eye of storm as well because the point mutation is located in the C-terminus and causes altered amino acid sequences of PRD-1 in the mutant. The failure to purify the C-terminus deleted *prd*-1 homokaryons demonstrated that the C-terminus is indispensable for the intact function of PRD-1 as expected. The N-terminus may also be important for the function of PRD-1 but the study of it is a lower priority since no evidence showed the N-terminus affects the circadian rhythm.

6.2 Dose effect of the expression of *prd*-1

In the *prd*-1 mutant, a small amount of wild-type *prd*-1 mRNA was detected76. The *prd*-1^{KO} heterokaryon possessed only a small proportion of wild-type nuclei under the stress of hygromycin selection (Figure 2.2). These data suggested that a small number of genomic copies of wild-type are sufficient for survival. Are they sufficient to maintain the circadian rhythm? The hypothesis is that a low expression level of *prd*-1 leads to the long period of the rhythm. In the *prd*-1 mutant, the expression of wild-type mRNA is very low since most of the pre-mRNA would be spliced aberrantly. The minimum amount of PRD-1 protein may need to be produced to maintain survival. The result of the Northern blot that the total expression of *prd*-1 mRNA in the mutant was much higher than that in wild type supported that (Figure 3.15). If the hypothesis is correct, normal expression level would lead to a wild-type period and overexpression of *prd*-1 would cause a shorter period. In Chapter 3, I constructed several strains carrying more than one copy of the wild-type *prd*-1 gene in a single nucleus. The periods of these strains were various – longer or shorter than the wild type. In contrast to the hypothesis, the strain with *ccg*-1 promoter which was expected to have the highest expression level showed the longest period. Although some unknown factors (such as the expression efficiency of each copy of *prd*-1 in one nucleus and the potential

effects of the FLAG tag) may contribute, no clear association could be found between the period of the circadian rhythm and the abundance of PRD-1.

6.3 Fluctuation of PRD-1-FLAG

The circadian rhythmic expression of a gene reflects a close association with the circadian clock. I assayed the rhythmicity of the mRNA and protein of *prd*-1 in Chapter 3. Neither one fit into the pattern of a circadian rhythm. A fluctuation of PRD-1-FLAG was found from the samples in constant dark while the *prd*-1 mRNA did not fluctuate. The lack of correlation between the expression level of the *prd*-1 mRNA and PRD-1 protein suggested post-transcriptional regulation of the *prd*-1 gene. Once the mRNA is synthesized, it will be transported to the cytoplasm for translation. The accumulation of a protein is modulated by many factors in the processes. The efficiency of transportation and translation initiation determine the synthesis of the protein. The post-translational modifications such as phosphorylation, ubiquitination and acetylation determine the decay of the protein. Hence, further study is needed to understand the post-transcriptional regulation of the *prd*-1 gene.

The samples for the assay of rhythmicity were collected every four hours and the expression levels were detected *in vitro*. Even though every effort was made to reduce the error during the experiment, the variation was still high among independent experiments. A proper reporter to demonstrate the expression levels of the *prd*-1 gene *in vivo* would be helpful to confirm these results.

6.4 The role of PRD-1 in ribosome-associated biological processes

The binding partners of PRD-1 provide direct clues for understanding its function. In Chapter 4, I performed co-IP and MS analysis to discover the proteins interacting with PRD-1. Ribosomal proteins from both subunits were found in the list. The results indicate that PRD-1 plays a role in ribosome-associated biological processes.

Taking the localization into account, PRD-1 may have two potential functions. In the nucleus PRD-1 may be a key component or a scaffold of ribosome biogenesis. PRD-1may be a component in both small and large ribosome subunits. Due to RNA helicase activity, PRD-1 may also bind with rRNAs which are the skeleton to form a ribosome. In the cytoplasm, PRD-1 may be an essential element in the translation machinery. Small and large subunits assemble when translation initiation factors bind to mRNAs. In this huge complex, ribosomal proteins and PRD-1 may cooperate to accomplish the translation. It is reported that PRD-1 is a nuclear protein so that the first role may be closer to the truth. However, it is also reported that PRD-1 was found in the cytoplasm when the hyphae were starved. Moreover, during protein extraction, the cells were homogenized and proteins from either the nucleus or the cytoplasm may seize the chance to bind onto PRD-1. Thus, I cannot draw conclusions about the functions of PRD-1 until more evidence is discovered. But at least, it is convincing that the PRD-1 protein is able to physically bind to ribosomal proteins.

DEAD-box RNA helicases are extensively implicated in ribosome biogenesis. 19 putative DEAD-box RNA helicases were considered to function in ribosome synthesis in yeast (Martin et al., 2013). In human cells, it was experimentally supported that several DEAD-box RNA helicases such as DDX3, DDX5, DDX10, DDX24, DDX47 were involved in ribosome biogenesis pathways (Linder and Jankowsky, 2011). PRD-1 is a DEAD-box RNA helicase and is homologous to DBP2 in yeast, DDX5 and DDX17 in mammals (Adhvaryu et al., 2016, Emerson et al., 2015). DBP2 has been implicated in ribosome synthesis and mRNA metabolism (Bond et al., 2001). DDX5 localizes to nuclei and nucleoli and is closely related to DDX17. The two helicases can form a heterodimer which is important in processing of the 32S rRNA precursor and 5.8S rRNA (Martin et al., 2013). Since the ribosome biogenesis pathway is highly conserved in eukaryotes, PRD-1 probably functions in ribosome biogenesis as well in *Neurospora*.

The heterokaryotic C-terminus deleted *prd*-1-flag strain could help us confirm the result

as well. In the heterokaryon, both wild type and partially deleted genes are expressed. If the C-terminus is the region that binds to ribosomal proteins, the list of binding partners to the truncated protein should be shortened or altered. The missing candidates between lists would give us information about the binding proteins of C-terminus, which may lead us to the function of PRD-1. If the same proteins showed up, which means DEAD-box domain and the helicase domain may be the binding site, the C-terminus probably is important for regulating the activity of PRD-1.

PRD-1 may also interact with the rRNAs. RNA IP-sequencing may be required to identify the composition of the RNAs and give more information on the function of PRD-1.

6.5 The potential role of PRD-1 in nutrient sensing

Evidence has been found to associate FLO with the nutrient sensing pathway as mentioned in Chapter 5. Growth experiments were conducted to assay the growth responses of the *prd*-1 mutant to different media. The *prd*-1 mutant behaved significantly differently from the wild type when arginine or leucine was present.

Arginine, which is the main nitrogen stock in the vacuole of *Neurospora*, inhibited the growth of the mutant. When excessive amino acids or nitrogen are absorbed in the cell, the extra will be converted to arginine or ornithine and stored in the vacuole (Davis, 1986). When the amino acids in the cytosol are depleted, the stored arginine will be released into the cytosol. The growth of the *prd*-1 mutant was inhibited by arginine in the media with and without ammonium nitrate, implying that the mutant could not utilize arginine efficiently for growth, or the mutant altered the regulation pathway so that the arginine functioned as a growth repressor instead of an enhancer.

Leucine, which stimulates TOR activity in mammals and yeast (Stracka et al., 2014), is not a preferred nitrogen resource in *Neurospora*. In contrast to glutamine, which is also a signal to stimulate the TOR pathway and promote growth, leucine dramatically inhibits the

growth of *Neurospora*. By itself it could scarcely be assimilated by *Neurospora* as shown in Figure 5.3. Intriguingly, the *prd*-1 mutant seems to be immune from the impacts of leucine. The additional leucine no longer suppressed the growth of the mutant. Leucine supplied as the only nitrogen source in the media could be utilized as efficiently as glutamine and arginine. These results suggest that in the *prd*-1 mutant, the nutrient sensing and metabolic pathways are dramatically altered. The inhibitory activity of leucine may be erased or bypassed. The catabolism of leucine somehow is reactivated even if it is barely possible that a novel catabolic pathway is created in the mutant. Unknown links among leucine, *prd*-1, the TOR pathway and other metabolic pathways are waiting to be discovered.

6.6 *Prd*-1 and the regulation of the circadian rhythm

So far I have discovered that the *prd*-1 gene is associated with ribosome-related processes and metabolic pathways of arginine and leucine, indirectly associated with the circadian clock and that the intact *prd*-1 gene especially the C-terminus is essential for its function relating to viability. However, it is still poorly understood why the circadian rhythm is altered in the *prd*-1 mutant and some *prd*-1-flag transformants.

Recently, crosstalk between metabolism and the circadian clock in mammals has been addressed more frequently. It has been reviewed that disruption of clock genes results in metabolic dysregulation (Huang et al., 2011). Some studies hint that amino acid metabolism may participate in the regulation of the temporal organization of feeding and the circadian clock. Studies have demonstrated that the cellular nutrient status can be relayed to the circadian clock by various nutrient sensors (Huang et al., 2011). In mammals, the mTOR pathway is a prime target to make a breakthrough to understand the crosstalk. The mTOR in the central nervous system (CNS) is present in the arcuate nucleus neurons modulating food intake (Cota et al., 2006). The expression of mTOR is activated by light within pacemaker neurons of the SCN (Cao et al., 2010). The light induction of the *Period* gene within the SCN

is altered when mTOR is inhibited (Cao et al., 2010).

My first hypothesis is that the alteration of the phenotype in the mutant is a consequence of effects on TOR pathway caused by the low expression of the wild-type *prd*-1 protein. From the MS analysis, ribosomal protein S6 is at the top of the candidate list. The S6 kinase in mammals or the homologue Sch9 in yeast is a substrate that could be phosphorylated by TOR complex 1 (Loewith and Hall, 2011). The activated S6 kinase phosphorylates the ribosomal protein S6 and stimulates anabolism which promotes growth. Since PRD-1 could physically bind to ribosomal protein S6, the *prd*-1 gene may play a crucial role in regulation downstream of the TOR pathway. Incorporating the association between the TOR pathway and the circadian clock, it is possible that the down-regulated TOR pathway in the *prd*-1 mutant lengthens the period and alters the period under different glucose concentrations. The dose effect could be included in this model. To verify this hypothesis, the phenotype of an inducible *prd*-1 knock-down strain will be informative.

In spite of some clues that the TOR pathway may affect the circadian clock, it is still unknown whether the impact of downstream regulation of the TOR pathway caused by the mutated PRD-1 indeed causes the change of the circadian rhythm. My second hypothesis is that the limited amount of PRD-1 in the mutant merely induces the slow growth rate due to its putative function in ribosome biogenesis and translation regulation; the circadian clock is not directly impacted by the low expression of the wild-type PRD-1. Since the C-terminus is essential for survival, the mutated PRD-1 protein cannot function normally whereas the wild-type PRD-1 functions normally and only the rate of growth is decreased. In this situation, the function of the mutated PRD-1 protein is the key to understand why the period is changed in the mutant. If the mutated C-terminus is dysfunctional, my first hypothesis will be the most possible explanation to the altered phenotype. If the mutated PRD-1 does influence the biological processes related to ribosomal protein S6, then the interaction between the TOR pathway and the mutated protein need to be verified. In both hypotheses, investigating the

mechanism of the regulation of the circadian clock by the TOR pathway is pivotal to build up the models.

My third hypothesis is that the mutated PRD-1 possesses 'neomorph functions' which might be the origin of the period change. The mutated PRD-1 may interact with something else that could directly influence the circadian clock. In this case, every mutated protein produced from the variety of mis-spliced mRNAs of *prd*-1 needs to be inspected for its potential effects on the circadian clock.

6.7 Future Work and Perspective

In this thesis, I discovered that the expression of the *prd*-1 gene is not circadianly rhythmic; that the C-terminus of the *prd*-1 gene is crucial for its function; that the binding partners of the protein product of the *prd*-1 gene are ribosomal proteins and that the strain with the mutated *prd*-1 gene responds differently to arginine and leucine. However, more experimental work needs to be carried out to confirm the results or to test the hypotheses.

In Chapter 3, only one strain which behaves most closely to the wild type was used for the time-series experiments to investigate the rhythmicity of the *prd*-1 gene. The strain (#588) carries wild-type *prd*-1 genes at both the native locus and *his*-3 locus, which might affect the circadian rhythm. In the future, the *prd*-1^{+}-flag KI strain would be better for assaying the rhythmicity of *prd*-1 expression to confirm the results.

To test the hypothesis that the *prd*-1 gene has a dose effect on the circadian rhythm and low expression level of PRD-1 causes the period alteration, I propose to construct an inducible *prd*-1 knock-down strain since the growth might be impaired by the knock-down. The expression level of *prd*-1 can be regulated by the inducible promoter and the period might vary with different levels of *prd*-1 expression.

To verify the association between the TOR pathway and the circadian rhythm, the phenotype of knockout strains of ribosomal protein S6 and S6 kinases may provide us with

some clues, since the ribosomal protein S6 kinases are major downstream effectors of the TOR complex (Loewith and Hall, 2011) and PRD-1 can bind to ribosomal protein S6.

In Chapter 4, the binding partners of PRD-1 were found to be ribosomal proteins. To confirm the results, some other techniques may be applied such as Bioluminescence / Fluorescence resonance energy transfer (BRET / FRET), reciprocal Co-IP, or Luciferase Complementary Imaging System. Other strains expressing PRD-1-FLAG could be used for Co-IP/MS to double-check the results. Taking the RNA helicase activity into account, RNA-IP/RNA-seq could be conducted to assay what RNA is binding to PRD-1. If the PRD-1 protein binds to rRNA, it would be more convincing that PRD-1 plays a key role on ribosome assembly.

In Chapter 5, the abnormal growth response to arginine and leucine suggested an interaction between amino acid sensing (specifically the TOR pathway) and the *prd*-1 gene. To confirm the results, different concentrations of amino acids could be added to the media and harvesting time may be optimized from medium to medium so that the real maximum growth could be obtained. To better understand the relationship between PRD-1 and the TOR pathway, growth experiments of strains possessing deficient TOR pathway could be carried out under the same conditions. If the deficient strains react similarly to the *prd*-1 mutant, I would be more confident to conclude that the PRD-1 protein can affect the amino acid sensing pathway.

In Chapter 2, I demonstrated that the C-terminal deletion of *prd*-1 is lethal, which suggests that the C-terminus of PRD-1 is indispensable for its function. The results of Co-IP/MS of the heterokaryon expressing truncated PRD-1-FLAG might help us to understand the reason for the lethality. The proteins missing from the list could indicate the impact of C-terminal deletion via impaired binding capability, which might inform us about the function of PRD-1.

Moreover, the hypothesis that mutated PRD-1 proteins have null function has not been

tested. The phenotypes of strains expressing each mutated PRD-1 protein and the binding partners of each need to be examined. To achieve this goal, each alternatively spliced mRNA sequence that leads to a mutated PRD-1 protein should be knocked into the *prd*-1 locus.

In my view, the current mainstream model of the circadian oscillator is too succinct to be true. It has been verified that circadian rhythms could be entrained by many zeitgebers, for instance, light, temperature and food availability. In mammals, "different zeitgebers may exert differing effects on circadian entrainment in the brain and peripheral tissues, leading to distinct effects on phase and amplitude of gene oscillation within these locales" (Huang et al., 2011), and the trend is for more research to be carried out on the circadian clock. In *Neurospora*, the FRQ-WCC oscillator is well characterized and is tightly interacting with light entrainment. However, the appearance of the FRQ-less rhythm indicates that there must be more than the FRQ-WCC oscillator. The effect of nutrition on the output of the circadian clock has been noticed decades ago but not an effect on the oscillating mechanism. The study of the *prd*-1 gene gives direct evidence linking the nutrient sensing pathway to the circadian clock, which could be a key to open the blackbox of the FLO.

Appendices

Appendix A: Genotype of the Strains

#1 *bd* (mat a)

#4 *bd* (mat A)

#26 *csp*-1; *chol*-1 *bd* (mat a)

#80 *csp*-1; *chol*-1 *bd* ; frq^{10} (mat a)

#170 *prd*-1; *bd* (mat A)

#260 *csp*-1; *prd*-1; *chol*-1 *bd* (mat a)

#274 *csp*-1 *his*-3; *chol*-1 (mat a)

#310 *csp*-1 *his*-3; *prd*-1; *chol*-1 *bd* (mat a)

#438 *rid*^delta ::hph^+ *his*-3::lpl^delta (5192-6040) ::hph^+::tk^+ ::flag-pcna; *inl*

#444 *csp*-1 *his*-3^+::$P_{ccg\text{-}1}$::NCU05950$^+$-flag; $NCU05950^{KO}$; *chol*-1 *bd* (mat a)

#471-476* *csp*-1 *his*-3^+:: $P_{ccg\text{-}1}$::*prd*-1^+-gfp ; *chol*-1 *bd* [ccg-*prd*-1-flag]

#477-479* *csp*-1 *his*-3^+*::* $P_{prd\text{-}1}$*::prd*-1^+-flag*; chol*-1 *bd* [native-*prd*-1-flag]

#480 *csp*-1 *his*-3^+:: $P_{ccg\text{-}1}$::prd-1^+-gfp ; *prd*-1; *chol*-1 *bd* (mat a)

#484-486* *csp*-1 *his*-3^+*::* $P_{prd\text{-}1}$*::prd*-1^+-flag*; chol*-1 *bd* [native-*prd*-1-flag]

#490 *csp*-1 *his*-3^+::$P_{prd\text{-}1}$::*prd*-1^+ ; *prd*-1; *chol*-1 *bd* (mat a)

#493-495*	*csp*-1 *his*-3^{+}:: $P_{ccg\text{-}1}$::*prd*-1^{+}-gfp ; *chol*-1 *bd*	[ccg-*prd*-1-flag]
#505-507*	*csp*-1 *his*-3^{+}:: $P_{ccg\text{-}1}$::*prd*-1^{+}-gfp ; *chol*-1 *bd*	[ccg-*prd*-1-flag]
#518	heterokaryon of [(*csp*-1 *his*-3^{+}::$P_{ccg\text{-}1}$:: rfp-*vam*-3; *chol*-1 *bd*), (*csp*-1 *his*-3^{+}::Pccg-1:: NCU05950-gfp; *chol*-1 *bd*; NCU05950^{KO})]	
#519*	*csp*-1 *his*-3^{+}*::* $P_{prd\text{-}1}$*::prd*-1^{+}-flag*; chol*-1 *bd*	[native-*prd*-1-flag]
#520*	*csp*-1 *his*-3^{+}*::* $P_{prd\text{-}1}$*::prd*-1^{+}-flag*; chol*-1 *bd*	[native-*prd*-1-flag]
#567	*his*-3; Δ*mus*-51:: bar^{+} (mat A)	
#586	*csp*-1 *his*-3^{+}::$P_{ccg\text{-}1}$::*prd*-1^{+}-flag ; *chol*-1 *bd* (mat a)	
#587	*csp*-1 *his*-3^{+}::$P_{ccg\text{-}1}$::*prd*-1^{+}-flag; *chol*-1 *bd*; *frq*^{10} (mat a)	
#588	*csp*-1 *his*-3^{+}::$P_{prd\text{-}1}$::*prd*-1^{+}-flag ; *chol*-1 *bd* (mat a)	
#589	*csp*-1 *his*-3^{+}::$P_{prd\text{-}1}$::*prd*-1^{+}-flag ; *prd*-1; *chol*-1 *bd* (mat a)	

*: Strains that were mis-labeled in the stock. Old names are in the spare parentheses.

Appendix B: Recipes

Trace element solution

In 95 ml distilled water, dissolve successively with stirring, at room temperature:

5 g Citric acid.$1H_2O$

5 g $ZnSO_4.7H_2O$

1 g $Fe(NH_4)_2(SO_4)_2.6H_2O$

0.25 g $CuSO_4.5H_2O$

0.05 g $MnSO_4.1H_2O$

0.05 g H_3BO_3 (anhydrous)

0.05 g $Na_2MoO_4.2H_2O$

Store in a stoppered bottle at room temperature, with 1 ml chloroform added as preservative.

Biotin stock solution:

Dissolve 5 mg biotin in 50 ml water or 50% ethanol. Tube 2.5 ml aliquots and store at -20°C.

50× Vogel's salt

755 ml water

125 g Na_3 citrate.$2H_2O$

250 g KH_2PO_4

100 g NH_4NO_3

10 g $MgSO_4.7\ H_2O$

5 g $CaCl_2$. $2H_2O$ (dissolved)

5 ml trace element solution

2.5 ml biotin stock solution

Dissolve constituents successively. Moderate heating is useful in speeding solution of the citrate and phosphate. Dissolve the calcium chloride separately in 20 ml water and add the solution slowly. Add about 5 ml chloroform as preservative and store the solution at room temperature. Dilute with water to 1× working solution to make Vogel's medium.

SC medium

For 2× stock, dissolve the following successively in 3 liters water:

6.0 g KNO_3

4.2 g K_2HPO_4 (anhydrous) (or K2HPO4.7 H2O) (5.49 g)

3.0 g KH_2PO_4 (anhydrous)

3.0 g $MgSO_4.7H_2O$
0.6 g NaCl
0.6 g $CaCl_2.2H_2O$ (dissolved separately)
0.3 ml biotin stock solution
0.6 ml trace element stock solution
Add 2 ml chloroform as preservative and store at 4°C.

12% SDS-PAGE

Separating gel:

Total volume	5.0 ml
Water	2.17 ml
1.5M Tris pH 8.8	1.25 ml
10% SDS	0.05 ml
40% acrylamide	1.50 ml

Add just before pouring:

10% APS	25 µl
TEMED	2.5 µl

Stacking gel:

Total volume	2.5 ml
Water	1.55 ml
0.5 M Tris pH 6.8	647 µl
10% SDS	25.9 µl
40% acrylamide	259 µl
0.4%Bromphenol blue stock	2.5 µl

Add just before pouring:

10% APS	12.9 µl
TEMED	2.59 µl

Fill up space above separating gel with stacking gel and insert comb to correct depth. Allow at least 30 min to polymerize.

Appendix C: Primer Information

native-prd-1 up-F (Not I):

AAGAATGCGGCCGCCTATAGAATGTGGTCAAGATTACAGAT

native-prd-1 up-R (Xba I):

ACGTCTAGAGACAAGAACCAAACGACACGCGTGAAG

PacI-NCU07839-3503-R (PacI(3xFLAG+7839)):

CCTTAATTAA CCACCGGCGGTTGTTAAGCGGA

SpeI-NCU07839-1040-F (SpeI(3xFLAG+7839)):

GGACTAGT ATGTCCGGATCTTACGGCGGC

rc 5r prd-1KO: GGTTCTTGTCTCTAGACGTC

rc 3f prd-1KO: CCTGTAGATGAGACTTTCCG

NCU07839-3136-F (Primer-F11): CTGCCATTACTTTCTTCACCACTGACA

pBM61-1: ATTCAGACCCCATTAGCCGTCCACGCC

His3-F1: TAGGTGGGAACGCTTGTATTGC

His3-R2: TTCAGGCTATTGAGGACGAGGTTC

NCU07839-1423-F: GAACTGGGACATGAGCGCTCTTCCC

NCU07839-1636-R: AGGGAAACCCTGAGCCTTGACCTCG

NCU07839-1662-F: GCTGGCCCATGGCCCTTTCTGGT

NCU07839-3161+Gly-R: TCCGCCGCCTCCGCCGTCAGTGGTGAAGAAAGTAAT

NCU07839-3161+Gly-F: ATTACTTTCTTCACCACTGACGGCGGAGGCGGCGGA

Flag+T trpC-R:

GAGGTAATCCTTCTTTCTAGAGGATCCTCACTACTTGTCATCGTCATCCTTGT

AGTCG

Flag+T trpC-F:

CGACTACAAGGATGACGATGACAAGTAGTGAGGATCCTCTAGAAAGAAGGA

TTACCTC

P trpC+downstreamNCU07839-R:

TTAGACAGCGAGCTAGGACAGAGACCTACCGTCGACAGAAGATGATATTGA

AGG

P trpC+downstreamNCU07839-F:

CCTTCAATATCATCTTCTGTCGACGGTAGGTCTCTGTCCTAGCTCGCTGTCTAA

Downstream NCU07839-R: TACGTAACCTTAGGGTCTCTACCGGTTCTATCCC

NCU07839-1600-F: CTACGTTATGGACGAGGTCAAGGCTC

NCU07839-2181-F: TCATCCAGGTCAACATCGGTTCCAT

NCU07839-2259-R: GACTCGGAAACAACCTCGACGATCT

NCU07839-2661-F: CGTGTCGACTTGGTCTATCTGAGTG

NCU07839-2733-R: GGGCGTAGCATAGTCCACTGTTTCT

T trpC-F1: ACCGTTGATCTGCTTGATCTCGTCTC

T trpC-R1: GCATTGACTGCAACCTAGTAACGCC

Hph-F1: CGAGTACTTCTACACAGCCATCGGT

Hph-R1: GGCAATTTCGATGATGCAGCTTGGG

Hph-F2: GTCGTCCATCACAGTTTGCCAGTGA

Hph-R2: GGACCGCAAGGAATCGGTCAATACA

Hph-F3: CCCTCCTACATCGAAGCTGAAAGCA

Hph-R3: ATGAAAAAGCCTGAACTCACCGCGA

Downstream NCU07839-F1: AATGAGCAACCTCCAACCACGTTTTG

Downstream NCU07839-R1: TGGCCATTCAGCAAAATCAACACCG

Downstream NCU07839-F2: CCGGGTTAAAAGAAGTAATGCGACCC

Downstream NCU07839-R2: CTTATAGGCGAACGGGCAAATCGTT

Downstream NCU07839-R3: ACGTAACCTTAGGGTCTCTACCGGT

NCU07839-3161+ PacI-R: GCCCTTAATTAAGTCAGTGGTGAAGAAAGTAAT

PtrpC+NotI-R: GACCTGCGGCCGCACCGTCGACAGAAGATGATATTGAAGG

NotI+downstreamNCU07839-F:

ACGGTGCGGCCGCAGGTCTCTGTCCTAGCTCGCTGTCTAA

Flag-R: TCACTACTTGTCATCGTCATCCTTG

KpnI-downstream7839-F: TCGACGGTGGTACCAGGTCTCTGTCCTAGCTCGCTGTCT

KpnI-PtrpC-R: AGAGACCTGGTACCACCGTCGACAGAAGATGATATTGAA

SbfI-NCU07839-1600-F:

ATAGAGCCTGCAGGCTACGTTATGGACGAGGTCAAGGCTC

SbfI-pJET-R: TAACGTAGCCTGCAGGCCTACAATATTCTCAGCTGCCATGG

NotI-downstream7839-R:

ATAGTTCAGCGGCCGCTACGTAACCTTAGGGTCTCTACCGG

Appendix D: Sequences

***Ccg*-1 promoter:**

GCTAGAAGGAGCAGTCCATCTGCGTGAATCACGAGAGAATCAGCTACTTTGAAT
CGATGGATGCAGCTACCAGAAGTCACTCAGTTCGTTCAAAGCCACATCACTGGG
CACTTCCATTGGGACAGGCATTGATCGGACGAGACCGACTTCTGGCCGCTTTCA
ACAGCCACATTATATCCATGTCACGGCTACGCGTCGGCCTTCGGTAACAGAAAA
GCACACAGACAGCGATTGTGACATGGATTCGGGCAAAGCATTGGTGGTCGCACC
AGGTCATCCTGAGTGTGCAGTGGCTGCTATTCAGATTTCATCTAACTGCGGGAGA
GGGGTTCAAAGGGGCGTGACGTCACAGACAACGGGTGAAGGACGAAGATTGC
CTCACTTCTTTGCTAGCAATTTGCCTGCAAAGAAGGCGCACATGACAAGCAAAC
AACTGGGAAACCACTATTGAATACCCACAATGCAAAGCTCGGAAGGTACGTCTT
GATTGCAGTGTGTCGAGTGTCAAAAAAGAAGCAAGTGTTCATGCAAGCCAAAA
TTGGCACCTCCTCCACTTCTCCGAGTGCCCCACCCGAACCTCCAGGCGAGATGG
CCGGAACATACCATCCGCGTTGGGATTATGACGTATCTCCTTCTTCTTCACATGAT
TCCATCCCGTTGTTGCTTGTTTGCGAGCTGTGACGGGAGATCGTAGATGCCACTT
CGGGCCAGGCAGGCAGTGCAGGCAGCCAGGAACACAAGCTTCCAACTTGGTCA
TCTCGATTGCCGATTAAGGGAACCAAATGCCTATATAAGACTGTCCTCCCACCTC
CCCAATACCATTCTTTTCTTCTTCCATCATCAGCCAACAAAGCAATCACATCTTCA
CTACTTCAAATCAACACAACACTCAAACCACTTTCACAACCCCTCACATCAACC
AAATCTAG

***Prd*-1 promoter:**

GCGGCCGCCTATAGAATGTGGTCAAGATTACAGATTCTCTTTTCCGTTCCCTGAC
AGCTGAGGTGAGCGACGACGGATGATTGCCCAACAACCGCGACGCGCAGCAAA
GACTGCCAAGCATAATCCGCCAGTGAAGCAAGAACGAGAACCCTTCTGGCAAA

GCGGAGTCGGTGAACCAGGTGACGCCAATTCCCGCAAAGGTGGACTTCTGCCT
GATTGATAAGGCCACACATGCCTTATCGGCGCTTTATCTGTGCTTATCTGTGCTTG
TCAACAGTGAAAGAATGCAGGCCCGCCAAGTGTTGCCAGTCGGGTCCAGTTTTT
TTTTTCTCTGGTGCCAGACCGCCCCTACATGGAAGTCTGGGGGACAGGTACGGC
AATGCCCGGTCCCCTCAAATCCGCCTTCGCTGTAACGACTGCAGTGAACTGAAG
GGAAGGGAAGAAAAAAAAAATATTTTTCTGGGGCACTTGCACGCAAGGGACGC
GTTGCGCCTTCCGCCTCCAACAAAAAGAAAGACTTTTTCTTCCCGCTTGGAGGC
GAGTCGGGTCTGGCACAGGATCCGCATCTCACATCCACTAGCACTGCACAGCGG
AACCCACCAATCCTCCATCGACATCTCCCTTTGGTCAGGTTCTTTTCCCATACTAA
CCTTACGTGACGGGTCCTTGTCCAGTGCCCCCAGAGTTTTTTTCGTTTCGACTTC
CGTCCAGAAAAACTTGCACTTCACCCTTCGCAGCAGCCCTTTTCTTCCTTCCTTC
CACCCACCCTCCATCTCCAATATCCCTTCCCGCCTACTTCTTGCGATTCTGCAAGA
TTCTTCATCCGCGATCCTTCTTTAACCAGTCGGACTGCTTACTTGTAACCACTTCA
CGCGTGTCGTTTGGTTCTTGTCTCTAGACGTCTGTCTTTTCCGACGTCTTCTTTTC
CCGACAATCGATACCCTTGCGCCTCTAGGCCTTGTTTGCTCGTCGTTTCGGTCTA
CCCTTCAGCAACCCCAATAACAACCGATCTTCAATTTTCAACCTTTTCTTAAACA
ACCAGCAAAC

10X Gly:

GGCGGAGGCGGCGGAGGCGGAGGCGGAGGC

3X FLAG:

GACTACAAAGACCATGACGGTGATTATAAAGATCATGACATCGACTACAAGGAT
GACGATGACAAG

GFP:

ATGGTGAGCAAGGGCGAGGAGCTGTTCACCGGGGTGGTGCCCATCCTGGTCGA
GCTGGACGGCGACGTAAACGGCCACAAGTTCAGCGTGTCCGGCGAGGGCGAGG
GCGATGCCACCTACGGCAAGCTGACCCTGAAGTTCATCTGCACCACCGGCAAGC
TGCCCGTGCCCTGGCCCACCCTCGTGACCACCTTCACCTACGGCGTGCAGTGCT
TCAGCCGCTACCCCGACCACATGAAGCAGCACGACTTCTTCAAGTCCGCCATGC
CCGAAGGCTACGTCCAGGAGCGCACCATCTTCTTCAAGGACGACGGCAACTAC
AAGACCCGCGCCGAGGTGAAGTTCGAGGGCGACACCCTGGTGAACCGCATCGA
GCTGAAGGGCATCGACTTCAAGGAGGACGGCAACATCCTGGGGCACAAGCTGG
AGTACAACTACAACAGCCACAACGTCTATATCATGGCCGACAAGCAGAAGAACG
GCATCAAGGTGAACTTCAAGATCCGCCACAACATCGAGGACGGCAGCGTGCAG
CTCGCCGACCACTACCAGCAGAACACCCCCATCGGCGACGGCCCCGTGCTGCTG
CCCGACAACCACTACCTGAGCACCCAGTCCGCCCTGAGCAAAGACCCCAACGA
GAAGCGCGATCACATGGTCCTGCTGGAGTTCGTGACCGCCGCCGGGATCACTCT
CGGCATGGACGAGCTGTACAAGTAA

***Prd*-1 CDS with intron:**

ATGTCCGGATCTTACGGCGGCGGCGGCTACGGTGGCCGCGGTGGCGGTGGTGGT
GGATATTCTAACGGGTACGATCGCAATGGCGGCGGCTACTCTAACAACTACTCCT
CACACGGGTATGATGTTTTAGCGCGAACCTGCTCATTTCCTCTCTCTCTCTCTCTC
TCTCTCTCTCTCTCTCTCTCTCTCTCTCTCTCTCTCTCTCTCTCTCTTTGCATTT
CAAGATCAAATTGCTAACATCTGGTTCAACAGTGGCTCGAATGGCTACGGAGGC
GGCGGCGGAGGATATGGCGGCGGTGGTGGTGGCTACGGAGGCGGCGGCTACGG
TGGTGGTGGCGGCGGTGATAGGATGTCTGCTCTCGGTGCTGGTCTGCAGAAGCA
GAACTGGGACATGAGCGCTCTTCCCAAGTTCGAGAAGTCCTTCTACCAAGAGCA
TCCTAGCGTCGCCAACCGATCTCCTGCTGAGGTCGACAAGTTCCGCGCAGACCA
CTCCATTGCCGTCTTCGGTAACAACGTTCCCAAGCCTGTCGAGACCTTCGACGA
GGCTGGTTTCCCTCGCTACGTTATGGACGAGGTCAAGGCTCAGGGTTTCCCTGC
TCCTACTGCCATTCAGTCGCAGGGCTGGCCCATGGCCCTTTCTGGTCGCGATGTC
GTCGGTATTGCCGAGACCGGTTCCGGAAAGACGCTCACCTACTGCCTTCCCGCC
ATCGTTCACATCAACGCTCAGCCTCTCCTCGCTCCCGGCGATGGCCCTATCGTCC
TCATCCTCGCCCCTACCCGTGAGTTGGCTGTCCAGATTCAGCAAGAAATCTCCAA
GTTCGGCAAGTCGTCCCGCATTCGCAACACCTGCGTCTACGGTGGTGTCCCCAA
GGGTCCCCAGATTCGCGATCTTTCCAGGGGAGTCGAGGTCTGTATCGCCACCCC
CGGCCGTTTGATCGATATGCTCGAGTCTGGCAAGACCAACCTCCGTCGTGTCAC
CTACCTTGTCCTCGATGAGGCTGATCGCATGTTGGACATGGGTTTCGAGCCCCAA
ATTCGCAAGATCATCGGCCAGATTCGCCCTGATCGTCAGACTCTCATGTGGTCTG
CTACCTGGCCCAAGGAGGTCCGCAACTTGGCCGCCGACTTCTTGACCGACTTCA
TCCAGGTCAACATCGGTTCCATGGATTTGGCTGCCAACCACCGTATCACCCAGAT
CGTCGAGGTTGTTTCCGAGTCCGAGAAGCGTGATCGCATGATCAAGCATCTTGA
GAAGATTATGGAGGGCCGCGAGAACCAGAACAAGATCCTCATCTTCACCGGCAC
CAAGCGTGTCGCCGACGACATCACCCGCTTCCTCCGCCAGGACGGCTGGCCCGC

TCTTTCCATCCACGGCGACAAGCAACAGAACGAGCGTGACTGGGTTTTGGACC
AGTTCAAGACTGGCAAGAGCCCTATCATGGTTGCCACCGACGTGGCTTCTCGTG
GTATCGGTATGTATCCATCTTACCCCTCCGCCCTGCCCAAACCCCTCCCCCCTTCT
TCTCTCCCCCATCTCAGGCGACTTCCAGCATACGTACGTGCTTGTGCTTTACTCTT
ATGTCTAGGGGCTCTCTTGATTGCGCGAACTTGCCTGACCTCGTGTCGACTTGGT
CTATCTGAGTGGAGTCTTGGGTTCGTGACGTAGCAGAAACAGTGGACTATGCTA
CGCCCGCGTGATTCTTCAATTGTACCTTTTTATCCCAGTTGTGGTACAAGCGAGG
AGTAGGCATTTCTTGATTCCCGTCAAGCTTGTCTCCAAGATTCCCAAGGGGATTT
GCATGCATGGCCCAAGGATCTCTGGAACCTTGGATCCCAACCCGGCATATTTTTC
GCAATGGACAGCCCACCTGCCAAGGAGAGAAGTACTACCAGAGGATCACAGAA
CATACCTAGATATTCGTGTTCTCCGTCCGTTCTGGAATGTCGTTATTCCAAACCCT
GCTATTGCTAACCACGGTCCTTTAAAAAAAGATGTGCGCAACATTACTCACGTGC
TCAACTATGACTACCCCAACAACTCCGAGGATTACATCCATCGTATCGGCCGAAC
TGGTCGTGCCGGTGCGAAGGGTACTGCCATTACTTTCTTCACCACTGACAGTAA
GTGTCACCTGAATCTGCCCATCCTTAGCCGAACGAAATTCTAATGTTATCTCTCCA
CAGACTCCAAGCAGGCTCGTGAGCTCGTCGGTGTGCTTCAAGAAGCTAAGCAG
CAGATTGACCCTAGACTTGCCGAGATGGCTCGCTACAGTGGTGGTGGAGGTGGC
CGCTTCGGTGGCTATCGCGGCCGTGGCGGCGGTGGATGGCGCGGTGGTAAGTCA
TTTTCACGCAGGTGAATTTGGCAGTTCCAATCCTAATAACCCTCATTAGGCCGTG
GCGGCGGTGGTGGCGGCGGCTCCGTCGGTGGTGCTAATGCTCT

P_{trpC}-*hph*-T_{trpC}:

ACCGTCGACAGAAGATGATATTGAAGGAGCACTTTTTGGGCTTGGCTGGAGCTA
GTGGAGGTCAACAATGAATGCCTATTTTGGTTTAGTCGTCCAGGCGGTGAGCAC
AAAATTTGTGTCGTTTGACAAGATGGTTCATTTAGGCAACTGGTCAGATCAGCCC
CACTTGTAGCAGTAGCGGCGGCGCTCGAAGTGTGACTCTTATTAGCAGACAGGA

ACGAGGACATTATTATCATCTGCTGCTTGGTGCACGATAACTTGGTGCGTTTGTC
AAGCAAGGTAAGTGAACGACCCGGTCATACCTTCTTAAGTTCGCCCTTCCTCCCT
TTATTTCAGATTCAATCTGACTTACCTATTCTACCCAAGCATCGATATGAAAAAGC
CTGAACTCACCGCGACGTCTGTCGAGAAGTTTCTGATCGAAAAGTTCGACAGCG
TCTCCGACCTGATGCAGCTCTCGGAGGGCGAAGAATCTCGTGCTTTCAGCTTCG
ATGTAGGAGGGCGTGGATATGTCCTGCGGGTAAATAGCTGCGCCGATGGTTTCTA
CAAAGATCGTTATGTTTATCGGCACTTTGCATCGGCCGCGCTCCCGATTCCGGAA
GTGCTTGACATTGGGGAATTCAGCGAGAGCCTGACCTATTGCATCTCCCGCCGTG
CACAGGGTGTCACGTTGCAAGACCTGCCTGAAACCGAACTGCCCGCTGTTCTGC
AGCCGGTCGCGGAGGCCATGGATGCGATCGCTGCGGCCGATCTTAGCCAGACGA
GCGGGTTCGGCCCATTCGGACCGCAAGGAATCGGTCAATACACTACATGGCGTG
ATTTCATATGCGCGATTGCTGATCCCCATGTGTATCACTGGCAAACTGTGATGGAC
GACACCGTCAGTGCGTCCGTCGCGCAGGCTCTCGATGAGCTGATGCTTTGGGCC
GAGGACTGCCCCGAAGTCCGGCACCTCGTGCACGCGGATTTCGGCTCCAACAAT
GTCCTGACGGACAATGGCCGCATAACAGCGGTCATTGACTGGAGCGAGGCGATG
TTCGGGGATTCCCAATACGAGGTCGCCAACATCTTCTTCTGGAGGCCGTGGTTG
GCTTGTATGGAGCAGCAGACGCGCTACTTCGAGCGGAGGCATCCGGAGCTTGCA
GGATCGCCGCGGCTCCGGGCGTATATGCTCCGCATTGGTCTTGACCAACTCTATC
AGAGCTTGGTTGACGGCAATTTCGATGATGCAGCTTGGGCGCAGGGTCGATGCG
ACGCAATCGTCCGATCCGGAGCCGGGACTGTCGGGCGTACACAAATCGCCCGCA
GAAGCGCGGCCGTCTGGACCGATGGCTGTGTAGAAGTACTCGCCGATAGTGGAA
ACCGACGCCCCAGCACTCGTCCGAGGGCAAAGGAATAGAGTAGATGCCGACCG
GGATCCACTTAACGTTACTGAAATCATCAAACAGCTTGACGAATCTGGATATAAG
ATCGTTGGTGTCGATGTCAGCTCCGGAGTTGAGACAAATGGTGTTCAGGATCTC
GATAAGATACGTTCATTTGTCCAAGCAGCAAAGAGTGCCTTCTAGTGATTTAATA
GCTCCATGTCAACAAGAATAAAACGCGTTTCGGGTTTACCTCTTCCAGATACAGC

TCATCTGCAATGCATTAATGCATTGGACCTCGCAACCCTAGTACGCCCTTCAGGC
TCCGGCGAAGCAGAAGAATAGCTTAGCAGAGTCTATTTTCATTTTCGGGAGACG
AGATCAAGCAGATCAACGGTCGTCAAGAGACCTACGAGACTGAGGAATCCGCT
CTTGGCTCCACGCGACTATATATTTGTCTCTAATTGTACTTTGACATGCTCCTCTTC
TTTACTCTGATAGCTTGACTATGAAAATTCCGTCACCAGCCCCTGGGTTCGCAAA
GATAATTGCACTGTTTCTTCCTTGAACTCTCAAGCCTACAGGACACACATTCATC
GTAGGTATAAACCTCGAAAATCATTCCTACTAAGATGGGTATACAATAGTAACCAT
GGTTGCCTAGTGAATGCTCCGTAACACCCAATACGCCGGCCGAAACTTTTTTACA
ACTCTCCTATGAGTCGTTTACCCAGAATGCACAGGTACACTTGTTTAGAGGTAAT
CCTTCTT

3’flank (downstream of *prd*-1)

AGGTCTCTGTCCTAGCTCGCTGTCTAAGTGATTGAGGTTGAATGTTTTGAGGTCT
ACGCTCAAGTAGATGTCTCGCTCAAGTGTGTACCTGTGACGATTTCCCAGAATTC
CTAGGGTAATTCAACGATTTGATTATGGAGTGCTCGCGATAAAGCTGTAGGTTTC
ACGTCGATGAGTCTTCTCTACGAGGTTAGTCCTTCACTTCCATATAGAAGATCAG
TATGAACATCTTTCTGATATATGTGTCTCGTAACATTCGACTTAATGCTCTGTACTT
TATGTTCGCAGAGTATTTCCTGTTCTACTCTCTCACTCTGAGGTACTGATTGACTG
TAGAGAAGCCGCTTGGCACGATTTGTGCTGCGTTCCAAGGTTAGTATGAATTGTG
TGCTTTGATATGTTAGTCTTGTGATTAGGTGAGAAAAATGAGCAACCTCCAACCA
CGTTTTGCGGGCTTCAGCGTCACGACTACTATAGTCTTATGATTCCGGTGTTGATT
TTGCTGAATGGCCATCAGGTTAACATATGGGCTCGAGTGTCTGCTGAGGTCCGAT
CGTCAAGTAACTAATGATGATGAGGAAGGAGCGATTCGAGGTAAGGAGAGAAC
GACTTGATGTTGGTGGGTCTCTGGCATTCACTGGGCACAGCACTGGGCACAGCC
CCAGTCCCCACTCTGTGCCCTGCCCAGACCGCACCATATCTAGCCTTCCAGATTC
GGCCAGTCTCCCTCTTCCTCTTTCTTCTCTATAGTACTTAATTAATTGTATCCAACC

GCTTGATTTCGTTGGTGATCCTATAGGTTATGAGCCCTCTCTAACCTTCCTTGTAA
TTGTATTTAACGAGCGTATCCTTAAAGTGTATCGTCGGCTTCAATTGCCAATTTCA
ATAAGGCGCTATAGTACCGGGTTAAAAGAAGTAATGCGACCCTTATTGATTTAAC
GATTTGCCCGTTCGCCTATAAGCTAGTATTGCTATATGAAGATTCTCGTTAATATTT
GTTGTATAGCGACCCTATCGAATTAGTTATTAATTTATTTAATGAATTAATTATTGGT
TTATTTATTATCGAATTAAGTAATTTAAATAATTCTATTATCGAATTAATTAAATTAA
TTAATAGTTAGTCTAGCGATTACTAACTTCCTTCTTCTTAATATATTGTCGAACCCT
CCTATACCTACTATAATTACTAGTTCGTCGCTGGTTCCCCTCCTTGGCGATTAGAA
TATTGCCGATTAGTAATAGGGATTTATAGTTGAGTTTAATTGCTTTTAGTTCGCTAA
TTATATTTTCGAGATAGTTCTGGAGCCTAATAAAGCGATTGAGTCCGAGAAGTAC
AATACTTAGTGGATTAGATATACTAATATTAATAAGATTCTATTTTCTACCTTTAAG
AATACTGATGTTACTATTACTTTAAACGTTAATAGTTGGGATAGAACCGGTAGAG
ACCCTAAGGTTACGTA

Probe Sequence:

GAACTGGGACATGAGCGCTCTTCCCAAGTTCGAGAAGTCCTTCTACCAAGAGCA
TCCTAGCGTCGCCAACCGATCTCCTGCTGAGGTCGACAAGTTCCGCGCAGACCA
CTCCATTGCCGTCTTCGGTAACAACGTTCCCAAGCCTGTCGAGACCTTCGACGA
GGCTGGTTTCCCTCGCTACGTTATGGACGAGGTCAAGGCTCAGGGTTTCCCT

gRNA: TCCCTTATTGTCATGCTTGCGGG

TCTTGGGCTAGCGGTAAAGGTGCGCATTTTTTCACACCCTACAATGTTCTGTTCA
AAAGATTTTGGTCAAACGCTGTAGAAGTGAAAGTTGGTGCGCATGTTTCGGCGT
TCGAAACTTCTCCGCAGTGAAAGATAAATGATCGCCCTTATTGTCATGCTTGCgtttt
agagctagaaatagcaagttaaaataaggctagtccgttatcaacttgaaaaagtggcaccgagtcggtggtgctttttttgttttttatg
tctTCGAGTCATGTAATTAGTTATGTCACGCTTACgTTCACGCCCTCCCCCCACATC
CGCTCTAACCGAAAAGGAAGGAGTTAGACAACCTGAAGTCTAGGTCCCTATTTA

TTTTTTTATAGTTATGTTAGTATTAAGAACGTTATTTATATTTCAAATTTTTCTTTTT
TTTCTGTACAGACGCGTGTACGCATGTAACATTATACTGAAAACCTTGCTTGAGA
AGGTTTTGGGACGCTCGAAGGCTTTAATTTGCGGCCGGTACCCAATTC

Appendix E: Mass Spectrometry Data

Table a. Total spectrum counts of selected protein (4.3.3). Data from four independent experiments are shown. The vacant cells represent that proteins were undetectable.

Gene ID	Identified proteins	#26 (WT)				#444 (NCU05950-FLAG)				#588(PRD-1-FLAG)			
		1	2	3	4	1	2	3	4	1	2	3	4
NCU00258	40S ribosomal protein S7				0				1		25	7	7
NCU00294	60S ribosomal protein L10a								1		23	2	6
NCU00413	60S ribosomal protein L2						3	4		4	46	8	1
NCU00475	40S ribosomal protein S18				1			2	3		14	8	7
NCU00634	60S ribosomal protein L14				1				4	2	23	5	7
NCU01221	60S ribosomal protein L16		1				3			1	23	3	1
NCU01452	40S ribosomal protein S1		1		4		4	1	11	1	31	6	11
NCU01552	ribosomal protein S28						1		2	2	22	1	4
NCU01776	60S ribosomal protein L15/ hypothetical protein GE21DRAFT_3246						0			3	28	3	3
NCU01827	60S ribosomal protein L27								1		6	1	6
NCU02181	40S ribosomal protein S4								1		18	6	2
NCU02707	60S ribosomal protein L6/ hypothetical protein GE21DRAFT_903						1		1		27	6	2
NCU03565	probable ribosomal protein L26			1			1	2	1	4	22	5	2
NCU03703	60S ribosomal protein L17		1	1	2				5	3	21	5	6
NCU03757	60S ribosomal protein L4-A		1	3			7	5	3	11	72	26	7
NCU04225	60S ribosomal protein L20						1	1		0	15	5	1
NCU04779	60S ribosomal protein L8		3	3		1	1	0	4	3	44	8	8
NCU05554	60S ribosomal protein L13		1	3		0	3	2	3	3	37	17	4
NCU05804	60S ribosomal protein L19		3	1		1	5	0	3	2	30	14	4
NCU06210	hypothetical protein GE21DRAFT_4187						2		3	1	34	5	3
NCU06432	40S ribosomal protein S12										4	1	1
NCU06843	60S ribosomal protein L3		1				2		2	1	36	4	6
NCU07735	Grp1p				0				0		4	5	1
NCU07829	60S ribosomal protein L7								1		27	13	4
NCU07830	40S ribosomal protein S14						5		2	1	23	5	
NCU07839	ATP-dependent RNA helicase dbp-2									139	571	87	41
NCU08500	40S ribosomal protein S8					1	2		1	2	26	10	1
NCU08502	40S ribosomal protein S6				1		2	1	1	3	50	13	3
NCU08960	60S acidic ribosomal protein P1/ hypothetical protein		1	3		2		1		1	3	9	1
NCU08964	60S ribosomal protein L10						0		0		29	2	2

Table b. Percent coverage of selected protein (4.3.3). Data from four independent experiments are shown. The vacant cells represent that proteins were undetectable.

Gene ID	Identified proteins	#26 (WT)				#444 (NCU05950-FLAG)				#588(PRD-1-FLAG)			
		1	2	3	4	1	2	3	4	1	2	3	4
NCU00258	40S ribosomal protein S7				16%				27%		53%	33%	28%
NCU00294	60S ribosomal protein L10a								9.70%		52%	17%	32%
NCU00413	60S ribosomal protein L2						16%	12%		16%	75%	19%	11%
NCU00475	40S ribosomal protein S18				4.50%			13%	28%		54%	35%	34%
NCU00634	60S ribosomal protein L14				8.50%				28%	9.20%	39%	29%	35%
NCU01221	60S ribosomal protein L16		6.90%				11%			4.00%	50%	16%	6.90%
NCU01452	40S ribosomal protein S1		5.50%		18%		16%	3.90%	31%	5.50%	62%	23%	37%
NCU01552	ribosomal protein S28						12%		25%	14%	53%	19%	38%
NCU01776	60S ribosomal protein L15/ hypothetical protein GE21DRAFT_3246						0.00%			13%	27%	22%	11%
NCU01827	60S ribosomal protein L27								13%		27%	5.90%	43%
NCU02181	40S ribosomal protein S4								4.60%		45%	34%	9.20%
NCU02707	60S ribosomal protein L6/ hypothetical protein GE21DRAFT_903						5.40%		5.90%		57%	20%	13%
NCU03565	probable ribosomal protein L26			15%			10%	15%	8.80%	27%	55%	34%	23%
NCU03703	60S ribosomal protein L17		6.50%	5.40%	10%				17%	22%	56%	32%	22%
NCU03757	60S ribosomal protein L4-A		3.90%	15%			23%	17%	15%	32%	72%	59%	24%
NCU04225	60S ribosomal protein L20						8.00%	8.00%		0.00%	34%	14%	10%
NCU04779	60S ribosomal protein L8		13%	16%		3.80%	4.60%	0.00%	14%	8.40%	63%	21%	24%
NCU05554	60S ribosomal protein L13		6.10%	15%		0.00%	16%	13%	18%	21%	67%	48%	18%
NCU05804	60S ribosomal protein L19		15%	9.40%		5.70%	24%	0.00%	13%	6.20%	37%	33%	13%
NCU06210	hypothetical protein GE21DRAFT_4187						8.00%		23%	8.00%	78%	25%	23%
NCU06432	40S ribosomal protein S12										21%	7.50%	6.80%
NCU06843	60S ribosomal protein L3		2.30%				2.30%		5.10%	2.30%	43%	15%	17%
NCU07735	Grp1p				0.00%				0.00%		8.50%	23%	3.70%
NCU07829	60S ribosomal protein L7								4.40%		57%	30%	15%
NCU07830	40S ribosomal protein S14						24%		15%	11%	65%	25%	
NCU07839	ATP-dependent RNA helicase dbp-2									65%	98%	47%	35%
NCU08500	40S ribosomal protein S8					5.90%	5.90%		6.40%	5.90%	61%	39%	6.40%
NCU08502	40S ribosomal protein S6				8.40%		7.50%	5.90%	8.40%	13%	68%	44%	17%
NCU08960	60S acidic ribosomal protein P1/ hypothetical protein		16%	16%		16%		13%		16%	16%	51%	13%
NCU08964	60S ribosomal protein L10						0.00%		0.00%		75%	9.50%	9.50%

Table c. Exclusive unique peptide counts of selected protein (4.3.3). Data from four independent experiments are shown. The vacant cells represent that proteins were undetectable.

Gene ID	Identified proteins	#26 (WT)				#444 (NCU05950-FLAG)				#588(PRD-1-FLAG)			
		1	2	3	4	1	2	3	4	1	2	3	4
NCU00258	40S ribosomal protein S7				0				1		12	5	3
NCU00294	60S ribosomal protein L10a								1		11	2	5
NCU00413	60S ribosomal protein L2						3	2		2	22	6	1
NCU00475	40S ribosomal protein S18				1			2	3		11	6	5
NCU00634	60S ribosomal protein L14				1				3	1	11	4	5
NCU01221	60S ribosomal protein L16		1				2			1	14	2	1
NCU01452	40S ribosomal protein S1		1		4		4	1	7	1	22	5	8
NCU01552	ribosomal protein S28						1		2	2	10	1	4
NCU01776	60S ribosomal protein L15/ hypothetical protein GE21DRAFT_3246						0			2	7	3	2
NCU01827	60S ribosomal protein L27								1		4	1	4
NCU02181	40S ribosomal protein S4								1		12	5	2
NCU02707	60S ribosomal protein L6/ hypothetical protein GE21DRAFT_903						1		1		14	4	2
NCU03565	probable ribosomal protein L26			1			1	2	1	3	11	3	2
NCU03703	60S ribosomal protein L17		1	1	2				3	3	15	4	4
NCU03757	60S ribosomal protein L4-A		1	3			6	5	3	8	28	15	6
NCU04225	60S ribosomal protein L20						1	1		0	8	3	1
NCU04779	60S ribosomal protein L8		3	3		1	1	0	3	2	22	6	7
NCU05554	60S ribosomal protein L13		1	2		0	1	2	3	3	21	11	3
NCU05804	60S ribosomal protein L19		3	1		1	5	0	2	2	13	9	2
NCU06210	hypothetical protein GE21DRAFT_4187						1		3	1	15	3	3
NCU06432	40S ribosomal protein S12										4	1	1
NCU06843	60S ribosomal protein L3		1				1		1	1	17	3	5
NCU07735	Grp1p				0				0		2	5	1
NCU07829	60S ribosomal protein L7								1		13	7	3
NCU07830	40S ribosomal protein S14						4		2	1	12	4	
NCU07839	ATP-dependent RNA helicase dbp-2									51	125	38	17
NCU08500	40S ribosomal protein S8					1	1		1	1	17	6	1
NCU08502	40S ribosomal protein S6				1		2	1	1	2	26	7	3
NCU08960	60S acidic ribosomal protein P1/ hypothetical protein		1	2		1		1		1	2	3	1
NCU08964	60S ribosomal protein L10						0		0		18	2	2

References

Adams, S., Manfield, I., Stockley, P., and Carre, I.A. (2015). Revised Morning Loops of the *Arabidopsis* Circadian Clock Based on Analyses of Direct Regulatory Interactions. PLoS One *10*, e0143943.

Adhvaryu, K., Firoozi, G., Motavaze, K., and Lakin-Thomas, P. (2016). PRD-1, a Component of the Circadian System of *Neurospora crassa*, Is a Member of the DEAD-box RNA Helicase Family. J Biol Rhythms *31*, 258-271.

Alabadi, D., Oyama, T., Yanovsky, M.J., Harmon, F.G., Mas, P., and Kay, S.A. (2001). Reciprocal regulation between TOC1 and LHY/CCA1 within the *Arabidopsis* circadian clock. Science *293*, 880-883.

Arble, D.M., Bass, J., Laposky, A.D., Vitaterna, M.H., and Turek, F.W. (2009). Circadian timing of food intake contributes to weight gain. Obesity (Silver Spring) *17*, 2100-2102.

Arendt, J. (2010). Shift work: coping with the biological clock. Occup Med-Oxford *60*, 10-20.

Aronson, B.D., Johnson, K.A., and Dunlap, J.C. (1994). Circadian clock locus frequency: protein encoded by a single open reading frame defines period length and temperature compensation. Proc. Nat. Acad. Sci. USA *91*, 7683-7687.

Avivi, A., Albrecht, U., Oster, H., Joel, A., Beiles, A., and Nevo, E. (2001). Biological clock in total darkness: The Clock/MOP3 circadian system of the blind subterranean mole rat. P Natl Acad Sci USA *98*, 13751-13756.

Baker, C.L., Loros, J.J., and Dunlap, J.C. (2012). The circadian clock of *Neurospora crassa*. FEMS Microbiol Rev *36*, 95-110.

Balzer, I., and Hardeland, R. (1988). Influence of Temperature on Biological Rhythms. Int J Biometeorol *32*, 231-241.

Boden, M.J., and Kennaway, D.J. (2006). Circadian rhythms and reproduction. Reproduction *132*, 379-392.

Bond A.T., Mangus D.A., He F., Jacobson A. (2001). Absence of Dbp2p alters both nonsense-mediated mRNA decay and rRNA processing. Mol Cell Biol *21*, 7366-7379

Bryksin, A.V., and Matsumura, I. (2010). Overlap extension PCR cloning: a simple and reliable way to create recombinant plasmids. Biotechniques *48*, 463-465.

Calderon, J., and Mora, J. (1989). Glutamine assimilation pathways in *Neurospora crassa* growing on glutamine as sole nitrogen and carbon source. J Gen Microbiol *135*, 2699-2707.

Cao, R., Li, A., Cho, H.Y., Lee, B., and Obrietan, K. (2010). Mammalian target of rapamycin signaling modulates photic entrainment of the suprachiasmatic circadian clock. J Neurosci *30*, 6302-6314.

Chang, Y.G., Tseng, R., Kuo, N.W., and LiWang, A. (2012). Rhythmic ring-ring stacking drives the circadian oscillator clockwise. Proc Natl Acad Sci U S A *109*, 16847-16851.

Chen, T.H., Chen, T.L., Hung, L.M., and Huang, T.C. (1991). Circadian Rhythm in Amino Acid Uptake by *Synechococcus RF-1*. Plant Physiol *97*, 55-59.

Cheng, P., He, Q., He, Q., Wang, L., and Liu, Y. (2005). Regulation of the *Neurospora* circadian clock by an RNA helicase. Genes Dev *19*, 234-241.

Christensen, M.K., Falkeid, G., Loros, J.J., Dunlap, J.C., Lillo, C., and Ruoff, P. (2004). A nitrate-induced *frq*-less oscillator in *Neurospora crassa*. J Biol Rhythms *19*, 280-286.

Cohen, S.E., and Golden, S.S. (2015). Circadian Rhythms in Cyanobacteria. Microbiol Mol Biol Rev *79*, 373-385.

Colot, H.V., Park, G., Turner, G.E., Ringelberg, C., Crew, C.M., Litvinkova, L., Weiss, R.L., Borkovich, K.A., and Dunlap, J.C. (2006). A high-throughput gene knockout procedure for *Neurospora* reveals functions for multiple transcription factors. Proc Natl Acad Sci U S A *103*, 10352-10357.

Cota, D., Proulx, K., Smith, K.A., Kozma, S.C., Thomas, G., Woods, S.C., and Seeley, R.J. (2006). Hypothalamic mTOR signaling regulates food intake. Science *312*, 927-930.

Czeisler, C.A., and Gooley, J.J. (2007). Sleep and circadian rhythms in humans. Cold Spring Harb Sym *72*, 579-597.

Davis, R.H. (1986). Compartmental and regulatory mechanisms in the arginine pathways of

Neurospora crassa and Saccharomyces cerevisiae. Microbiol Rev *50*, 280-313.

Davis, R.H. (2000). *Neurospora*: contributions of a model organism (Oxford University Press). pp. 11-19.

Davis, R.H., and Weiss, R.L. (1988). Novel mechanisms controlling arginine metabolism in *Neurospora*. Trends Biochem Sci *13*, 101-104.

de Paula, R.M., Lewis, Z.A., Greene, A.V., Seo, K.S., Morgan, L.W., Vitalini, M.W., Bennett, L., Gomer, R.H., and Bell-Pedersen, D. (2006). Two circadian timing circuits in *Neurospora crassa* cells share components and regulate distinct rhythmic processes. J Biol Rhythms *21*, 159-168.

DiCarlo, J.E., Norville, J.E., Mali, P., Rios, X., Aach, J., and Church, G.M. (2013). Genome engineering in Saccharomyces cerevisiae using CRISPR-Cas systems. Nucleic Acids Res *41*, 4336-4343.

Dunlap, J.C. (1999). Molecular bases for circadian clocks. Cell *96*, 271-290.

Dunlap, J.C., Loros, J.J., Colot, H.V., Mehra, A., Belden, W.J., Shi, M., Hong, C.I., Larrondo, L.F., Baker, C.L., Chen, C.H.*, et al.* (2007). A circadian clock in *Neurospora*: how genes and proteins cooperate to produce a sustained, entrainable, and compensated biological oscillator with a period of about a day. Cold Spring Harb Symp Quant Biol *72*, 57-68.

Ebbole, D., and M.S. Sachs (1990) A rapid and simple method for isolation of *Neurospora crassa* homokaryons using microconidia. Fungal Genetics Reports *37*, 7

Emerson, J.M., Bartholomai, B.M., Ringelberg, C.S., Baker, S.E., Loros, J.J., and Dunlap, J.C. (2015). period-1 encodes an ATP-dependent RNA helicase that influences nutritional compensation of the *Neurospora* circadian clock. Proc Natl Acad Sci U S A *112*, 15707-15712.

Feldman, J.F. (1982). Genetic Approaches to Circadian Clocks. Annu Rev Plant Phys *33*, 583-608.

Feldman, J.F., and Hoyle, M.N. (1973). Isolation of circadian clock mutants of *Neurospora crassa*. Genetics *75*, 605-613.

Fuller, K.K., Chen, S., Loros, J.J., and Dunlap, J.C. (2015). Development of the

CRISPR/Cas9 System for Targeted Gene Disruption in Aspergillus fumigatus. Eukaryotic Cell *14*, 1073-1080.

Galagan, J.E., Calvo, S.E., Borkovich, K.A., Selker, E.U., Read, N.D., Jaffe, D., FitzHugh, W., Ma, L.J., Smirnov, S., Purcell, S.*, et al.* (2003). The genome sequence of the filamentous fungus *Neurospora crassa*. Nature *422*, 859-868.

Gallego, M., and Virshup, D.M. (2007). Post-translational modifications regulate the ticking of the circadian clock. Nat Rev Mol Cell Bio *8*, 139-148.

Gardner, G.F., and Feldman, J.F. (1980). The *frq* locus in *Neurospora crassa*: a key element in circadian clock organization. Genetics *96*, 877-886.

Gnocchi, D., and Bruscalupi, G. (2017). Circadian Rhythms and Hormonal Homeostasis: Pathophysiological Implications. Biology (Basel) *6*.

Golombek, D.A., and Rosenstein, R.E. (2010). Physiology of Circadian Entrainment. Physiol Rev *90*, 1063-1102.

Greenham, K., and McClung, C.R. (2015). Integrating circadian dynamics with physiological processes in plants (vol 16, pg 598, 2015). Nature Reviews Genetics *16*, 682-682.

Guo, J., and Liu, Y. (2010). Molecular mechanism of the *Neurospora* circadian oscillator. Protein Cell *1*, 331-341.

Harmer, S.L. (2009). The Circadian System in Higher Plants. Annu Rev Plant Biol *60*, 357-377.

He, Q., Cheng, P., Yang, Y., He, Q., Yu, H., and Liu, Y. (2003). FWD1-mediated degradation of FREQUENCY in *Neurospora* establishes a conserved mechanism for circadian clock regulation. EMBO J *22*, 4421-4430.

Honda, S., and Selker, E.U. (2009). Tools for fungal proteomics: multifunctional *neurospora* vectors for gene replacement, protein expression and protein purification. Genetics *182*, 11-23.

Hsu, P.Y., Devisetty, U.K., and Harmer, S.L. (2013). Accurate timekeeping is controlled by a cycling activator in *Arabidopsis*. Elife *2*.

Huang, T.C., Tu, J., Chow, T.J., and Chen, T.H. (1990). Circadian Rhythm of the Prokaryote

Synechococcus sp. RF-1. Plant Physiol *92*, 531-533.

Huang, W., Perez-Garcia, P., Pokhilko, A., Millar, A.J., Antoshechkin, I., Riechmann, J.L., and Mas, P. (2012). Mapping the Core of the *Arabidopsis* Circadian Clock Defines the Network Structure of the Oscillator. Science *336*, 75-79.

Huang, W.Y., Ramsey, K.M., Marcheva, B., and Bass, J. (2011). Circadian rhythms, sleep, and metabolism. J Clin Invest *121*, 2133-2141.

Ishida, N., Kaneko, M., and Allada, R. (1999). Biological clocks. P Natl Acad Sci USA *96*, 8819-8820.

Ishiura, M., Kutsuna, S., Aoki, S., Iwasaki, H., Andersson, C.R., Tanabe, A., Golden, S.S., Johnson, C.H., and Kondo, T. (1998). Expression of a gene cluster kaiABC as a circadian feedback process in cyanobacteria. Science *281*, 1519-1523.

King, D.P., and Takahashi, J.S. (2000). Molecular genetics of circadian rhythms in mammals. Annu Rev Neurosci *23*, 713-742.

Lakin-Thomas, P.L. (1998). Choline depletion, *frq* mutations, and temperature compensation of the circadian rhythm in *Neurospora crassa*. J Biol Rhythm *13*, 268-277.

Lakin-Thomas, P.L. (2006). Circadian clock genes frequency and white collar-1 are not essential for entrainment to temperature cycles in *Neurospora crassa*. Proc Natl Acad Sci U S A *103*, 4469-4474.

Lakin-Thomas, P.L., and Brody, S. (2000). Circadian rhythms in *Neurospora crassa*: lipid deficiencies restore robust rhythmicity to null frequency and white-collar mutants. Proc Natl Acad Sci U S A *97*, 256-261.

Lakin-Thomas, P.L., and Brody, S. (1985). Circadian-Rhythms in *Neurospora Crassa* - Interactions between Clock Mutations. Genetics *109*, 49-66.

Lakin-Thomas, P.L., Cote, G.G., and Brody, S. (1990). Circadian-Rhythms in *Neurospora Crassa* Biochemistry and Genetics. Crit Rev Microbiol *17*, 365-416.

Lee, C., Etchegaray, J.P., Cagampang, F.R., Loudon, A.S., and Reppert, S.M. (2001). Posttranslational mechanisms regulate the mammalian circadian clock. Cell *107*, 855-867.

Li, S., and Lakin-Thomas, P. (2010). Effects of *prd* circadian clock mutations on FRQ-less

rhythms in *Neurospora*. J Biol Rhythms *25*, 71-80.

Li, S., Motavaze, K., Kafes, E., Suntharalingam, S., and Lakin-Thomas, P. (2011). A new mutation affecting FRQ-less rhythms in the circadian system of *Neurospora crassa*. PLoS Genet *7*, e1002151.

Linder, P., and Jankowsky, E. (2011). From unwinding to clamping — the DEAD box RNA helicase family. Nat Rev Mol Cell Bio *12*, 505.

Liu, Y. (2003). Molecular mechanisms of entrainment in the *Neurospora* circadian clock. J Biol Rhythm *18*, 195-205.

Liu, Y., and Bell-Pedersen, D. (2006). Circadian rhythms in *Neurospora crassa* and other filamentous fungi. Eukaryot Cell *5*, 1184-1193.

Liu, Y., Garceau, N.Y., Loros, J.J., and Dunlap, J.C. (1997). Thermally regulated translational control of FRQ mediates aspects of temperature responses in the *Neurospora* circadian clock. Cell *89*, 477-486.

Liu, Y., He, Q., and Cheng, P. (2003). Photoreception in *Neurospora*: a tale of two White Collar proteins. Cell Mol Life Sci *60*, 2131-2138.

Loewith, R., and Hall, M.N. (2011). Target of rapamycin (TOR) in nutrient signaling and growth control. Genetics *189*, 1177-1201.

Lombardi, L., Schneider, K., Tsukamoto, M., and Brody, S. (2007). Circadian rhythms in *Neurospora crassa*: clock mutant effects in the absence of a *frq*-based oscillator. Genetics *175*, 1175-1183.

Loros, J.J., and Feldman, J.F. (1986). Loss of temperature compensation of circadian period length in the *frq*-9 mutant of *Neurospora crassa*. J Biol Rhythms *1*, 187-198.

Maheshwari, R. (1999). Microconidia of *Neurospora crassa*. Fungal Genet Biol *26*, 1-18.

Markson, J.S., Piechura, J.R., Puszynska, A.M., and O'Shea, E.K. (2013). Circadian control of global gene expression by the cyanobacterial master regulator RpaA. Cell *155*, 1396-1408.

Martin R., Straub A.U., Doebele C., Bohnsack M.T. (2013). DExD/H-box RNA helicases in ribosome biogenesis. RNA Biol *10*, 4-18.

Matsu-Ura, T., Baek, M., Kwon, J., and Hong, C. (2015). Efficient gene editing in *Neurospora crassa* with CRISPR technology. Fungal Biol Biotechnol *2*, 4.

McClung, C.R. (2006). Plant circadian rhythms. Plant Cell *18*, 792-803.

Merrow, M., Brunner, M., and Roenneberg, T. (1999). Assignment of circadian function for the *Neurospora* clock gene frequency. Nature *399*, 584-586.

Ninomiya, Y., Suzuki, K., Ishii, C., and Inoue, H. (2004). Highly efficient gene replacements in *Neurospora* strains deficient for nonhomologous end-joining. Proc Natl Acad Sci U S A *101*, 12248-12253.

Nishiwaki, T., Satomi, Y., Nakajima, M., Lee, C., Kiyohara, R., Kageyama, H., Kitayama, Y., Temamoto, M., Yamaguchi, A., Hijikata, A.*, et al.* (2004). Role of KaiC phosphorylation in the circadian clock system of *Synechococcus elongatus* PCC 7942. Proc Natl Acad Sci U S A *101*, 13927-13932.

Padmanabhan, K., Robles, M.S., Westerling, T., and Weitz, C.J. (2012). Feedback regulation of transcriptional termination by the mammalian circadian clock PERIOD complex. Science *337*, 599-602.

Panda, S., Antoch, M.P., Miller, B.H., Su, A.I., Schook, A.B., Straume, M., Schultz, P.G., Kay, S.A., Takahashi, J.S., and Hogenesch, J.B. (2002). Coordinated transcription of key pathways in the mouse by the circadian clock. Cell *109*, 307-320.

Perkins, D.D., and Davis, R.H. (2000). *Neurospora* at the millennium. Fungal Genet Biol *31*, 153-167.

Pittendrigh, C.S., Bruce, V.G., Rosensweig, N.S., and Rubin, M.L. (1959). Growth Patterns in *Neurospora*: A Biological Clock in *Neurospora*. Nature *184*, 169.

Preitner, N., Damiola, F., Lopez-Molina, L., Zakany, J., Duboule, D., Albrecht, U., and Schibler, U. (2002). The orphan nuclear receptor REV-ERBalpha controls circadian transcription within the positive limb of the mammalian circadian oscillator. Cell *110*, 251-260.

Reddy, A.B., Karp, N.A., Maywood, E.S., Sage, E.A., Deery, M., O'Neill, J.S., Wong, G.K., Chesham, J., Odell, M., Lilley, K.S.*, et al.* (2006). Circadian orchestration of the hepatic

proteome. Curr Biol *16*, 1107-1115.

Sanchez, S.E., and Kay, S.A. (2016). The Plant Circadian Clock: From a Simple Timekeeper to a Complex Developmental Manager. Csh Perspect Biol *8*.

Sargent, M.L., Briggs, W.R., and Woodward, D.O. (1966). Circadian nature of a rhythm expressed by an invertaseless strain of *Neurospora crassa*. Plant Physiol *41*, 1343-1349.

Shevchuk, N.A., Bryksin, A.V., Nusinovich, Y.A., Cabello, F.C., Sutherland, M., and Ladisch, S. (2004). Construction of long DNA molecules using long PCR-based fusion of several fragments simultaneously. Nucleic Acids Res *32*.

Steinlechner, S. (2012). Chapter 2.12 - Biological Rhythms of the Mouse A2 - Hedrich, Hans J. In The Laboratory Mouse (Second Edition) (Boston: Academic Press), pp. 383-407.

Stracka, D., Jozefczuk, S., Rudroff, F., Sauer, U., and Hall, M.N. (2014). Nitrogen source activates TOR (target of rapamycin) complex 1 via glutamine and independently of Gtr/Rag proteins. J Biol Chem *289*, 25010-25020.

Takahashi, J.S. (2017). Transcriptional architecture of the mammalian circadian clock. Nat Rev Genet *18*, 164-179.

Takai, N., Nakajima, M., Oyama, T., Kito, R., Sugita, C., Sugita, M., Kondo, T., and Iwasaki, H. (2006). A KaiC-associating SasA-RpaA two-component regulatory system as a major circadian timing mediator in cyanobacteria. Proc Natl Acad Sci U S A *103*, 12109-12114.

Tataroglu, O., and Emery, P. (2015). The molecular ticks of the *Drosophila* circadian clock. Curr Opin Insect Sci *7*, 51-57.

Tomita, J., Nakajima, M., Kondo, T., and Iwasaki, H. (2005). No transcription-translation feedback in circadian rhythm of KaiC phosphorylation. Science *307*, 251-254.

Tsang, A.H., Barclay, J.L., and Oster, H. (2014). Interactions between endocrine and circadian systems. J Mol Endocrinol *52*, R1-R16.

Tsarmpopoulos, I., Gourgues, G., Blanchard, A., Vashee, S., Jores, J., Lartigue, C., and Sirand-Pugnet, P. (2016). In-Yeast Engineering of a Bacterial Genome Using CRISPR/Cas9. Acs Synth Biol *5*, 104-109.

Wollnik, F. (1989). Physiology and Regulation of Biological Rhythms in Laboratory-

Animals - an Overview. Lab Anim *23*, 107-125.

Xiong, A.S., Yao, Q.H., Peng, R.H., Li, X., Fan, H.Q., Cheng, Z.M., and Li, Y. (2004). A simple, rapid, high-fidelity and cost-effective PCR-based two-step DNA synthesis method for long gene sequences. Nucleic Acids Res *32*.

Xu, Y., Mori, T., Pattanayek, R., Pattanayek, S., Egli, M., and Johnson, C.H. (2004). Identification of key phosphorylation sites in the circadian clock protein KaiC by crystallographic and mutagenetic analyses. Proc Natl Acad Sci U S A *101*, 13933-13938.

Yamanaka, Y., Honma, K.-i., Hashimoto, S., Takasu, N., Miyazaki, T., and Honma, S. (2006). Effects of physical exercise on human circadian rhythms. Sleep and Biological Rhythms *4*, 199-206.

Yang, G., Wang, S., Wei, H., Ping, J., Liu, J., Xu, L., and Zhang, W. (2012). Patch oligodeoxynucleotide synthesis (POS): a novel method for synthesis of long DNA sequences and full-length genes. Biotechnol Lett *34*, 721-728.

Yang, P., Sampson, H.M., and Krause, H.M. (2006). A modified tandem affinity purification strategy identifies cofactors of the *Drosophila* nuclear receptor dHNF4. Proteomics *6*, 927-935.

Young, M.W., and Kay, S.A. (2001). Time zones: a comparative genetics of circadian clocks. Nat Rev Genet *2*, 702-715.

Zhang, Y., Fang, B., Emmett, M.J., Damle, M., Sun, Z., Feng, D., Armour, S.M., Remsberg, J.R., Jager, J., Soccio, R.E.*, et al.* (2015). GENE REGULATION. Discrete functions of nuclear receptor Rev-erbalpha couple metabolism to the clock. Science *348*, 1488-1492.